



Seasonal and temporal variation in water quality in New Zealand rivers and lakes

Prepared for The Ministry for the Environment

February 2019

Prepared by:
Amy Whitehead
Craig Depree
John Quinn

For any information regarding this report please contact:

Amy Whitehead
Quantitative Freshwater Ecologist
Freshwater Ecology
+64-3-343 7854
amy.whitehead@niwa.co.nz

National Institute of Water & Atmospheric Research Ltd
PO Box 8602
Riccarton
Christchurch 8011

Phone +64 3 348 8987

NIWA CLIENT REPORT No: 2019024CH
Report date: February 2019
NIWA Project: MFE18502

Quality Assurance Statement		
	Reviewed by:	Ton Snelder
	Formatting checked by:	Rachel Wright
	Approved for release by:	Scott Larned

© All rights reserved. This publication may not be reproduced or copied in any form without the permission of the copyright owner(s). Such permission is only to be given in accordance with the terms of the client's contract with NIWA. This copyright extends to all forms of copying and any storage of material in any kind of information retrieval system.

Whilst NIWA has used all reasonable endeavours to ensure that the information contained in this document is accurate, NIWA does not give any express or implied warranty as to the completeness of the information contained herein, or that it will be suitable for any purpose(s) other than those specifically contemplated during the Project or agreed by NIWA and the Client.

Contents

- Executive summary6**

- 1 Introduction7**

- 2 Data8**
 - 2.1 River water quality data.....8
 - 2.2 Lake water quality data9
 - 2.3 Predictor data11

- 3 Modelling methods.....14**
 - 3.1 Comparison of summer and winter water quality state14
 - 3.2 Relationships between summer and winter water quality state and land cover.....14
 - 3.3 Spatial models of summer and winter water quality state14

- 4 Seasonal variation in river water quality state18**
 - 4.1 Comparison of summer and winter water quality state18
 - 4.2 Relationships between seasonal water quality state and land cover27
 - 4.3 Spatial models of summer and winter river water quality state28

- 5 Seasonal variation in lake water quality state44**
 - 5.1 Comparison of summer and winter water quality state44
 - 5.2 Spatial models of summer and winter lake water quality state51

- 6 Diel variation in water quality57**
 - 6.1 Tukituki River case study site.....57
 - 6.2 Results.....58

- 7 Discussion and conclusions70**
 - 7.1 Patterns of seasonal water quality70
 - 7.2 Comparison with previous studies71

- 8 Acknowledgments72**

- 9 References.....73**

Tables

Table 2-1:	River water quality variables, measurement units and site numbers used for seasonality analyses.	8
Table 2-2:	Lake water quality variables, measurement units and site numbers used for seasonality analyses.	10
Table 2-3:	Predictor variables used in spatial models of river water quality.	12
Table 2-4:	Predictor variables used in spatial models of lake water quality.	13
Table 4-1:	Seasonal differences between river water quality variables under different REC landcover and climate classes.	18
Table 4-2:	Performance of river water quality state random forest models.	28
Table 4-3:	Rank order of importance of predictor variables retained in the river random forest models for at least one water quality variable.	31
Table 4-4:	Comparisons of the minimum and maximum observed and predicted median values of seasonal river water quality.	34
Table 5-1:	Seasonal differences between lake water quality variables in lakes in different elevation × depth classes.	44
Table 5-2:	Performance of lake water quality state random forest models.	51
Table 5-3:	Rank order of importance of predictor variables retained in the lake random forest models for at least one water quality variable.	53
Table 5-4:	Comparisons of the minimum and maximum observed and predicted median values of seasonal lake water quality.	55

Figures

Figure 2-1:	Distribution of river water quality sites used for seasonality analyses.	9
Figure 2-2:	Distribution of lake water quality sites used for seasonality analyses.	10
Figure 4-1:	Seasonal patterns of visual clarity at river monitoring sites in different REC landcover and climate classes.	19
Figure 4-2:	Seasonal patterns of turbidity at river monitoring sites in different REC landcover and climate classes.	20
Figure 4-3:	Seasonal patterns of NH ₄ N at river monitoring sites in different REC landcover and climate classes.	21
Figure 4-4:	Seasonal patterns of NO ₃ N at river monitoring sites in different REC landcover and climate classes.	22
Figure 4-5:	Seasonal patterns of TN at river monitoring sites in different REC landcover and climate classes.	23
Figure 4-6:	Seasonal patterns of DRP at river monitoring sites in different REC landcover and climate classes.	24
Figure 4-7:	Seasonal patterns of TP at river monitoring sites in different REC landcover and climate classes.	25
Figure 4-8:	Seasonal patterns of <i>E. coli</i> at river monitoring sites in different REC landcover and climate classes.	26
Figure 4-9:	Relationships between median seasonal river water-quality and proportion of the upstream catchment with high-intensity agricultural land cover.	27
Figure 4-10:	Comparison of observed river water quality versus values predicted by the random forest models.	29

Figure 4-11:	Partial plot for the predictor variable season in random forest models of water quality.	32
Figure 4-12:	Partial plots for 11 of the 12 most important predictor variables in random forest models of river water quality.	33
Figure 4-13:	Predicted seasonal median visual clarity in New Zealand rivers.	36
Figure 4-14:	Predicted seasonal median turbidity in New Zealand rivers.	37
Figure 4-15:	Predicted median NH ₄ N in New Zealand rivers.	38
Figure 4-16:	Predicted seasonal median NO ₃ N in New Zealand rivers.	39
Figure 4-17:	Predicted seasonal median TN in New Zealand rivers.	40
Figure 4-18:	Predicted seasonal median DRP in New Zealand rivers.	41
Figure 4-19:	Predicted seasonal median TP in New Zealand rivers.	42
Figure 4-20:	Predicted seasonal median ECOLI in New Zealand rivers.	43
Figure 5-1:	Seasonal patterns of SECCHI in lakes in different altitude and depth classes.	45
Figure 5-2:	Seasonal patterns of CHLA in lakes in different altitude and depth classes.	46
Figure 5-3:	Seasonal patterns of NH ₄ N in lakes in different altitude and depth classes.	47
Figure 5-4:	Seasonal patterns of TN in lakes in different altitude and depth classes.	48
Figure 5-5:	Seasonal patterns of TP in lakes in different altitude and depth classes.	49
Figure 5-6:	Seasonal patterns of TLI3 in lakes in different altitude and depth classes.	50
Figure 5-7:	Comparison of observed lake water quality versus values predicted by the random forest models.	52
Figure 5-8:	Partial plots for the 12 most important predictor variables in random forest models of lake water quality.	54
Figure 5-9:	Predicted median water quality for six variables in New Zealand lakes.	56
Figure 6-1:	Examples of benthic periphyton blooms in the Tukituki River (Feb 2016 and Feb 2017).	57
Figure 6-2:	Location map of the Tukituki River showing the study sites and sewerage treatment plant discharges (black arrows).	58
Figure 6-3:	Diel pH values at Tukituki sites T7, T8, T9 and T11 (Feb 2017).	59
Figure 6-4:	The average duration (hours) that river water pH was ≥ 9 at sites along a 31km reach of the Tukituki River (Feb 2017).	59
Figure 6-5:	Fraction of ammonium (NH ₄) and ammonia (NH ₃) at different pH values.	61
Figure 6-6:	The relationship between free dissolved phosphate from the dissolution of iron(II) phosphate with increasing pH value.	62
Figure 6-7:	Continuous pH (black line) and two-hourly DRP concentrations (blue dashed line) for site T9, Tukituki River (Feb 2017).	63
Figure 6-8:	Dissolved oxygen (DO) concentrations g/m ³ at two sites on the Tukituki River (T2 and T9) and one site on a tributary, Papanui Stream.	64
Figure 6-9:	Chlorophyll- <i>a</i> (Chl _a) concentrations (a proxy measure of sloughed algal biomass) of biomass trapped in nets positioned at mid-depth and surface level.	65
Figure 6-10:	Diel variations in nitrate-N concentrations at Tukituki sites T8, T9 and T11 (Feb 2017).	66
Figure 6-11:	Concentration of nitrate-N attenuated between sites T8 and T9 (3 km distance) on the Tukituki River.	68
Figure 6-12:	Diel concentrations of nitrate-N at sites T9 and T11 (22 km apart) on the Tukituki River before (solid line) and one week after (dashed line) a 85 m ³ /s stormflow event on 20 Feb 2017.	69

Executive summary

This report provides an analysis of seasonal patterns in river and lake water quality across New Zealand, using data from 2013-2017. This report is the fifth in a series of reports prepared for the Ministry for the Environment on national-scale state and trends in river and lake water quality. The first two reports provided site-specific water quality state and trends for over 1000 river and lake monitoring sites operated by Regional Councils and NIWA. The water quality data acquired and processed for these two reports were used in the current report to assess seasonal patterns in water quality. The third and fourth reports made national-scale water quality predictions for all New Zealand rivers and lakes (> 1ha) using random forest models. The current report uses the same datasets and methodologies to identify seasonal patterns in the spatial and environmental distribution of water quality variables. Large scale assessments of seasonality were carried out using river sites grouped into River Environment Classification (REC) classes, lake sites grouped into elevation × depth classes, and spatial models of all river segments and all large lakes in New Zealand.

There were significant differences between summer and winter water quality for river monitoring sites associated with some REC landcover classes. For example, monitoring sites in catchments dominated by agricultural and natural landcover were typically associated with lower clarity and higher turbidity and nutrient concentrations in winter compared to summer. Clarity, turbidity, and nitrogen (NH₄N, NO₃N, TN) showed significant seasonal relationships with high-intensity agriculture, with the difference between summer and winter water quality increasing as the proportion of high-intensity agriculture in a catchment increased. The spatial modelling supported these findings, with regions dominated by high-intensity agriculture typically having poorer clarity, turbidity and nutrients concentrations in winter than in summer. In contrast, *E. coli* concentrations were significantly higher in summer compared to winter. Spatial patterns of *E. coli* showed greater differences between summer and winter concentrations in catchments dominated by agricultural and urban environments. This study supports the common perception that river water quality is poorer in winter, with the exception of *E. coli*, which is used to evaluate human health risks associated with contact recreation. There have been recent discussions suggesting that monitoring of *E. coli* should be limited to summer when contact recreation is more common. Our findings suggest that summer-only monitoring would result in poorer water quality gradings of sites representing catchments that are dominated by agricultural and urban land cover.

Most variation in lake water quality was accounted for by catchment topography and lake characteristics, not by season or catchment landcover. However, biases in the geographic spread of lake data mean that spatial predictions are uncertain at the lake-scale and actual data should be used in preference to the modelled predictions.

This report also includes an assessment of diel variation in water quality using the Tukituki River as a case study. Data from sonde deployments and grab samples revealed strong diel fluctuations in pH, dissolved oxygen and nitrate-nitrogen concentrations. These patterns were driven by fluctuations in photosynthetic carbon fixation, ecosystem respiration, nutrient uptake and sorption-desorption processes. Such diel variation is likely to have potential implications for ecosystem and human health.

1 Introduction

River and lake water quality across New Zealand was characterised by recent national analyses of state and trends at over 1000 monitoring sites (Larned et al., 2018a, 2018b). The sites are monitored as part of the State of Environment (SOE) programmes operated by regional councils, unitary authorities and the national river water quality network operated by NIWA. Larned et al. (2018a, 2018b) provided information on water quality variables measured at 887 river sites and 155 lakes. The datasets underlying these analyses contain quarterly or monthly measurements over periods from as early as 1990 to 2018.

The current report uses river and lake water quality data from Larned et al. (2018a, 2018b) to assess differences in summer and winter water quality across New Zealand. The data were also used to develop spatial models that predict summer and winter water quality in all New Zealand rivers and all lakes with an area greater than one hectare. Spatial modelling provides a more representative assessment of national scale water quality than assessments based on aggregating raw monitoring site data as the latter approach can lead to biased conclusions about water quality patterns due to the non-random locations of monitoring sites (Larned and Unwin, 2012).

This report provides a detailed description of the methods used to prepare the data and assess seasonal differences in water quality. Detailed methods for predicting summer and winter water quality at unmonitored sites are also described. The results provide an analysis of summer and winter water quality across River Environment Classification climate and landcover classes for rivers and lake elevation × depth classes, as well as national-scale maps of predicted summer and winter river and lake water quality. Measures of model performance and the important relationships between water quality variables and predictors are described and discussed.

This report also assesses diel variation in water quality, using data from the Tukituki River to show how diel fluctuations in river metabolism (gross and net primary production and ecosystem respiration) lead to corresponding fluctuations in pH and dissolved oxygen (DO) and nitrogen concentrations. We also briefly discuss the potential implications of this diel variation, with respect to the compulsory NPS-FM values (MFE 2017) of ecosystem and human health.

2 Data

2.1 River water quality data

The monitoring sites and data used in the Stage 1 study that analysed water quality state (Larned et al., 2018b) were also used for the current study. The water quality data consisted of measurements of eight physical, chemical, microbiological and invertebrate variables from river monitoring sites in council SOE networks and the NRWQN sites (Table 2-1). Detailed methods for processing the water quality data are given in Larned et al (2018b). The monitoring sites had the following properties: 1) less than 50% of the values for a variable were censored (i.e., below the detection limit (left-censored) or above reporting limit (right-censored)); 2) values for at least 90% of monthly or quarterly sampling dates were available, including censored values; 3) at least 14 values per season (summer: Dec-Feb; winter: Jun-Aug) were distributed over four of the five years from 2013 to 2017. Invertebrate data was not included in this report because annual sampling means that seasonal values of state cannot be calculated. Seasonal state medians were calculated for summer and winter for all site and variable combinations.

The Stage 1 study used the original version of the River Environment Classification (REC1; Snelder and Biggs, 2002) as a spatial framework to provide environmental context for the analysis. In the current study, we used a recently updated version of the REC, referred to as REC2 (see Section 2.2 for details). Shifting to REC2 allowed us to use associated updated predictor variables to each monitoring site for use in spatial modelling. All monitoring sites from the Stage 1 study were projected on to the REC2 digital river network, then manually checked. In the final dataset used for RF modelling, between 596 and 891 sites met the inclusion criteria for at least one of the eight water quality variables (Table 2-1).

The geographic distribution of river monitoring sites used for modelling is shown in Figure 2-1. The sites are reasonably well-distributed, although there are gaps in the central North and central South Islands. There is a high degree of overlap among the sites used for physical, chemical and microbiological water quality monitoring, as some or all of the corresponding variables are measured at each site in council SOE programmes.

Table 2-1: River water quality variables, measurement units and site numbers used for seasonality analyses.

Variable type	Variable	Abbreviation	Units	Number of monitoring sites
Physical	Visual clarity	CLAR	m	490
	Turbidity	TURB	NTU	760
Chemical	Ammoniacal nitrogen	NH4N	mg m ⁻³	774
	Nitrate-nitrogen	NO3N	mg m ⁻³	773
	Total nitrogen (unfiltered)	TN	mg m ⁻³	705
	Dissolved reactive phosphorus	DRP	mg m ⁻³	774
	Total phosphorus (unfiltered)	TP	mg m ⁻³	706
Microbiological	<i>Escherichia coli</i>	ECOLI	cfu/100 mL	758

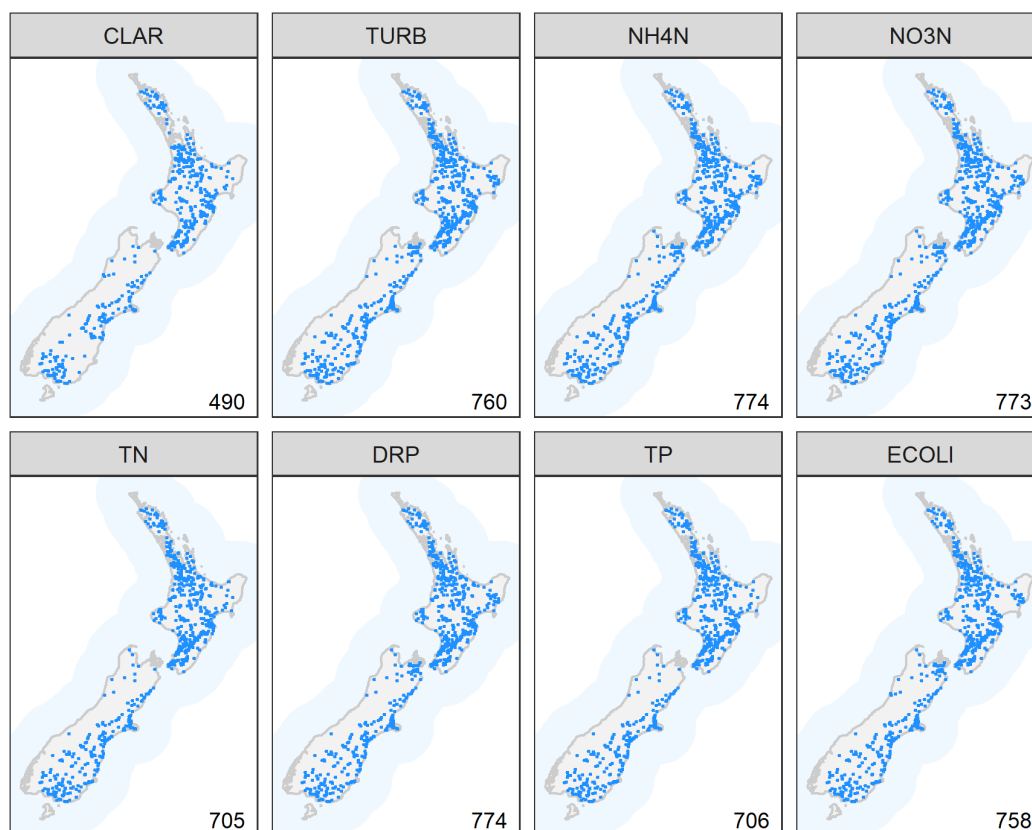


Figure 2-1: Distribution of river water quality sites used for seasonality analyses. The number of sites available for each variable is indicated in the bottom corner of each panel.

2.2 Lake water quality data

We used the SOE data for lakes analysed by Larned et al. (2018a) for the current study for spatial modelling. Detailed methods for obtaining and grooming these data are provided by Larned et al. (2018b). These lake SOE data included six water quality variables that correspond to physical, chemical and biological conditions (Table 2-2). The variables included total nitrogen (TN), total phosphorus (TP), ammoniacal nitrogen (NH4N), the visual clarity indicator Secchi depth (SECCHI), phytoplankton biomass as chlorophyll *a* (CHLA), and the trophic level index (TLI3, comprising TN, TN and CHLA; Burns et al., 1999).

This study used only lake SOE data for the five-year period from 2013 to 2017. Two filtering rules were applied to ensure that the SOE data were representative of each lake and variable, following the approach of Snelder et al. (Snelder et al., 2016) First, at least eight samples were available per season (summer: Dec-Feb; winter: Jun-Aug) for the five-year period. Second, less than 50% of the observations of each variable were censored. A summary of the number of lakes per variable used in this study is show in Table 2-2. These filtering rules are the same as those used by Fraser and Snelder (2018) but are a relaxation of the inclusion rule of Larned et al. (Larned et al., 2018a) who required lake × variable combinations in the state analyses to have measurements for at least 80% of the years (four out of five years) and at least 80% of the seasons in the period (either 48 of 60 months, or 16 of 20 quarters). The relaxation of the inclusion rules by this study increased the number of lakes

for which water quality state was assessed compared to Larned et al. (2018a) (Figure 2-2). Seasonal state medians were calculated for summer and winter separately.

Table 2-2: Lake water quality variables, measurement units and site numbers used for seasonality analyses.

Variable type	Variable	Abbreviation	Units	Number of lakes
Physical	Secchi depth	SECCHI	m	58
Chemical	Ammoniacal nitrogen	NH4N	mg m ⁻³	60
	Total nitrogen (unfiltered)	TN	mg m ⁻³	97
	Total phosphorus (unfiltered)	TP	mg m ⁻³	90
Biological	Chlorophyll <i>a</i>	CHLA	mg m ⁻³	95
Index	Trophic Level Index	TLI3	Unitless	87

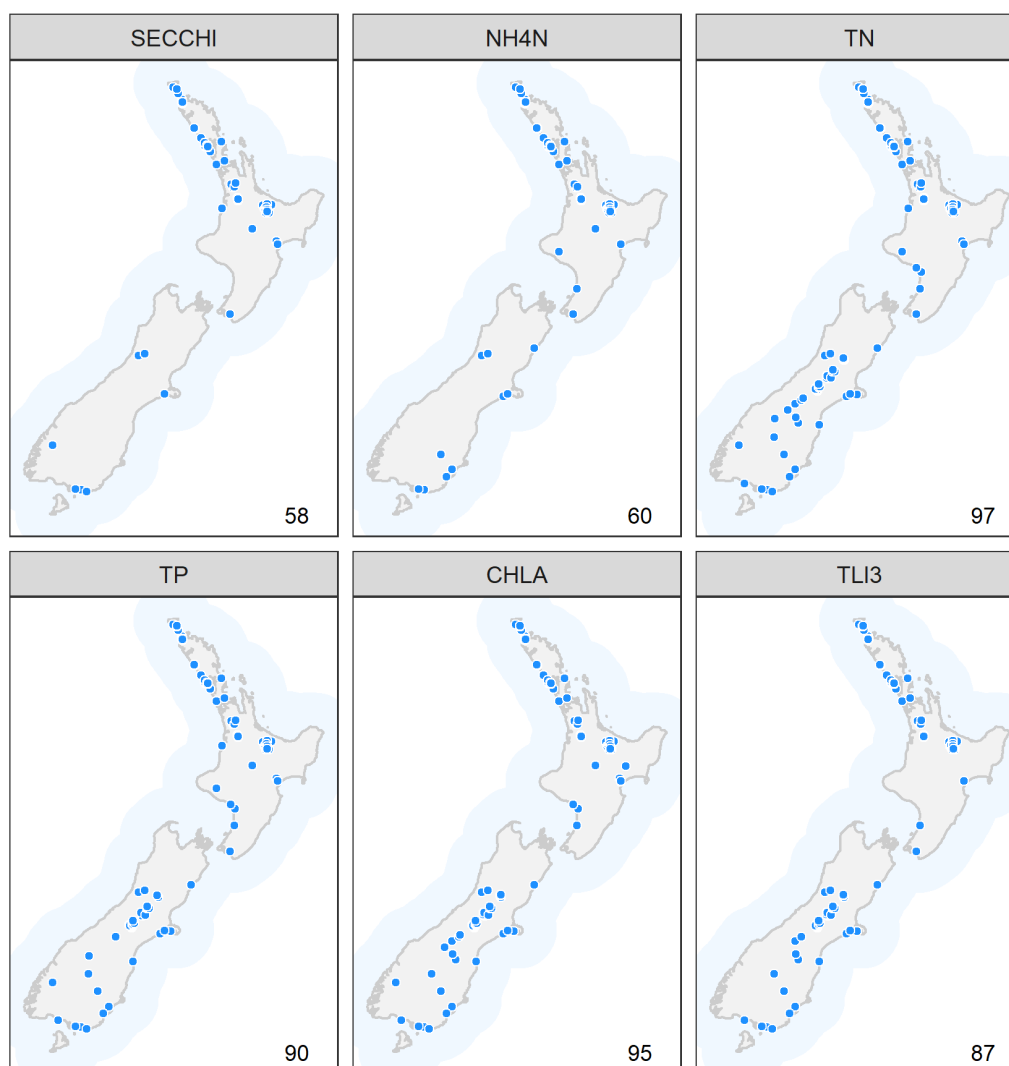


Figure 2-2: Distribution of lake water quality sites used for seasonality analyses. The number of sites available for each variable is indicated in the bottom corner of each panel.

2.3 Predictor data

2.3.1 Rivers

The digital river network and catchment boundaries used to define the REC provided the spatial framework for the random forest models of river water quality state. The river network and catchment boundaries were derived from a digital elevation model (DEM) with a spatial resolution of 50 m. The digital network represents New Zealand's rivers as ~ 560,000 segments (bounded by upstream and downstream confluences) and their corresponding catchments. Each segment in the digital network has a unique identifier, the nzsegment number. The links between each nzsegment and its catchment, between adjacent nzsegments and between adjacent catchments facilitate analyses of upstream-downstream connectivity and the accumulation of catchment characteristics in the downstream direction. The digital network has been recently updated to correct errors and to improve its representation of rivers nationally; the REC geodatabase with the updated network is referred to as REC2.

In addition to the digital network, REC2 contains spatial data layers describing the climate, topography, geology, vegetation, infrastructure and hydrology of New Zealand (<https://www.niwa.co.nz/freshwater-and-estuaries/management-tools/river-environment-classification-0>). These spatial data are used to link each nzsegment to many attributes that describe the environmental characteristics of the segment and its catchment. Catchment landcover in REC2 is derived from the national Land Cover Database-4 (LCDB4) which differentiates 33 categories based on analysis of satellite imagery from 2012 ([Iris.scinfo.org.nz](http://iris.scinfo.org.nz)). Descriptions of catchment regolith are derived from the Land Resources Inventory (LRI) including interpretations of the LRI categories made by Leathwick et al (2003). Additional variables for each segment have been derived from national-scale hydrological modelling (e.g., Booker and Snelder, 2012).

We selected 32 network attributes from the REC2 (Table 2-2) for predictor variables in spatial models of the eight water quality variables listed in Table 2-1. The predictor variables were selected based on their predicted mechanistic or correlative relationships with water quality, and on previous experience with national scale modelling of water quality (e.g., Unwin et al., 2010) and invertebrate communities (Clapcott et al., 2013; Leathwick et al., 2011).

Table 2-3: Predictor variables used in spatial models of river water quality. *Geological variables are based on regolith, using averages of ordinal values assigned to LRI top-rock categories by Leathwick et al. (2003). The variables usHard and usPsize characterise physical regolith conditions; usPhos and usCalc characterise regolith fertility.

Predictor	Description	Abbreviation	Unit
Season	Summer (Dec – Feb), Winter (Jun – Aug)	season	factor
Geography & topography	Catchment area	usArea	m ²
	Mean annual catchment rainfall	usRain	mm
	Mean annual catchment potential evapotranspiration	usPET	mm/yr
	Estimated mean flow	MeanFlow	m ³ /s
	Segment mean elevation	segElev	m ASL
	Percentage of catchment occupied by lakes	usLakePerc	%
	Mean catchment elevation	usElev	m ASL
	Mean catchment slope	usSlope	degrees
	Distance to the coast	DistToCoast	m
	Mean segment slope	SegSlope	degrees
Climate & flow	Segment sinuosity (segment length divided by the straight-line distance between endpoints)	Sinuosity	unitless
	Distance to furthest headwater segment	DistToHead	m
	Mean segment June air temperature	segTmin	degrees C x 10
	Mean segment January air temperature.	segTwarm	degrees C x 10
	Mean catchment June air temperature	usTmin	degrees C x 10
	Mean catchment January air temperature	usTwarm	degrees C x 10
	Mean catchment coefficient of variation of annual rainfall	usRainvar	mm/yr
	Mean catchment rain days > 10mm	usRainDays10	days/mo
Mean catchment rain days > 200mm	usRainDays20	days/mo	
Mean catchment rain days > 100mm	usRainDays100	days/mo	
Geology*	Mean catchment induration (hardness) of regolith	usHard	Ordinal
	Mean catchment phosphorous content of regolith	usPhos	Ordinal
	Mean catchment particle size of regolith	usPsize	Ordinal
	Mean catchment calcium content of regolith	usCalc	Ordinal
Landcover	Proportion of catchment occupied by combination of high producing exotic grassland, short-rotation cropland, orchard, vineyard and other perennial crops (LCDB4 classes 40, 30, 33)	usIntensiveAg	%
	Proportion of catchment in low producing grassland (LCDB4 class 41)	usPastoralLight	%
	Proportion of catchment in native forest (LCDB4 class 69)	usNativeForest	%
	Proportion of catchment in built-up areas, urban parkland, surface mines, dumps and transport infrastructure (LCDB4 classes 1,2,6,5)	usUrban	%
	Proportion of catchment in scrub and shrub cover (LCDB4 classes 50, 51, 52, 54, 55, 56, 58)	usScrub	%
	Proportion of catchment occupied by lake and pond, river and estuarine open water (LCDB4 classes 20, 21, 22)	usWetland	%
	Proportion of catchment in exotic forest (LCDB4 class 71)	usExoticForest	%
	Proportion of catchment occupied in bare or lightly-vegetated cover (LCDB4 classes 10, 12, 14, 15, 16)	usBare	%

2.3.2 Lakes

The FENZ database provides characteristics of all 3821 lakes greater than one hectare in area occurring across the North and South Islands and some of the smaller outlying islands. Details of these variables and their derivation are provided by Snelder et al. (2006). Characteristics include descriptors of climatic, geological, topographic, bathymetric, landcover, and hydrological conditions in New Zealand lakes and their catchments.

The FENZ dataset includes estimates of average lake depth that were made using a geospatial statistical model (Snelder et al., 2006). We also had measured maximum depth for all monitored lakes. We tested including maximum lake depth in our spatial models. However, because we used our models to make predictions for all lakes, we used the estimated average lake depth in our spatial models.

Table 2-4: Predictor variables used in spatial models of lake water quality.

Predictor	Description	Abbreviation	Unit
Season	Summer (Dec – Feb), Winter (Jun – Aug)	season	factor
Lake	Lake surface area	lkArea	m ²
	Straight line distance to coast	lkDistCoast	km
	Estimated average lake depth	lkDepth	m
	Lake elevation	lkElev	m ASL
Catchment topography	Catchment average slope	catSlope	Degrees
	Catchment area	catArea	m ²
	Catchment elevation	catElev	m ASL
Climate and flow	Lake summer (December) solar radiation	lkDecSolRad	W m ⁻²
	Lake winter (June) solar radiation	lkJuneSolRad	W m ⁻²
	Lake average summer (December) air temperature	lkDecTemp	Degrees
	Lake average winter (June) air temperature	lkJunTemp	Degrees
	Lake wind fetch	lkFetch	m
	Lake summer (December) wind speed	lkSumWind	m s ⁻¹
	Lake winter (June) wind speed	lkWinWind	m s ⁻¹
	Catchment average summer (December) air temperature	catSumTemp	Degrees
	Catchment average winter (June) air temperature	catWinTemp	Degrees
	Catchment average annual discharge	catFlow	m ³ yr ⁻¹
Geology	Catchment average phosphorous	catPhos	Ordinal*
	Catchment average calcium	catCalc	Ordinal*
	Catchment average induration or hardness value	catHard	Ordinal*
	Catchment average particle size	catPsize	Ordinal*
	Proportion of catchment occupied by peat	catPeat	Proportion
	Proportion of catchment occupied by alluvium	catAlluv	Proportion
Landcover	Proportion of catchment occupied by permanent snow	catGlacial	Proportion
	Proportion of catchment occupied by indigenous forest	catIndigForest	Proportion
	Proportion of catchment occupied by bare ground	catBare	Proportion
	Proportion of catchment occupied by exotic forest	catExoticForest	Proportion
	Proportion of catchment occupied by pasture	catPastoral	Proportion

3 Modelling methods

3.1 Comparison of summer and winter water quality state

We used the median summer and winter state of each river and lake water quality variable to identify seasonal patterns in water quality. River sites were grouped by REC classes (climate, landcover) to help determine whether differences between summer and winter water quality were associated with catchment land use and climate, while lakes were grouped by depth and altitude classes. For each water quality variable in each group, inter-seasonal comparisons were made by non-parametric pairwise Wilcoxon signed rank tests, with comparisons limited to groups that contained at least five sites.

3.2 Relationships between summer and winter water quality state and land cover

Following the method of Larned et al (2018b), we used multiple linear regressions to evaluate whether water quality varied by season and the proportion of high-intensity agricultural land cover in the catchments upstream of the monitoring sites. The proportion of high-intensity agricultural landcover was defined as the sum of proportional landcover in three LCDB4 classes (high-producing exotic grassland, short-rotation crops, and orchards and vineyards). The same composite classification for high-intensity agricultural land cover was used in previous national-scale water-quality analyses (Larned et al., 2016b; McDowell et al., 2013). All water quality variable values were log-transformed to improve the normality of residuals.

3.3 Spatial models of summer and winter water quality state

The summer and winter site medians for each water quality variable were used to fit water quality state to the predictor variables (Table 2-3, Table 2-4) using random forest (RF) models. We included season as a predictor to determine if there were spatial patterns in summer and winter water quality. The RF models were then used to predict water quality state for all segments of the digital network. Note that the training datasets used for the seasonal RF models had fewer sites than for the mean annual models developed in Whitehead (2018) and Fraser and Snelder (2018) as some river sites and lakes did not have sufficient data after subdividing the data into summer and winter subsets. National-scale maps of predicted water quality were produced for each water quality variable. For models where season was retained as an important predictor (see Section 3.3.1), we produced separate maps of summer and winter water quality, and a third map showing the summer – winter difference mapped to each reach.

3.3.1 Random forest models

We modelled log-transformed median summer and winter values of each water quality variable (i.e., the \log_{10} of the median of the untransformed raw data) as a function of the predictor variables using RF models (Breiman, 2001, 1984; Cutler et al., 2007). An RF model is an ensemble of individual classification and regression trees (CART). In a regression context, CART partitions observations (in this case the individual water quality variables) into groups that minimise the sum of squares of the response (i.e. assembles groups that minimise differences between observations) based on a series of binary rules or splits that are constructed from the predictor variables. CART models have several desirable features including requiring no distributional assumptions and the ability to automatically fit non-linear relationships and high order interactions. However, single regression trees have the limitations of not searching for optimal tree structures, and of being sensitive to small changes in

input data (Hastie et al., 2001). RF models reduce these limitations by using an ensemble of trees (a forest) and making predictions based on the average of all trees (Breiman, 2001). An important feature of RF models is that each tree is grown with a bootstrap sample of the fitting data (i.e. the observation dataset). In addition, a random subset of the predictor variables is made available at each node to define the split. Introducing these random components and then averaging over the forest increases prediction accuracy while retaining the desirable features of CART.

An RF model produces a limiting value of the generalization error (i.e., the model maximises its prediction accuracy for previously unseen data; Breiman, 2001). The generalization error converges asymptotically as the number of trees increases, so the model cannot be over-fitted. The number of trees needs to be set high enough to ensure an appropriate level of convergence, and this value depends on the number of variables that can be used at each split. We used default options that included making one third of the total number of predictor variables available for each split, and 500 trees per forest. Some studies report that model performance is improved by including more than ~ 50 trees per forest, but that there is little improvement associated with increasing the number of trees beyond 500 (Cutler et al., 2007). Our models took less than a minute to fit when using the default of 500 trees per forest.

Unlike linear models, RF models cannot be expressed as equations. However, the relationships between predictor and response variables produced by RF models can be represented by importance measures and partial dependence plots (Breiman, 2001; Cutler et al., 2007). During the fitting process, RF model predictions are made for each tree for observations that were excluded from the bootstrap sample; these excluded observations are known as out-of-bag (OOB) observations. To assess the importance of a specific predictor variable, the values of the response variable are randomly permuted for the OOB observations, and predictions are obtained from the tree for these modified data. The importance of the predictor variable is indicated by the degree to which prediction accuracy decreases when the response variable is randomly permuted. Importance is defined in this study as the loss in model performance (i.e. the increase in the mean square error; MSE) when predictions are made based on the permuted OOB observations compared to those based on the original observations. The differences in MSE between trees fitted with the original and permuted observations are averaged over all trees and normalised by the standard deviation of the differences (Cutler et al., 2007).

A partial dependence plot is a graphical representation of the marginal effect of a predictor variable on the response variable, when the values of all other predictor variables are held constant. The benefit of holding the other predictors constant (generally at their respective mean values) is that the partial dependence plot effectively ignores their influence on the response variables. Partial dependence plots do not perfectly represent the effects of each predictor variable, particularly if predictor variables are highly correlated or strongly interacting, but they do provide an approximation of the modelled predictor-response relationships that are useful for model interpretation (Cutler et al., 2007).

RF models can include any of the original set of predictor variables that are chosen during the model fitting process. Inclusion of marginally important and correlated predictor variables does not degrade the performance of the RF models. However, these predictor variables may be redundant (i.e. their removal does not affect model performance) and their inclusion can complicate model interpretation. We used a backward elimination procedure to remove redundant predictor variables from the initial 'saturated' models (i.e., models that included any of the original predictor variables). The procedure first assesses the model error (MSE) using a 10-fold cross validation process. The

predictions made to the hold out observations during cross validation are used to estimate the MSE and its standard error. The model's least important predictor variables are then removed in order, with the MSE and its standard error being assessed for each successive model. The final, 'reduced' model is defined as the model with the fewest predictor variables whose error is within one standard error of the best model (i.e., the model with the lowest cross validated MSE). This is equivalent to the "one standard error rule" used for cross validation of classification trees (Breiman, 1984).

An alternative approach is to choose the model with the smallest error. We used the former procedure as it retains fewer predictor variables than the latter procedure, while achieving an error rate that is not different, within sampling error, from the "best solution". Importance levels for predictor variables were not recalculated at each reduction step to avoid over-fitting (Svetnik et al., 2004).

We note that, because fitting a RF model involves randomly selecting observations and predictor variables throughout the fitting process, successive models fitted to the same data set will exhibit subtle differences in structure and diagnostics such as total explained deviance, MSE, partial dependence plots, and the order of predictor importance. In the current study, the variability in model error between individual fits of the model for each water quality variable were within the reported model performance (see Section 3.2).

All calculations were performed in the R statistical computing environment (R Core Team, 2017) using the *randomForest* package and other specialised packages.

3.3.2 Model performance

Model performance was assessed by comparing observations with independent predictions (i.e. sites that were not used in fitting the model), which were obtained from the out-of-bag (OOB) samples. We summarised the models using four statistics; regression R^2 , Nash-Sutcliffe Efficiencies (NSE), bias and root mean square deviation (RMSD).

The regression R^2 value is the coefficient of determination derived from a regression of the observations against the predictions. The R^2 value shows the proportion of the total variance explained by the regression model (Piñeiro et al., 2008). However, the regression R^2 is not a complete description of model performance. The NSE (Nash and Sutcliffe, 1970) provides a measure of overall model performance by indicating how closely a plot of observed versus predicted values lies to the 1:1 line (i.e. the degree to which two sets of values coincide). NSE values range from $-\infty$ to 1. An NSE of 1 corresponds to a perfect match between predictions and the observed data, an NSE of 0 indicates that the model predictions are as accurate as the mean of the observed data; and an NSE < 0 indicates that the observed mean is a better predictor than the model. Model bias measures the average tendency of the predicted values of water quality variables to be larger or smaller than the observed values. Positive values indicate underestimation bias and negative values indicate overestimation bias (Moriassi et al., 2007). The RMSD is a measure of the characteristic model uncertainty. RMSD is mean deviation of predicted values with respect to the observed values (distinct from the standard error of the regression model).

3.3.3 Model predictions

Predictions are made with RF models by "running" new cases down every tree in the fitted forest and averaging the predictions made by each tree (Cutler et al., 2007). The models in this study were fitted to \log_{10} -transformed water quality data. When these models are back-transformed, the model error

term no longer has a mean of zero. Ignoring this results retransformation bias, i.e. predictions that systematically underestimate the response. We corrected the retransformation bias using the smearing estimate (S) developed by Duan (1983):

$$S = \frac{1}{n} \sum_{i=1}^n 10^{\hat{\varepsilon}_i} \quad (\text{Equation 1}),$$

where $\hat{\varepsilon}$ are the residuals of an RF model. The predictions were back-transformed by raising them to the power of 10, then corrected for retransformation bias by multiplying by S . The back-transformed and corrected predictions for all river segments in New Zealand were projected on a single national map for each water quality variable.

4 Seasonal variation in river water quality state

4.1 Comparison of summer and winter water quality state

There were some seasonal patterns for most water quality variables, although these patterns were not consistent across REC landcover classes (Table 4-1). TURB and nutrient concentrations (NH₄N, NO₃N, TN, DRP, TP) were typically higher and CLAR lower during the winter (Figure 4-1 to Figure 4-7), particularly in the pastoral landcover class. However, sites in the natural landcover class also had higher winter values of TURB, NO₃N, TN and DRP. In contrast, ECOLI was higher in the summer in all landcover types (Figure 4-8). The observed patterns were similar when monitoring sites were divided into landcover x climate classes, with non-significant results often associated with low numbers of sites in a given class.

Table 4-1: Seasonal differences between river water quality variables under different REC landcover and climate classes. Cell values show site numbers in each class with both summer and winter observations. Cells shaded red indicate situations where the median summer value for a given water quality variable is significantly ($p < 0.05$) higher in summer than winter, while blue cells indicate the opposite seasonal pattern. Unshaded cells indicate either no significant difference between the seasons or insufficient data (< 5 sites), while blank cells represent landcover x climate classes not represented in the data. See Figures 4-1 to 4-8 for corresponding boxplots. Landcover: N = natural, EF = exotic forest, P = pasture, U = Urban. Climate: CD = Cool-dry, CW = cool-wet, CX = cool-extremely wet, WD = warm-dry, WW = warm-wet, WX = warm-extremely wet.

Landcover	Climate	CLAR	TURB	NH ₄ N	NO ₃ N	TN	DRP	TP	ECOLI	Total
N	All	106	169	171	171	158	171	159	168	171
EF	All	13	18	18	18	16	18	16	18	18
P	All	224	477	499	498	464	499	465	485	500
U	All	12	48	52	52	39	52	39	53	54
N	CD	9	19	19	19	18	19	18	19	19
	CW	64	95	96	96	89	96	89	94	96
	CX	21	33	34	34	29	34	30	33	34
	WD		2	2	2	2	2	2	2	2
	WW	12	20	20	20	20	20	20	20	20
EF	CW	7	9	9	9	8	9	8	9	9
	WW	6	9	9	9	8	9	8	9	9
P	CD	45	143	146	146	130	146	130	145	146
	CW	90	181	185	185	177	184	178	179	185
	CX	2	3	3	3	3	3	3	3	3
	WD	7	31	42	41	36	42	36	39	42
	WW	76	115	118	118	113	119	113	115	119
	WX	4	4	5	5	5	5	5	4	5
U	CD	2	23	27	27	15	27	15	27	27
	CW	2	2	2	2	2	2	2	2	2
	WD	2	14	14	14	13	14	13	15	16
	WW	6	9	9	9	9	9	9	9	9
Total		355	712	740	739	677	740	679	724	743

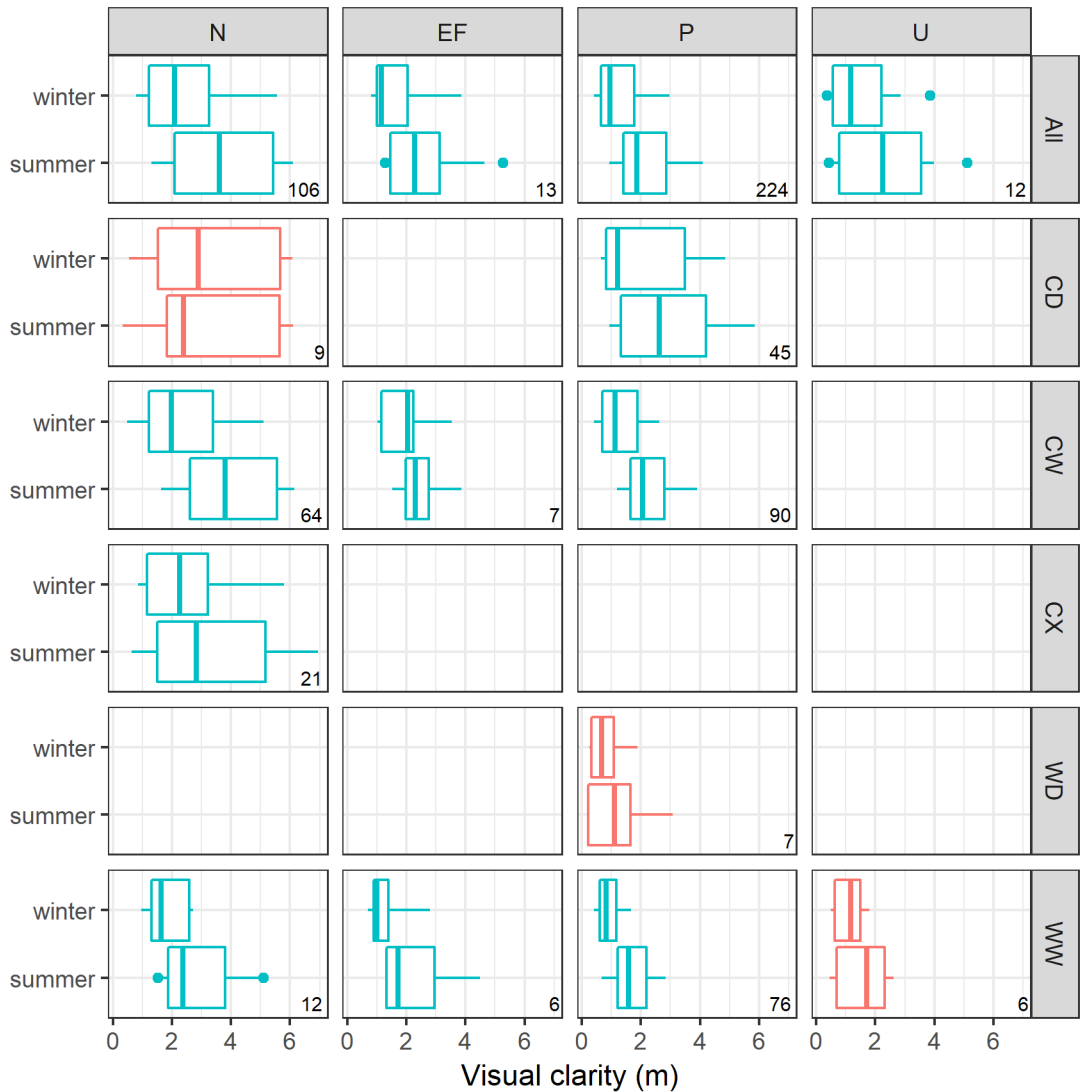


Figure 4-1: Seasonal patterns of visual clarity at river monitoring sites in different REC landcover and climate classes. Columns represent sites with both summer and winter observations grouped by natural (N), exotic forest (EF), pastoral (P) and urban (U) landcover classes. The top row represents all sites irrespective of climate, while the remaining rows are sites grouped by climate classes within each landcover class. Blue boxplots indicate significant differences ($p < 0.05$) in seasonal state within a panel, while red boxplots within a panel are not significantly different. Percentiles: boxes = 25% and 75%; horizontal bars = medians; whiskers = 10% and 90%; closed circles = 5% and 95% (for classes with > 10 sites). Panel numbers indicate the number of sites in each class, with classes with fewer than five sites not shown.

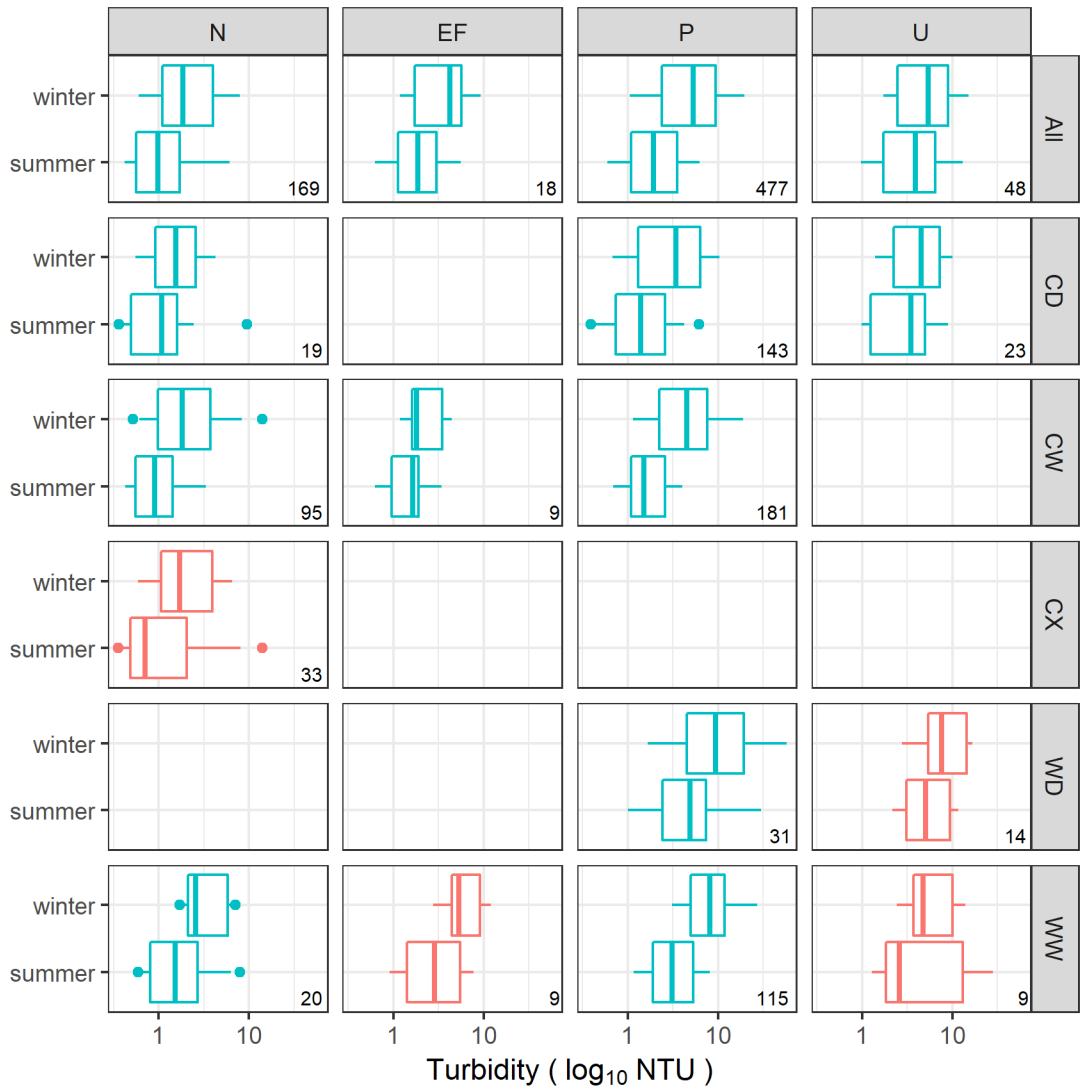


Figure 4-2: Seasonal patterns of turbidity at river monitoring sites in different REC landcover and climate classes. Columns represent sites with both summer and winter observations grouped by natural (N), exotic forest (EF), pastoral (P) and urban (U) landcover classes. The top row represents all sites irrespective of climate, while the remaining rows are sites grouped by climate classes within each landcover class. Blue boxplots indicate significant differences ($p < 0.05$) in seasonal state within a panel, while red boxplots within a panel are not significantly different. Percentiles: boxes = 25% and 75%; horizontal bars = medians; whiskers = 10% and 90%; closed circles = 5% and 95% (for classes with > 10 sites). Panel numbers indicate the number of sites in each class, with classes with fewer than five sites not shown.

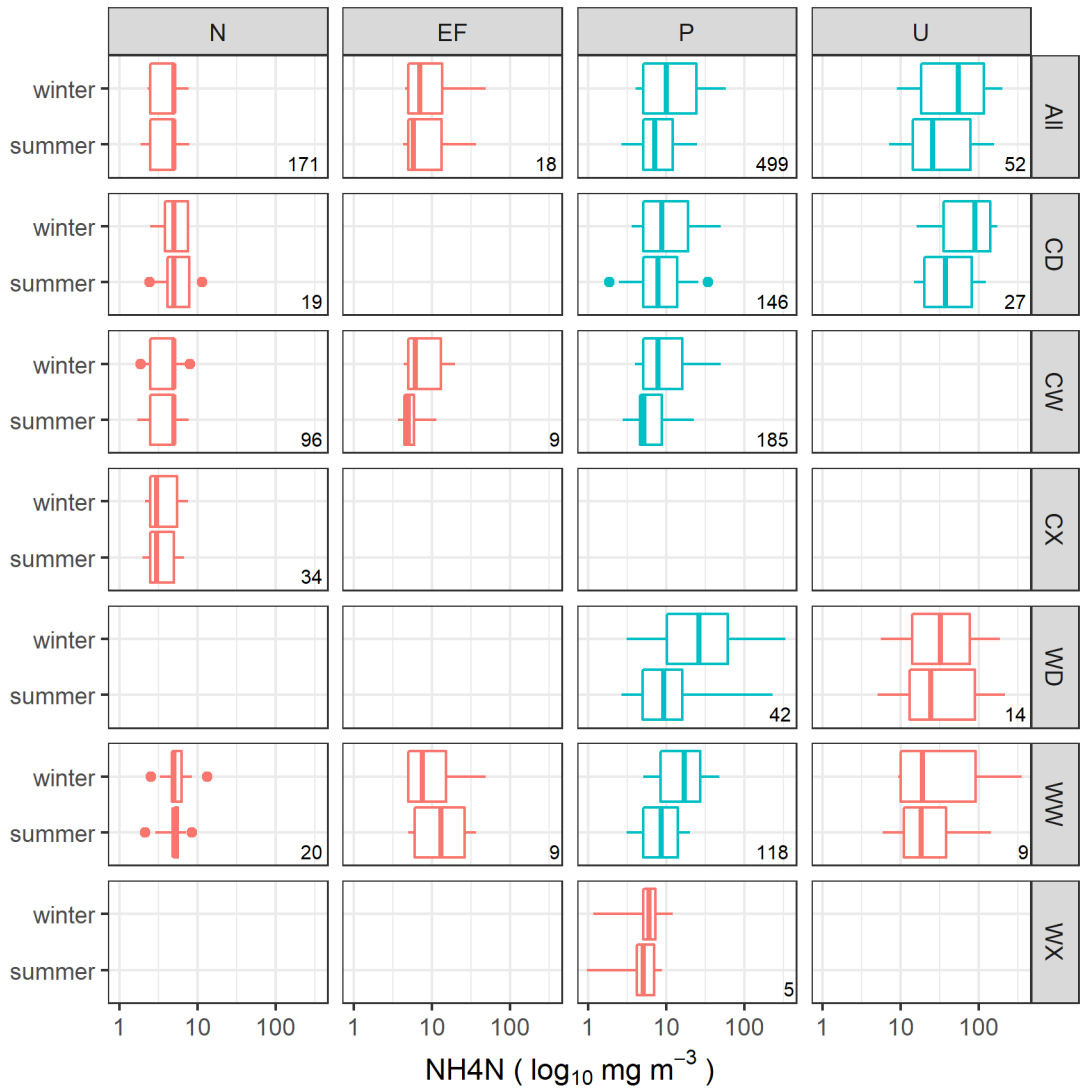


Figure 4-3: Seasonal patterns of NH4N at river monitoring sites in different REC landcover and climate classes. Columns represent sites with both summer and winter observations grouped by natural (N), exotic forest (EF), pastoral (P) and urban (U) landcover classes. The top row represents all sites irrespective of climate, while the remaining rows are sites grouped by climate classes within each landcover class. Blue boxplots indicate significant differences ($p < 0.05$) in seasonal state within a panel, while red boxplots within a panel are not significantly different. Percentiles: boxes = 25% and 75%; horizontal bars = medians; whiskers = 10% and 90%; closed circles = 5% and 95% (for classes with > 10 sites). Panel numbers indicate the number of sites in each class, with classes with fewer than five sites not shown.

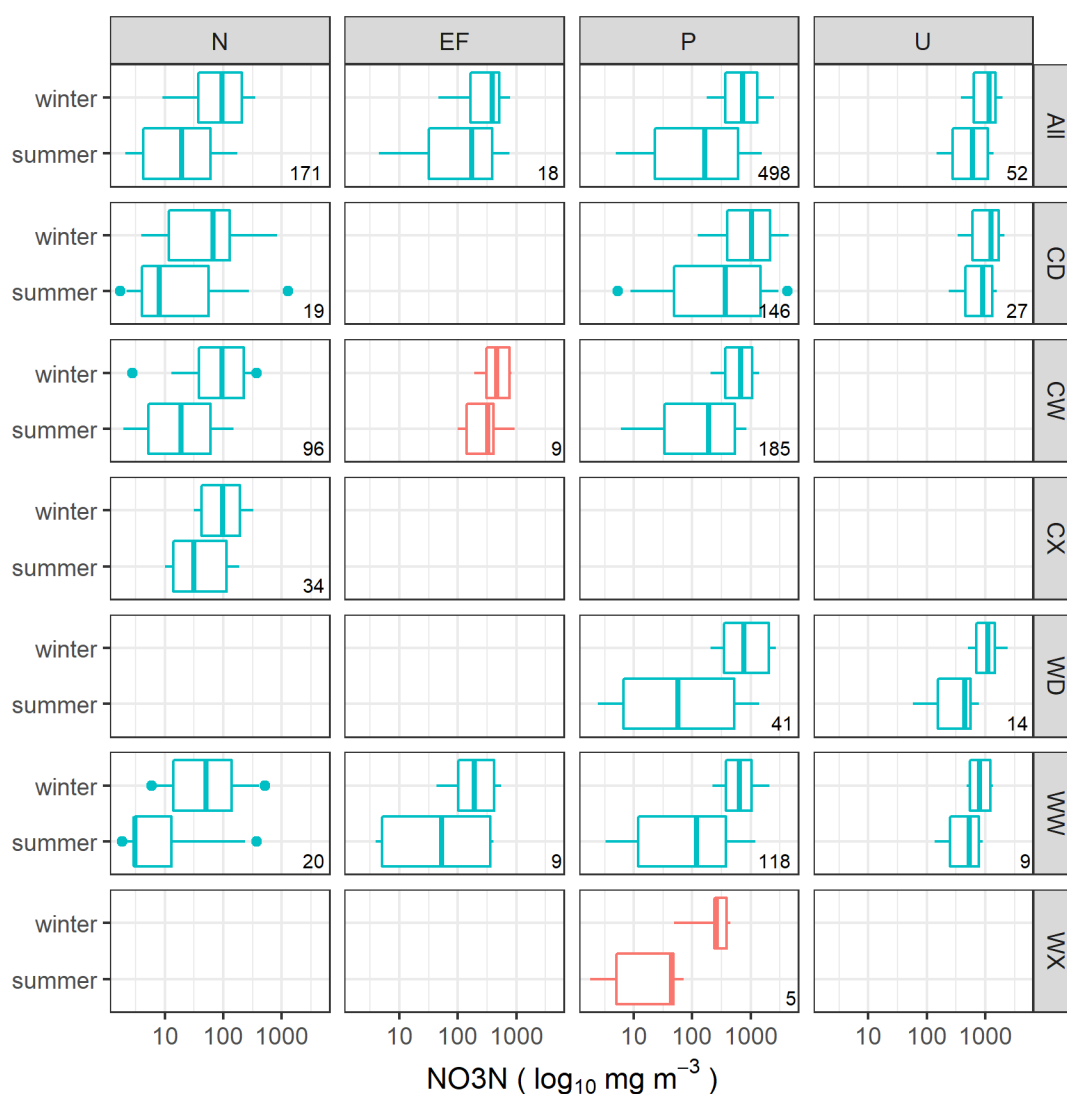


Figure 4-4: Seasonal patterns of NO3N at river monitoring sites in different REC landcover and climate classes. Columns represent sites with both summer and winter observations grouped by natural (N), exotic forest (EF), pastoral (P) and urban (U) landcover classes. The top row represents all sites irrespective of climate, while the remaining rows are sites grouped by climate classes within each landcover class. Blue boxplots indicate significant differences ($p < 0.05$) in seasonal state within a panel, while red boxplots within a panel are not significantly different. Percentiles: boxes = 25% and 75%; horizontal bars = medians; whiskers = 10% and 90%; closed circles = 5% and 95% (for classes with > 10 sites). Panel numbers indicate the number of sites in each class, with classes with fewer than five sites not shown.

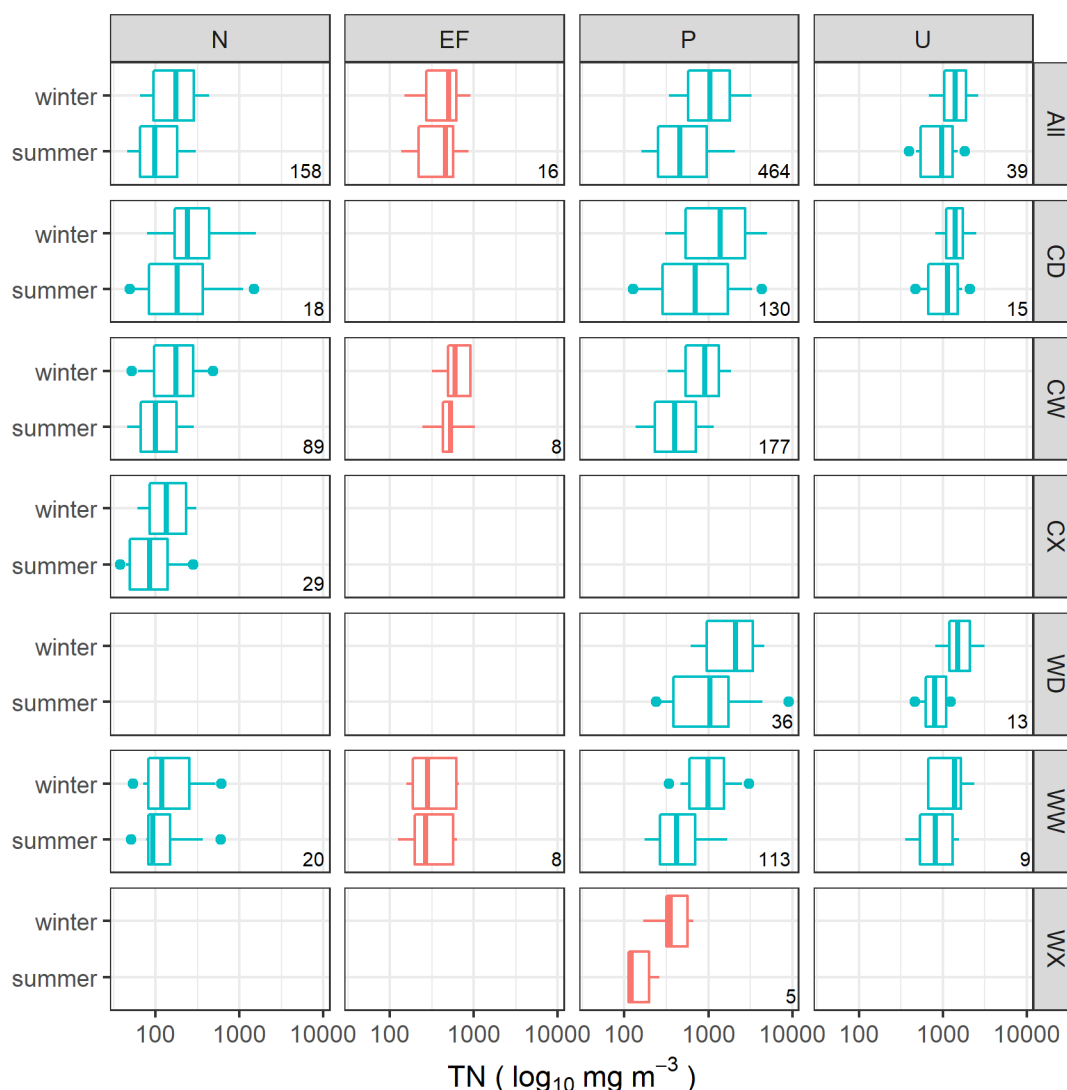


Figure 4-5: Seasonal patterns of TN at river monitoring sites in different REC landcover and climate classes. Columns represent sites with both summer and winter observations grouped by natural (N), exotic forest (EF), pastoral (P) and urban (U) landcover classes. The top row represents all sites irrespective of climate, while the remaining rows are sites grouped by climate classes within each landcover class. Blue boxplots indicate significant differences ($p < 0.05$) in seasonal state within a panel, while red boxplots within a panel are not significantly different. Percentiles: boxes = 25% and 75%; horizontal bars = medians; whiskers = 10% and 90%; closed circles = 5% and 95% (for classes with > 10 sites). Panel numbers indicate the number of sites in each class, with classes with fewer than five sites not shown.

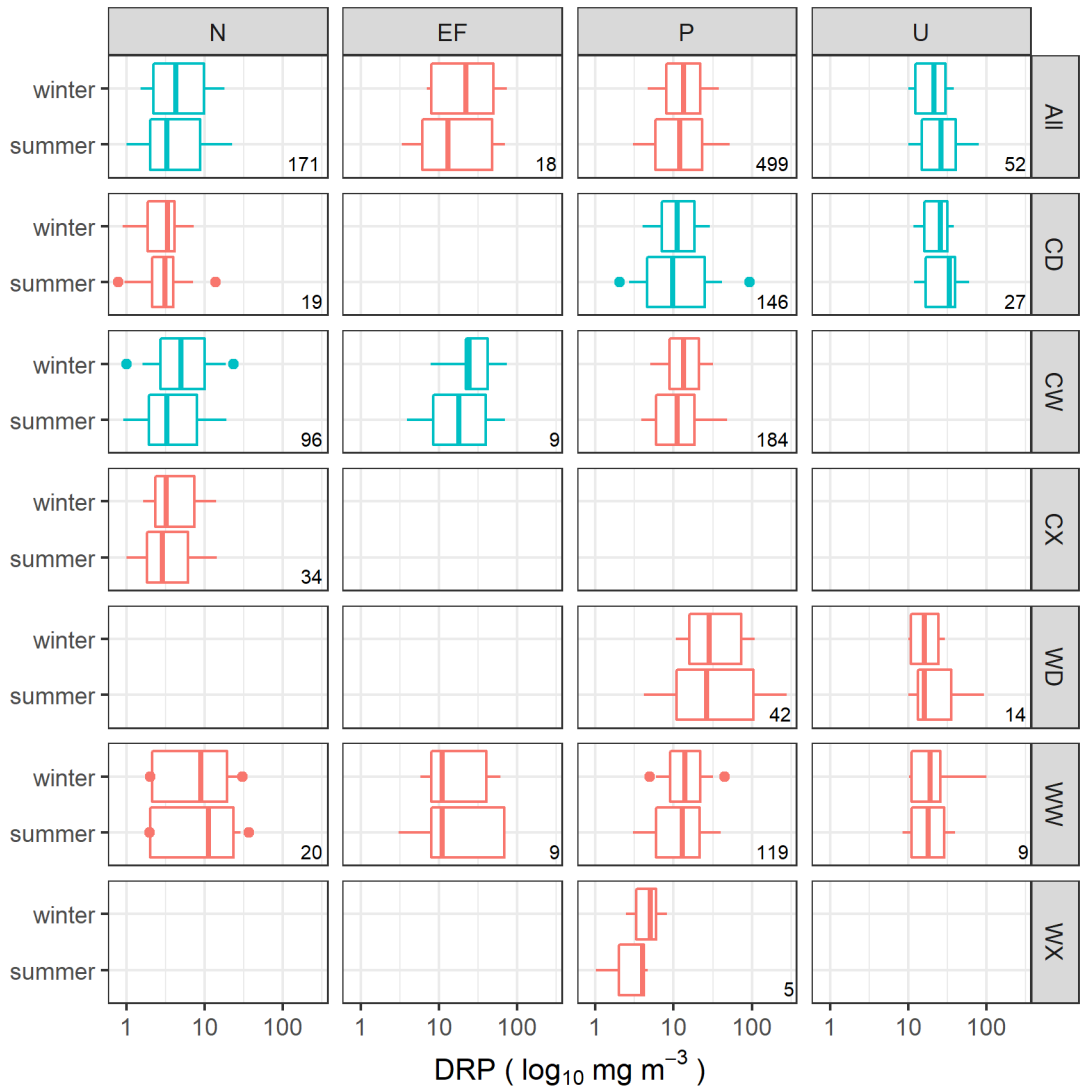


Figure 4-6: Seasonal patterns of DRP at river monitoring sites in different REC landcover and climate classes. Columns represent sites with both summer and winter observations grouped by natural (N), exotic forest (EF), pastoral (P) and urban (U) landcover classes. The top row represents all sites irrespective of climate, while the remaining rows are sites grouped by climate classes within each landcover class. Blue boxplots indicate significant differences ($p < 0.05$) in seasonal state within a panel, while red boxplots within a panel are not significantly different. Percentiles: boxes = 25% and 75%; horizontal bars = medians; whiskers = 10% and 90%; closed circles = 5% and 95% (for classes with > 10 sites). Panel numbers indicate the number of sites in each class, with classes with fewer than five sites not shown.

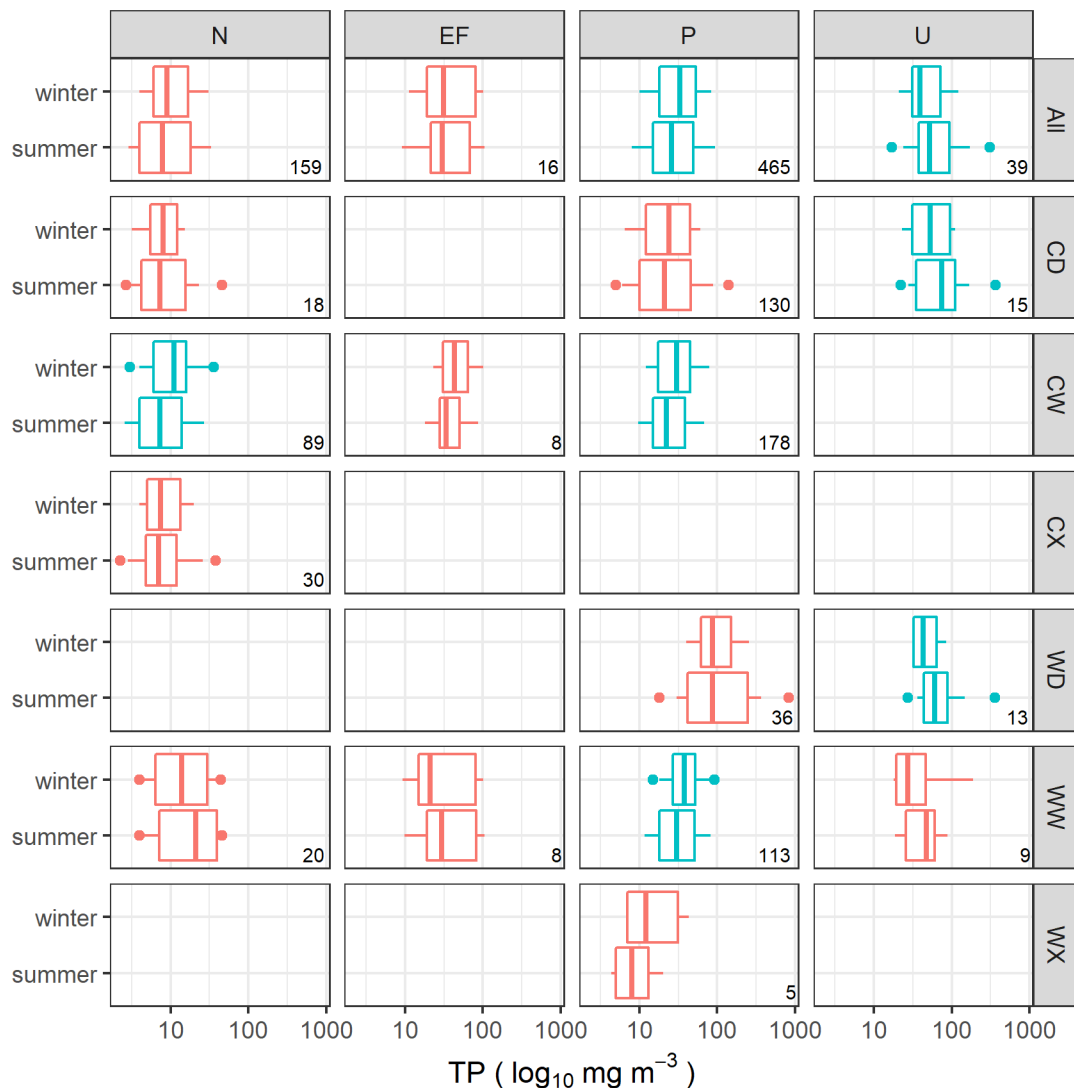


Figure 4-7: Seasonal patterns of TP at river monitoring sites in different REC landcover and climate classes. Columns represent sites with both summer and winter observations grouped by natural (N), exotic forest (EF), pastoral (P) and urban (U) landcover classes. The top row represents all sites irrespective of climate, while the remaining rows are sites grouped by climate classes within each landcover class. Blue boxplots indicate significant differences ($p < 0.05$) in seasonal state within a panel, while red boxplots within a panel are not significantly different. Percentiles: boxes = 25% and 75%; horizontal bars = medians; whiskers = 10% and 90%; closed circles = 5% and 95% (for classes with > 10 sites). Panel numbers indicate the number of sites in each class, with classes with fewer than five sites not shown.

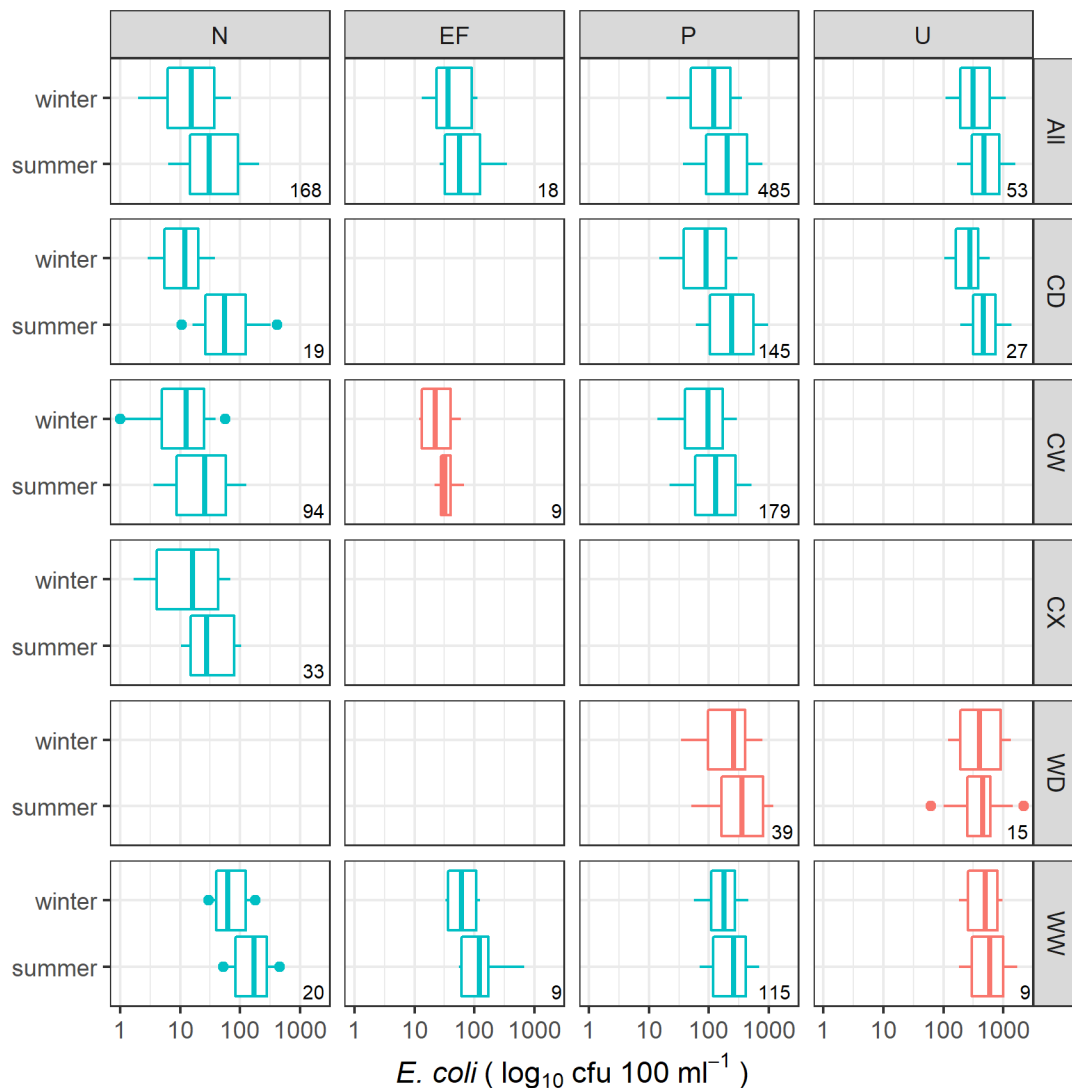


Figure 4-8: Seasonal patterns of *E. coli* at river monitoring sites in different REC landcover and climate classes. Columns represent sites with both summer and winter observations grouped by natural (N), exotic forest (EF), pastoral (P) and urban (U) landcover classes. The top row represents all sites irrespective of climate, while the remaining rows are sites grouped by climate classes within each landcover class. Blue boxplots indicate significant differences ($p < 0.05$) in seasonal state within a panel, while red boxplots within a panel are not significantly different. Percentiles: boxes = 25% and 75%; horizontal bars = medians; whiskers = 10% and 90%; closed circles = 5% and 95% (for classes with > 10 sites). Panel numbers indicate the number of sites in each class, with classes with fewer than five sites not shown.

4.2 Relationships between seasonal water quality state and land cover

Water quality state varied significantly with the proportion of high-intensity agriculture upstream of river monitoring sites (Figure 4-9) for all measured variables, with CLAR declining and TURB, ECOLI and all five nutrients increasing as the proportion of high-intensity agriculture (usIntensiveAg) increased. These patterns are consistent with previous research showing negative associations between water quality and agricultural landcover (Larned et al., 2016b). There were also significant interactions between season and high-intensity agricultural cover, with higher TURB ($p = 0.031$), NH4N ($p = 0.007$), NO3N ($p = 0.019$) and TN ($p = 0.003$) associated with high proportions of agricultural landcover during the winter.

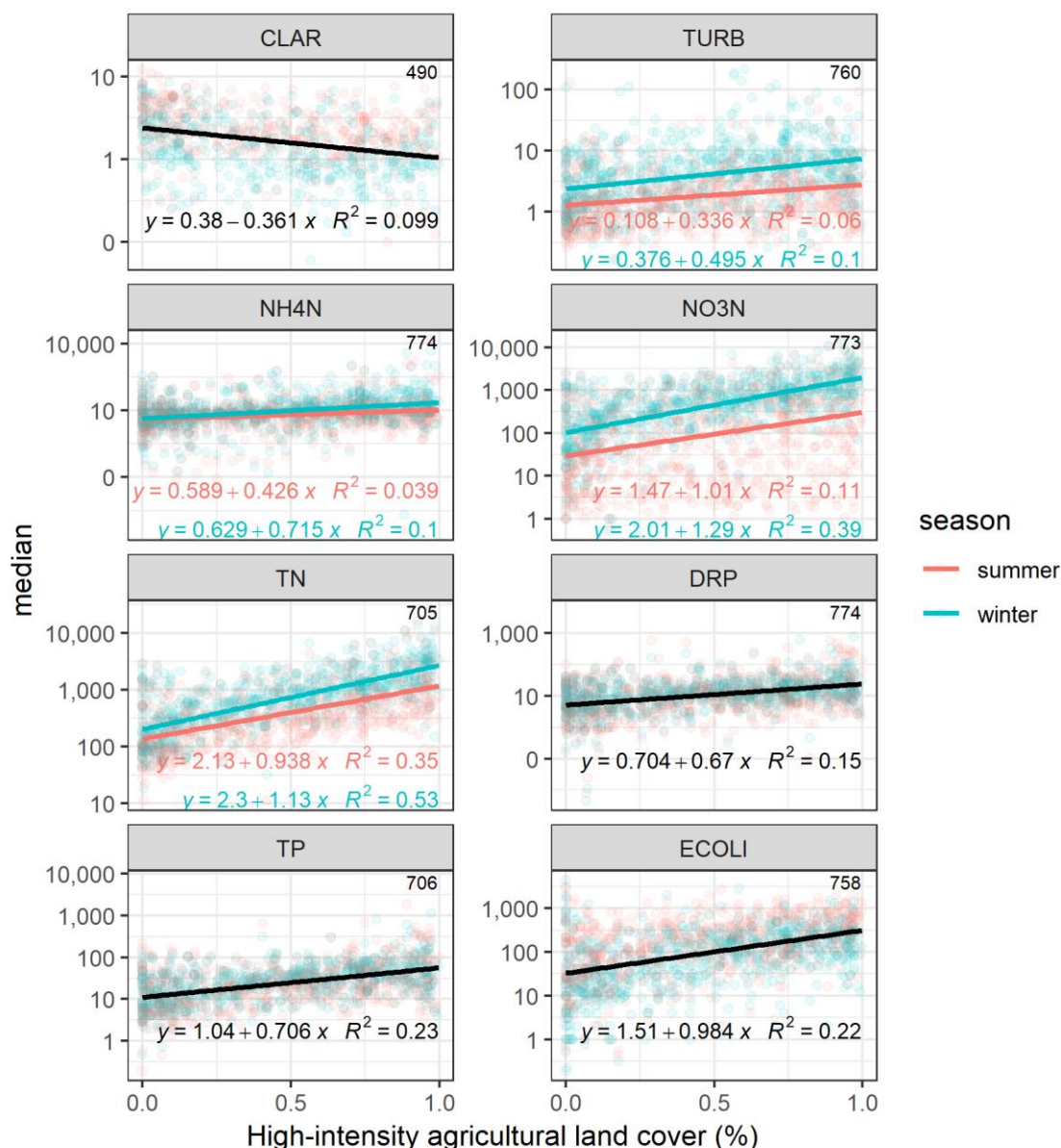


Figure 4-9: Relationships between median seasonal river water-quality and proportion of the upstream catchment with high-intensity agricultural land cover. Solid lines indicate least squares linear regression models, with black lines indicating no significant effect of season. The number of monitoring sites shown in the top corner of each panel. Note that the y-axes are on a \log_{10} scale.

4.3 Spatial models of summer and winter river water quality state

4.3.1 Model performance

The RF models for all water quality variables performed well, as indicated by the following statistics: $R^2 > 0.60$, $NSE > 0.60$, and $RMSD < 0.52$ for all models (Table 4-2). Bias in the RF models was low as indicated by the close match between the line representing the regression of the observed versus predicted values (red dashed line in Figure 4-10) and the one-to-one line (blue solid line in Figure 4-10). The close match between the regression and one to one line also indicates that the models are consistent (i.e. that low or high values are not under or over-estimated). Based on NSE values, models for TN, TP, DRP and ECOLI models had the best overall performance, the TURB and CLAR models had the worst overall performance, and the NH4N and NO3N models had intermediate performance.

Table 4-2: Performance of river water quality state random forest models. Performance was determined using independent predictions (i.e. sites that were not used in fitting the models) generated from the out-of-bag observations. Regression R^2 = coefficient of determination, NSE = Nash-Sutcliffe efficiency, RMSD = root mean square deviation). Units for RMSD and bias are the log10 transformed units of the respective water quality variables.

Water quality variable	N	Regression R^2	NSE	Bias	RMSD
CLAR	845	0.65	0.63	0.004	0.22
TURB	1470	0.65	0.63	-0.003	0.30
NH4N	1513	0.61	0.61	-0.005	0.33
NO3N	1511	0.68	0.67	0.002	0.51
TN	1382	0.81	0.80	-0.002	0.23
DRP	1513	0.77	0.76	-0.002	0.25
TP	1385	0.80	0.80	-0.001	0.21
ECOLI	1480	0.73	0.72	-0.003	0.35

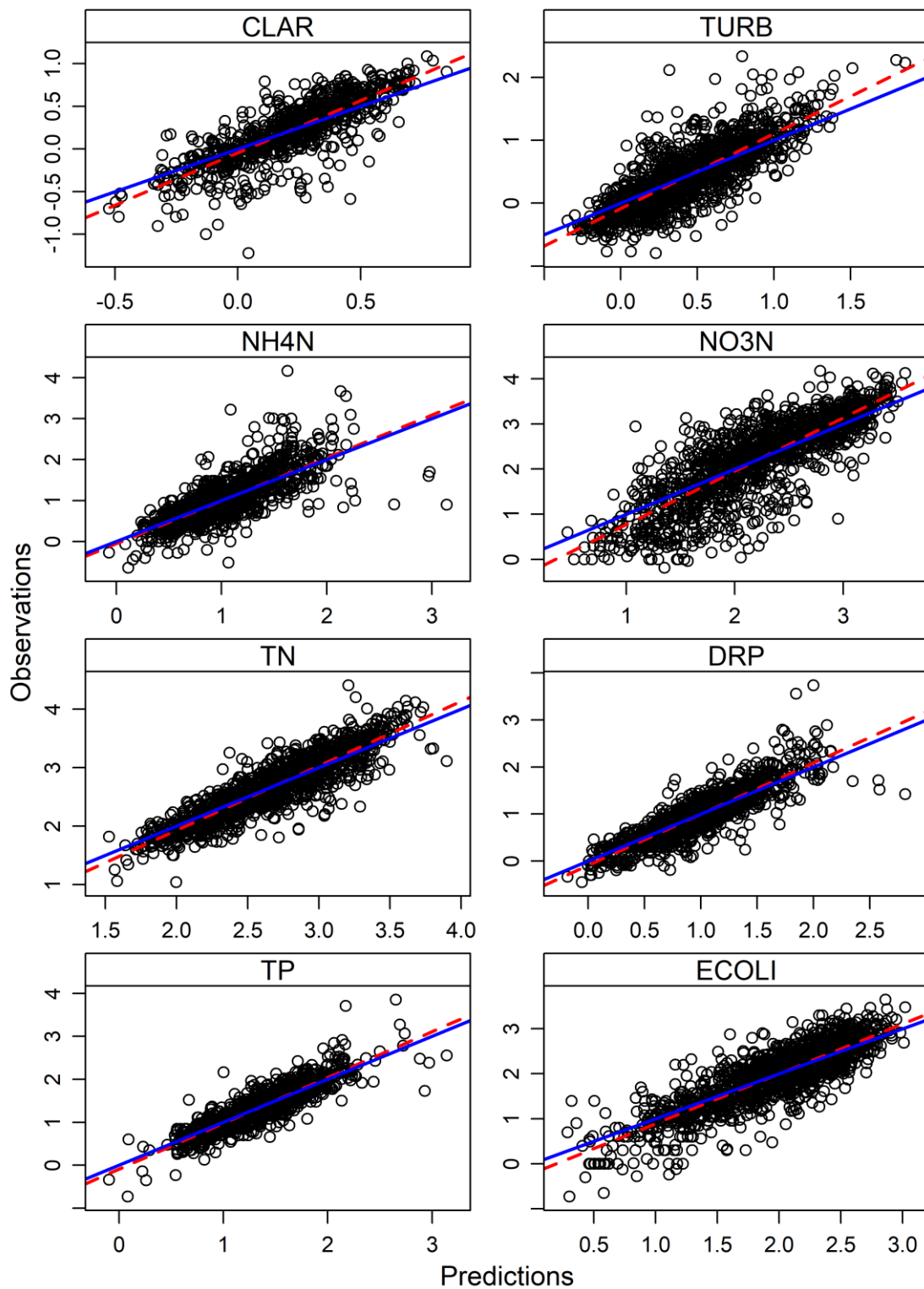


Figure 4-10: Comparison of observed river water quality versus values predicted by the random forest models. Note that the observed values are plotted on the Y-axis and predicted values on the X-axis, following Piñeiro et al. (2008). Solid lines: best fit linear regression of the observed and predicted values. Black dashed line: one-to-one line. Units are the \log_{10} transformed units of all water quality variables

4.3.2 Modelled relationships

The predictor variables with high importance in all RF models reflected strong associations between water quality and landcover and catchment topography, with season retained in the final random forest model for all variables (Table 4-3). Overall, season was the 8th most important predictor of river water quality (based on the median importance rank across all models) and the most important predictor for CLAR, TURB and NO₃N. However, season was the least important predictor for DRP, TP and NH₄N. Estimated median TURB, NH₄N, NO₃N, TN, DRP and TP concentrations were higher and CLAR lower in winter than in summer, while ECOLI concentration was higher in summer (Figure 4-11). This pattern of higher summer ECOLI is consistent with previous findings (Muirhead and Meenken, 2018; Snelder et al., 2016) and may be due to lower summer flows or increased microbial growth during periods of elevated water temperature. High winter nutrient and TURB, and low CLAR, values are likely linked with increased winter rainfall and runoff, particularly in areas dominated by agriculture.

The predictors usSlope and usElev, which represent the mean slope and mean elevation of the catchment, had the 1st and 7th highest overall importance ranks (Table 4-3). The partial plots indicated that CLAR increased with increasing values of usSlope and usElev and the values of all other water quality variables decreased (Figure 4-12). The predictor distToCoast was the 12th most important predictor, being retained in models of TURB, NH₄N, DRP and TP.

The predictors usRain and usRainvar were the 2nd and 5th most important overall predictors of the water quality variables (Table 4-3). CLAR increased with increasing usRainvar and usRain, while the values of all other water quality variables decreased (Figure 4-12). These results suggest that there is a moderately strong positive association between water quality and catchment rainfall. The mechanisms that drive this association may include solute dilution and sustained low water temperatures.

Landcover variables describing the proportion of the upstream catchment that is occupied by urban landcover (usUrban) and intensive agriculture (usIntensiveAg) were ranked 3rd and 4th, respectively (Table 4-3). The partial plots indicated that CLAR decreased with increasing values of usIntensiveAg, while the values of all other water quality variables increased (Figure 4-12). Predicted ECOLI and nutrient concentrations increased with increasing values of usUrban. These associations are consistent with observations of negative correlations between intensive agriculture, urban landcover and water quality state (e.g., Larned et al., 2016a; Unwin et al., 2010; Whitehead, 2018).

Upstream particle size (usPsize) and phosphorus (usPhos) were the 6th and 8th most important overall predictors, respectively (Table 4-3). These predictors indicate that the regolith of the catchment is associated with water quality state. Water quality decreased with increasing values of usPsize and increased with increasing usPhos (Figure 4-12). These patterns suggest that water quality generally declines as regolith fertility increases.

A predictor describing local summer temperature (segTwarm) was also important, ranking 11th (Table 4-3). NO₃N, TP and ECOLI increased with increasing temperature, while CLAR declined at high temperatures (Figure 4-12). Temperature may influence water quality by altering rates of nutrient cycling and microbial and periphyton growth.

Table 4-3: Rank order of importance of predictor variables retained in the river random forest models for at least one water quality variable. Blank cells indicate that the predictor was not included in the reduced model. The predictor variables in the first column are listed in descending order of the median of the rank importance over all eight models, with season indicated in bold.

predictor	CLAR	TURB	NH4N	NO3N	TN	DRP	TP	ECOLI
usSlope	9	22	4	3	2	1	1	10
usRain	4	4	27	-	-	3	4	-
usUrban	-	-	1	4	5	19	25	4
usIntensiveAg	8	6	3	2	1	25	6	2
usRainvar	2	2	5	19	10	5	8	3
usPsize	-	7	9	5	-	2	7	-
usElev	3	21	2	11	3	17	14	1
usPhos	5	18	6	7	8	18	26	6
season	1	1	33	1	4	33	33	12
usBare	6	5	29	17	-	14	3	9
segTwarm	10	3	15	10	7	28	30	-
distToCoast	-	8	10	-	-	10	13	-
usExoticForest	-	-	19	16	6	6	9	11
usHard	-	11	11	22	-	7	2	-
usWetland	-	-	20	13	9	4	18	5
usNativeForest	-	9	8	20	11	23	11	8
segTmin	-	12	13	6	12	13	10	-
usScrub	-	-	18	8	13	16	12	-
usPET	13	10	21	14	15	11	17	7
distToHead	16	13	7	-	-	21	15	13
usRainDays20	7	14	30	-	-	12	20	-
meanFlow	12	15	14	-	-	20	23	15
segElev	15	-	12	23	-	31	16	14
usTmin	-	16	26	15	16	9	27	-
usArea	14	17	16	-	-	30	24	16
usRainDays10	11	19	28	18	-	8	19	-
segSlope	-	-	17	9	-	29	22	-
usTwarm	-	20	23	12	-	26	21	-
usPastoralLight	-	-	22	21	-	15	28	-
sinuosity	-	-	25	-	-	22	5	-
usRainDays100	-	23	31	-	14	24	32	-
usCalc	-	-	24	-	-	32	29	-
usLakePerc	-	-	32	-	-	27	31	-

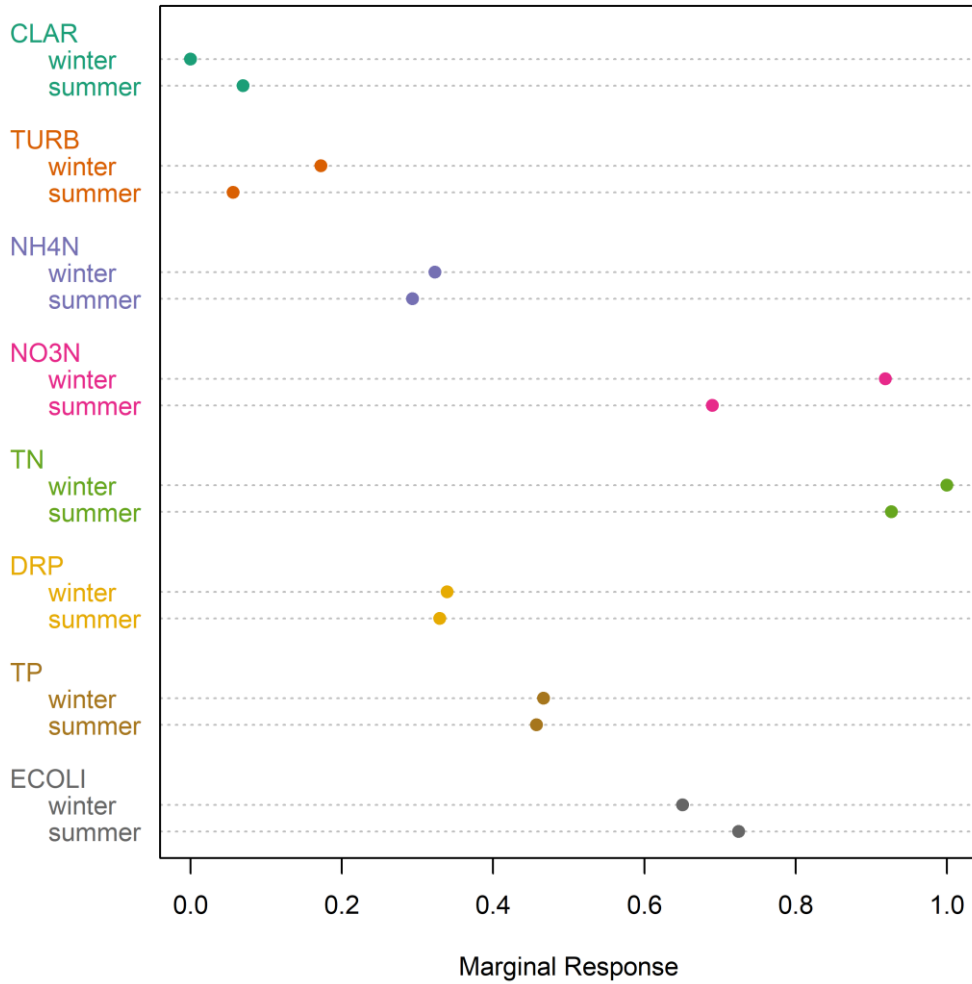


Figure 4-11: Partial plot for the predictor variable season in random forest models of water quality. The X-axis scale shows the standardised value of the marginal response for each of the eight modelled variables. Note that season was not included in the final model for NH4N.

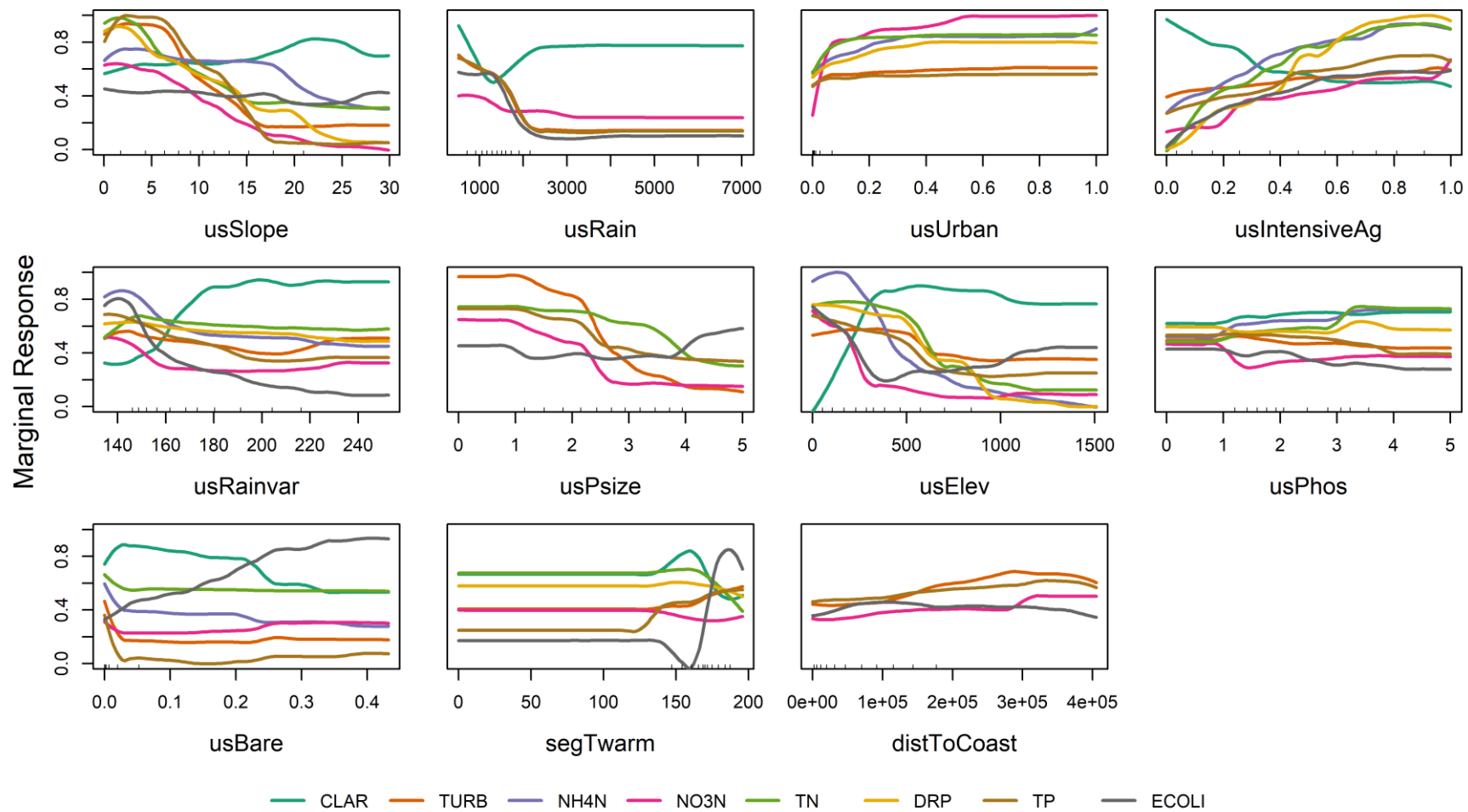


Figure 4-12: Partial plots for 11 of the 12 most important predictor variables in random forest models of river water quality. Each panel corresponds to one predictor. The Y-axis scales: standardised value of the marginal response for each of the eight modelled variables. In each case, the original marginal responses over all eleven predictors were standardised to have a range between zero and one. Plot amplitude (the range of the marginal response on the Y-axis) is directly related to a predictor variable's importance; amplitude is large for predictor variables with high importance. The partial plot of season is shown in Figure 4-11.

4.3.3 Model predictions

The minimum values predicted by the RF models were always somewhat larger than the minimum of the observed values and the maximum predicted values were always somewhat smaller than the maximum observed values (Table 4-4). This is an expected outcome of RF models, which are based on partitioned data with predictions derived from the means of observations that are assigned to a particular partition. Therefore, the predictions for each water quality variable were always within the range of the observations.

Table 4-4: Comparisons of the minimum and maximum observed and predicted median values of seasonal river water quality. Observed and predicted values are based on combined summer and winter data.

Variable and unit	Minimum observed value	Maximum observed value	Minimum predicted value	Maximum predicted value
CLAR (m)	0.06	12	0.22	9
TURB (NTU)	0.16	215	0.33	111
NH4N (mg m ⁻³)	0.23	14760	0.66	511
NO3N (mg m ⁻³)	0.65	15000	1.90	8816
TN (mg m ⁻³)	11.00	25600	21.33	8970
NO3N (mg m ⁻³)	0.36	5450	0.56	357
TP (mg m ⁻³)	0.19	7108	0.53	1095
ECOLI (cfu 100ml)	0.19	4400	0.78	2171

Overall, the predicted spatial patterns of river water quality were similar to those predicted in Whitehead (2018), with relatively high nutrient concentrations, TURB and ECOLI in low-elevation areas on the east coasts of the North and South Island, and in the inland Waikato, Wairarapa Valley, Rangitikei-Manawatu coastal plain, Taranaki Ring Plain, and Auckland Region (Figure 4-13 to Figure 4-20). In contrast, predicted nutrient, TURB and ECOLI concentrations are generally low in major mountain ranges, in large areas of the Department of Conservation estate, and in smaller, native forest-dominated areas of Northland and the Coromandel Peninsula. Predicted median clarity typically showed the opposite pattern to the other variables. See Whitehead (2018) for more detail about these broad spatial patterns and their potential drivers.

While the spatial patterns in the seasonal RF models were similar to those of Whitehead (2018), we also observed strong seasonal patterns in the spatial predictions for most water quality variables. Clarity was predicted to be lower and turbidity higher during the winter months throughout most of the North and South Islands, with the exception of parts of Westland, the Southern Alps and central Otago (Figure 4-13 and Figure 4-14). Higher winter values of NH4N, NO3N and TN were predicted throughout Southland, eastern Otago and Canterbury, as well as most of the North Island (Figure 4-15 to Figure 4-17). In contrast, ECOLI was predicted to be higher in the summer months in almost all regions, with the exception of some larger mainstem rivers in Southland and throughout the North Island (Figure 4-20). This pattern of higher summer ECOLI values is consistent with previous studies (Muirhead and Meenken, 2018; Snelder et al., 2016) but may be contrary to perceptions that ECOLI concentrations are typically higher during winter because runoff and river flows are higher. DRP and TP showed minimal variation between predictions of summer and winter median values

(Figure 4-18 and Figure 4-19), likely driven by the low importance rank of season in these models. However, there were concentrations were predicted to be elevated in winter along the east coast of the North Island and in parts of Manawatu and Taranaki.

Note that the maps in Figure 4-13 to Figure 4-20 consist of nzsegments of Order 3 and above, and some extensive lowland areas are dominated by low order streams (e.g., eastern Auckland, Tauranga). Steep coastal areas of the Marlborough Sounds, Fiordland, Coromandel and Banks Peninsulas and offshore islands are also dominated by low order streams. The predicted water quality in low order streams in these areas is not shown on the maps in Figure 4-13 to Figure 4-20.

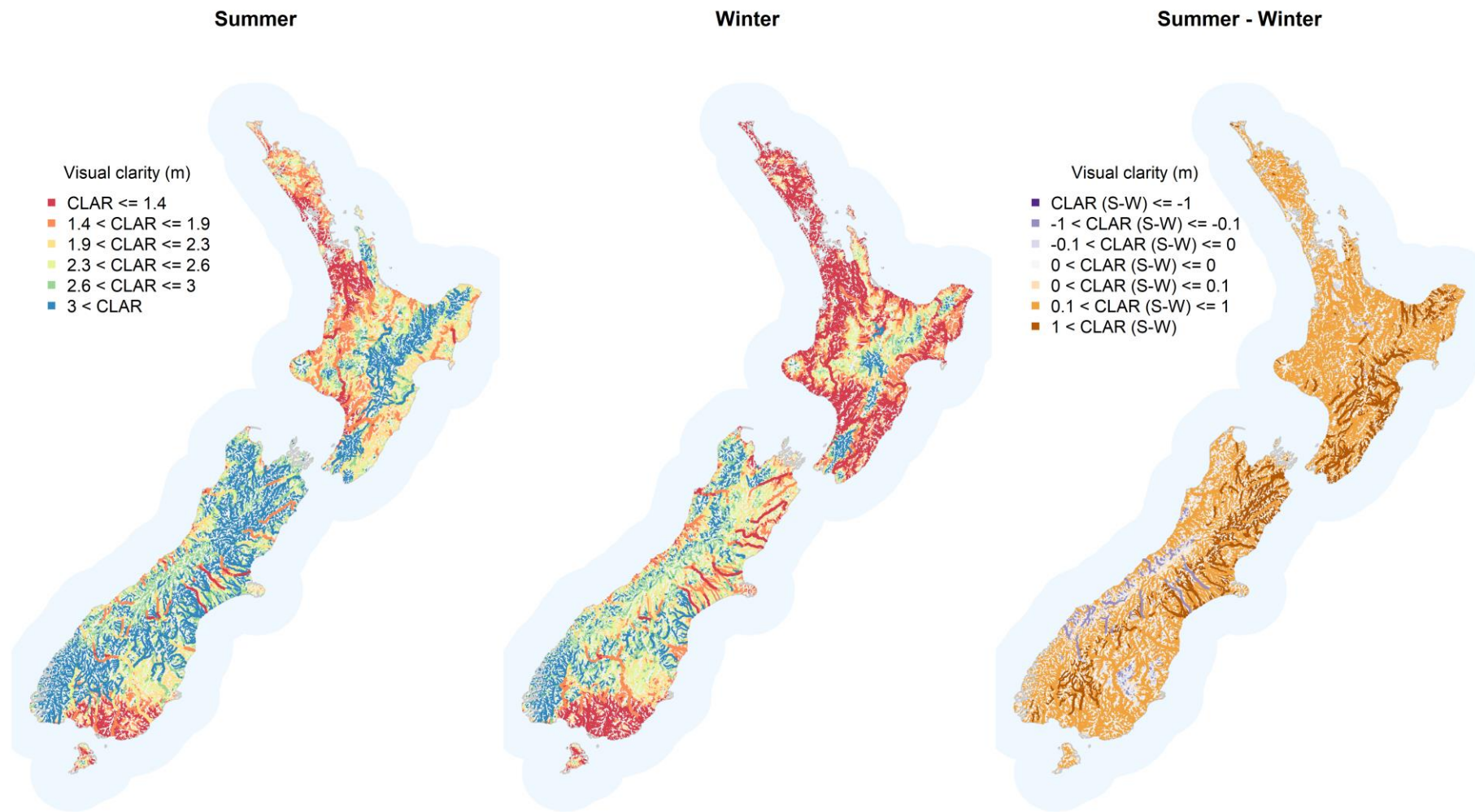


Figure 4-13: Predicted seasonal median visual clarity in New Zealand rivers. The first two panels show predicted summer and winter medians, respectively, while the third panel shows the difference between summer and winter (orange represents lower winter clarity; purple represents higher winter clarity). Maps show all nzsegments of Order 3 and higher. Smaller rivers are omitted to make river networks distinguishable.

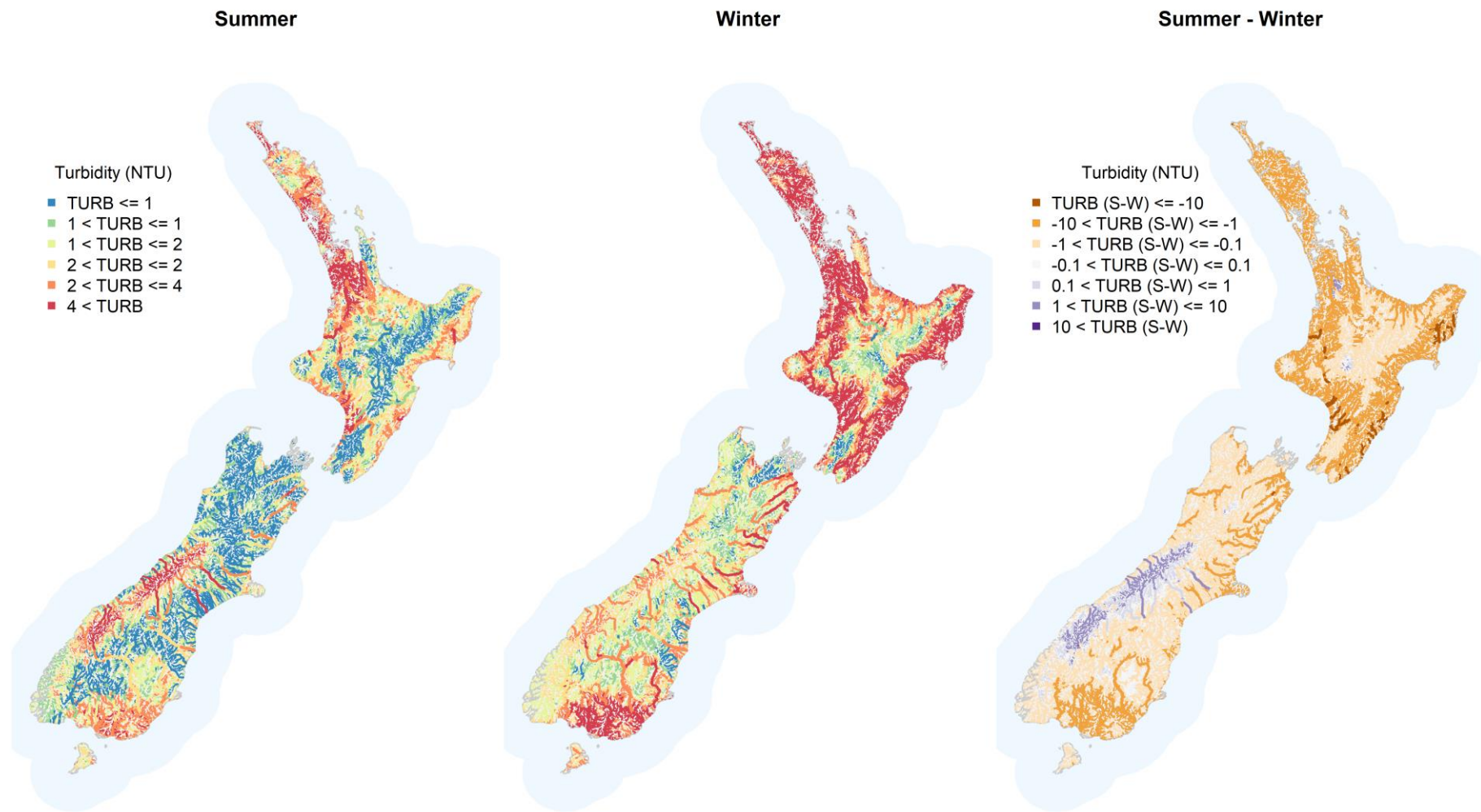


Figure 4-14: Predicted seasonal median turbidity in New Zealand rivers. The first two panels show predicted summer and winter medians, respectively, while the third panel shows the difference between summer and winter (orange represents higher winter turbidity; purple represents lower winter turbidity). Maps show all nzssegments of Order 3 and higher. Smaller rivers are omitted to make river networks distinguishable.

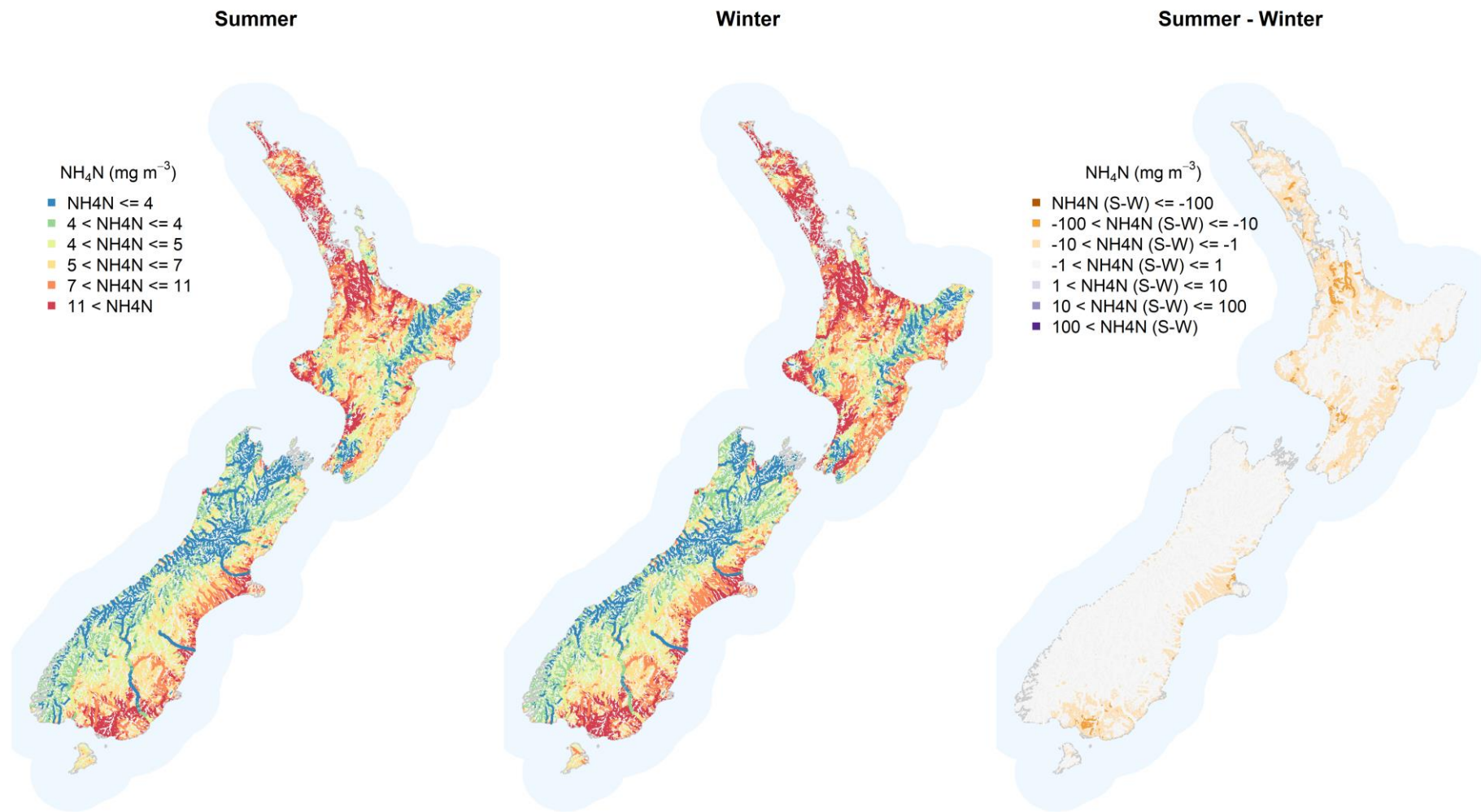


Figure 4-15: Predicted median NH₄N in New Zealand rivers. The first two panels show predicted summer and winter medians, respectively, while the third panel shows the difference between summer and winter (orange represents higher winter turbidity; purple represents lower winter turbidity). Maps show all nzsegments of Order 3 and higher. Smaller rivers are omitted to make river networks distinguishable.

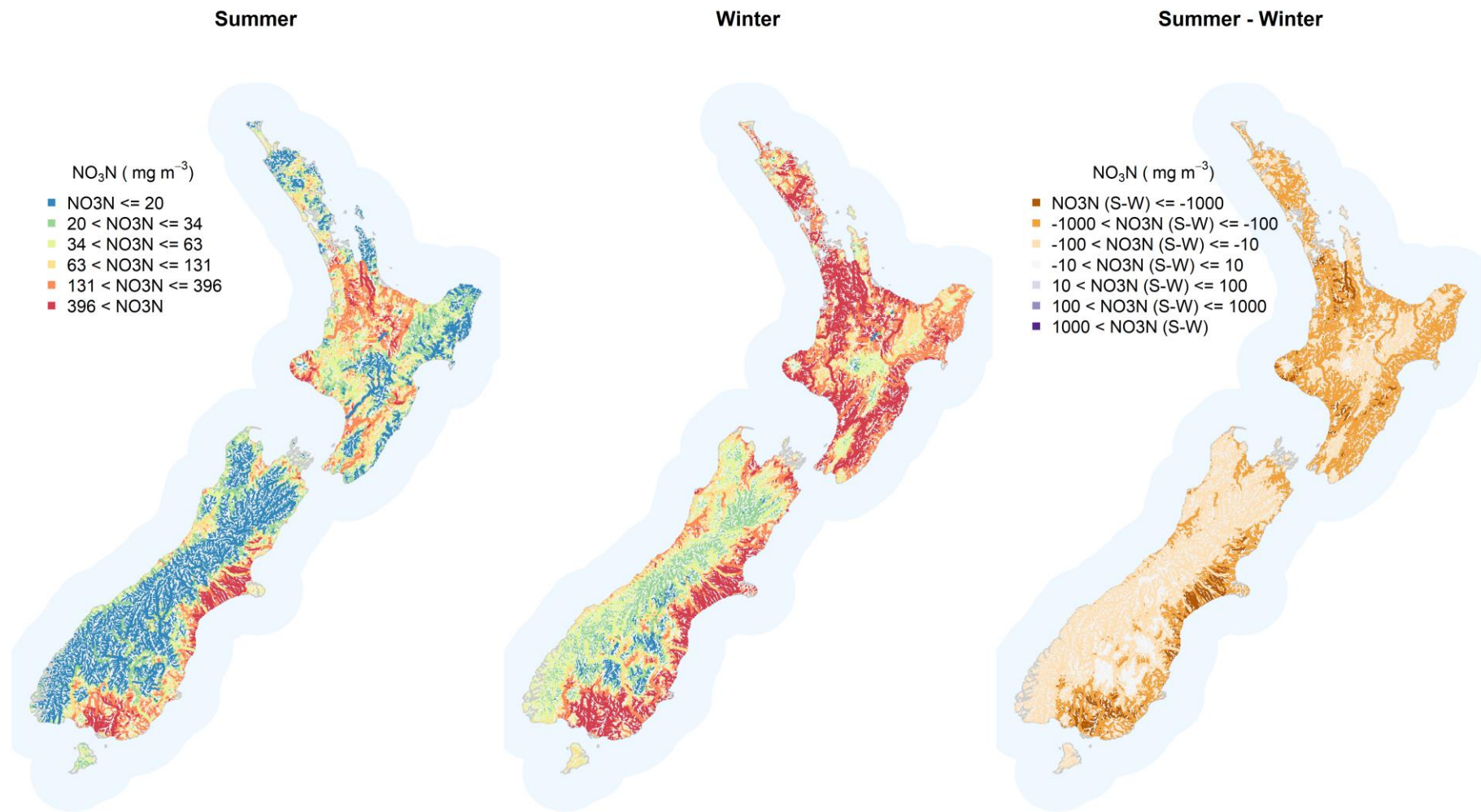


Figure 4-16: Predicted seasonal median NO₃N in New Zealand rivers. The first two panels show predicted summer and winter medians, respectively, while the third panel shows the difference between summer and winter (orange represents higher winter concentrations; purple represents lower winter concentrations). Maps show all nzsegments of Order 3 and higher. Smaller rivers are omitted to make river networks distinguishable.

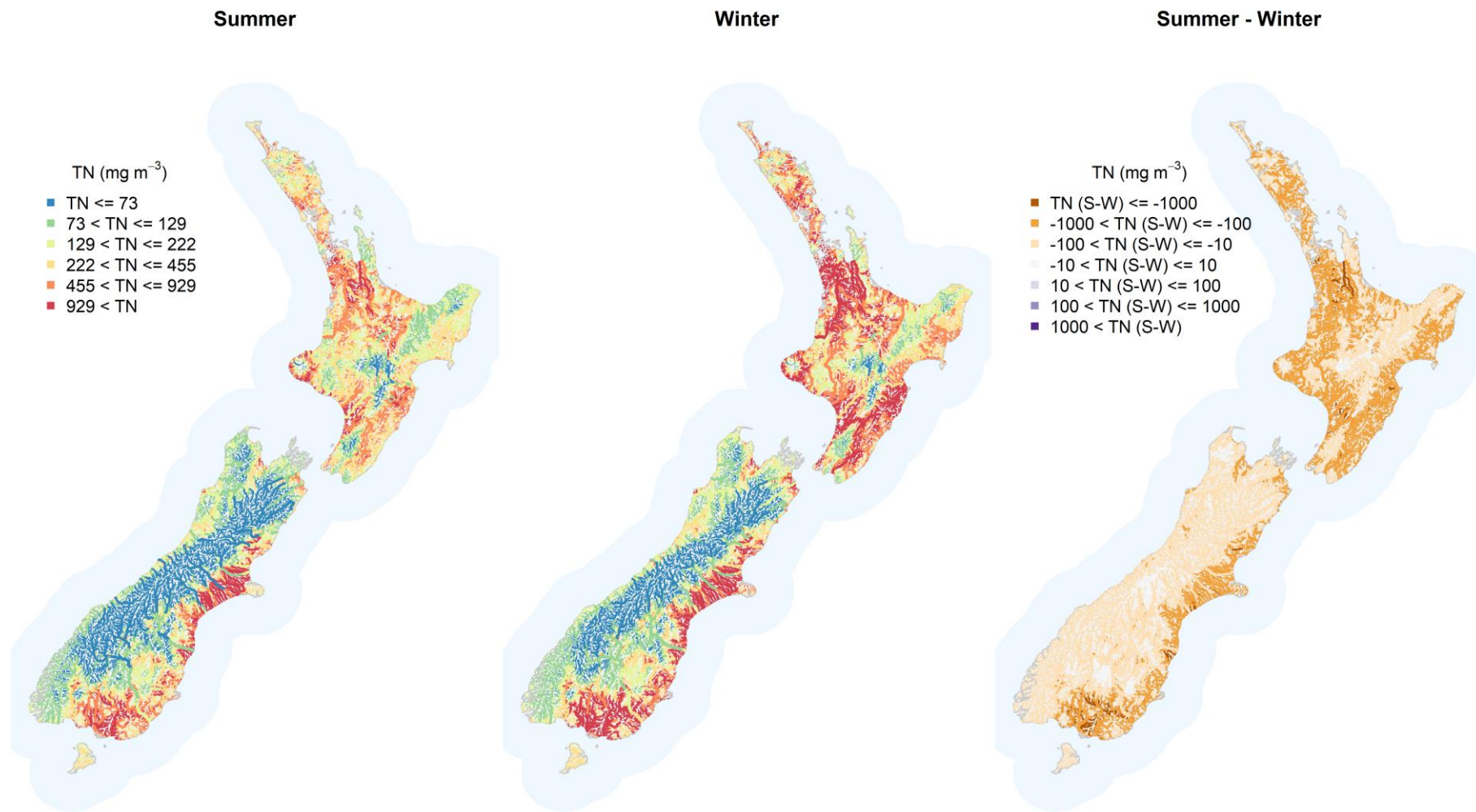


Figure 4-17: Predicted seasonal median TN in New Zealand rivers. The first two panels show predicted summer and winter medians, respectively, while the third panel shows the difference between summer and winter (orange represents higher winter concentrations; purple represents lower winter concentrations). Maps show all nzsegments of Order 3 and higher. Smaller rivers are omitted to make river networks distinguishable.

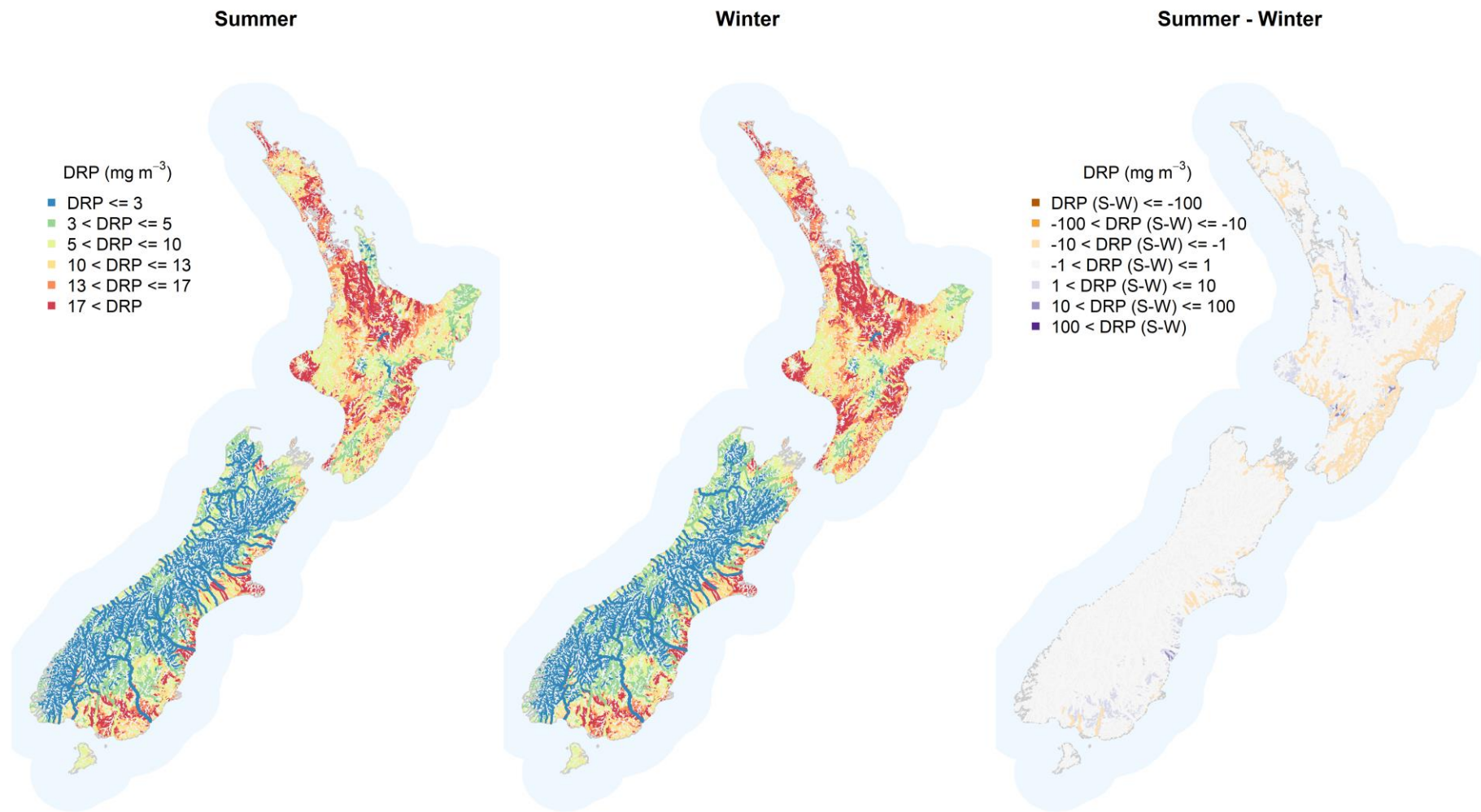


Figure 4-18: Predicted seasonal median DRP in New Zealand rivers. The first two panels show predicted summer and winter medians, respectively, while the third panel shows the difference between summer and winter (orange represents higher winter concentrations; purple represents lower winter concentrations). Maps show all nzsegments of Order 3 and higher. Smaller rivers are omitted to make river networks distinguishable.

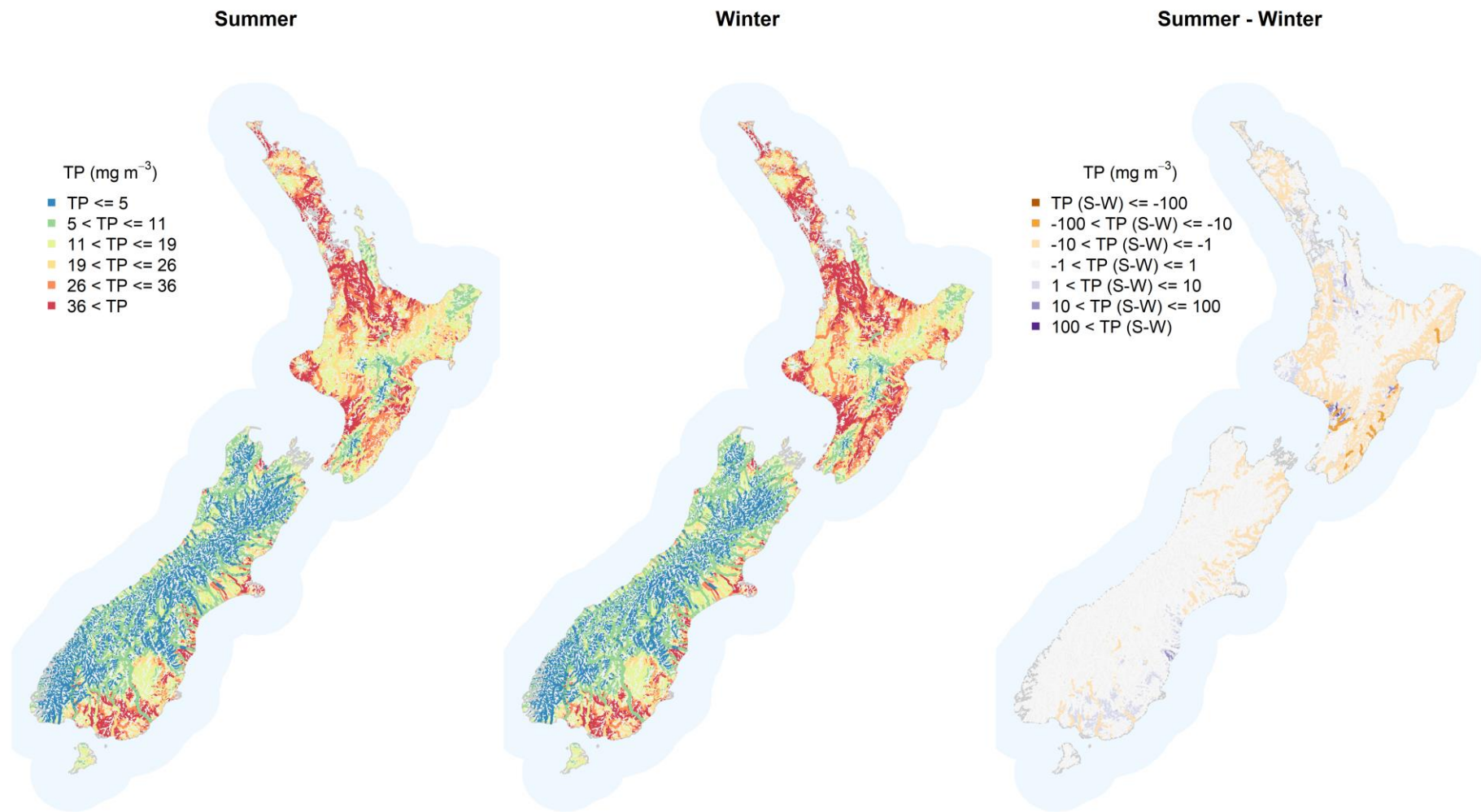


Figure 4-19: Predicted seasonal median TP in New Zealand rivers. The first two panels show predicted summer and winter medians, respectively, while the third panel shows the difference between summer and winter (orange higher winter concentrations; purple represents lower winter concentrations). Maps show all nzsegments of Order 3 and higher. Smaller rivers are omitted to make river networks distinguishable.

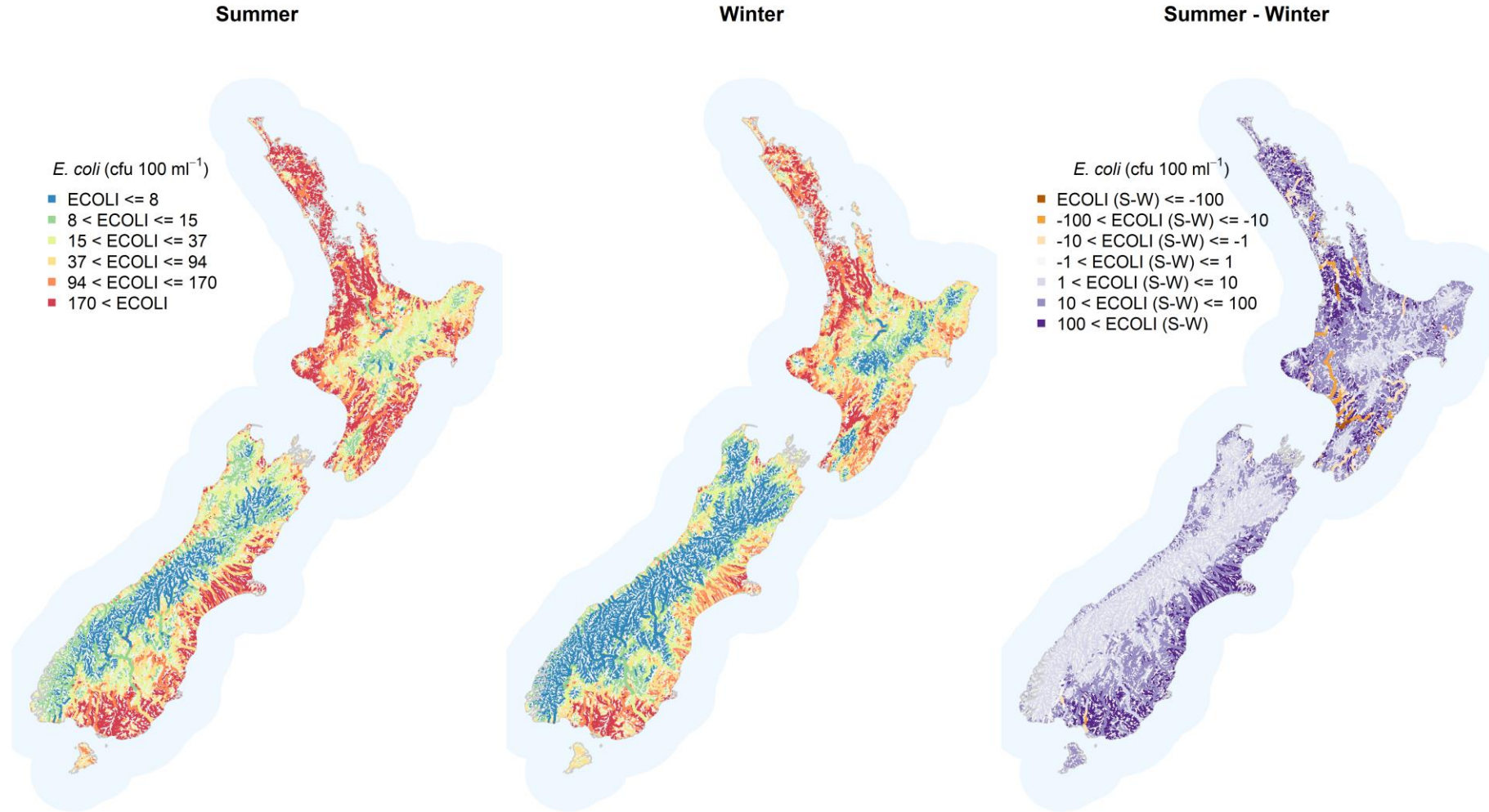


Figure 4-20: Predicted seasonal median ECOLI in New Zealand rivers. The first two panels show predicted summer and winter medians, respectively, while the third panel shows the difference between summer and winter (orange represents higher winter concentrations; purple represents lower winter concentrations). Maps show all nzsegments of Order 3 and higher. Smaller rivers are omitted to make river networks distinguishable.

5 Seasonal variation in lake water quality state

5.1 Comparison of summer and winter water quality state

The monitored lakes did not show any significant seasonal variation in water quality for most variables (Table 5-1). However, CHLA was statistically higher in high elevation lakes deeper than 50 m during the winter and NH₄N was higher during the winter in low elevation lakes between 5-15 m deep. Stratification in deeper lakes is likely to drive these seasonal patterns in CHLA due to differences in nutrient dynamics and algal biomass, with the breakdown of the thermocline in winter often bringing nutrient-rich water to the surface. In contrast, wind mixing throughout the water depth of shallow lakes prevents stratification. Higher winter concentrations of NH₄N are likely driven by reduced rates of nutrient uptake and denitrification in the winter.

Table 5-1: Seasonal differences between lake water quality variables in lakes in different elevation × depth classes. Cell values represent the number of lakes in each class with both summer and winter observations. Cells shaded blue indicate classes for which the median winter value for a given water quality variable is statistically higher in the winter than in the summer. Unshaded cells indicate either no significant difference between the seasons or insufficient data (< 5 samples), while blank cells represent landcover × climate combinations that did not exist in the data set. Boxplots showing these relationships are presented in Figure 5-1 to Figure 5-6.

Altitude	Depth	SECCHI	NH ₄ N	TN	TP	CHLA	TLI3	Total
0-300 m	0-5 m	14	16	20	20	19	19	20
	5-15 m	21	19	22	22	21	20	22
	15-50 m	9	10	12	11	12	10	12
	> 50 m	5	4	5	5	5	4	5
> 300 m	0-5 m							
	5-15 m							
	15-50 m	5	5	7	7	6	5	7
	> 50 m	4	6	5	6	6	4	7
Total		54	56	71	71	69	54	73

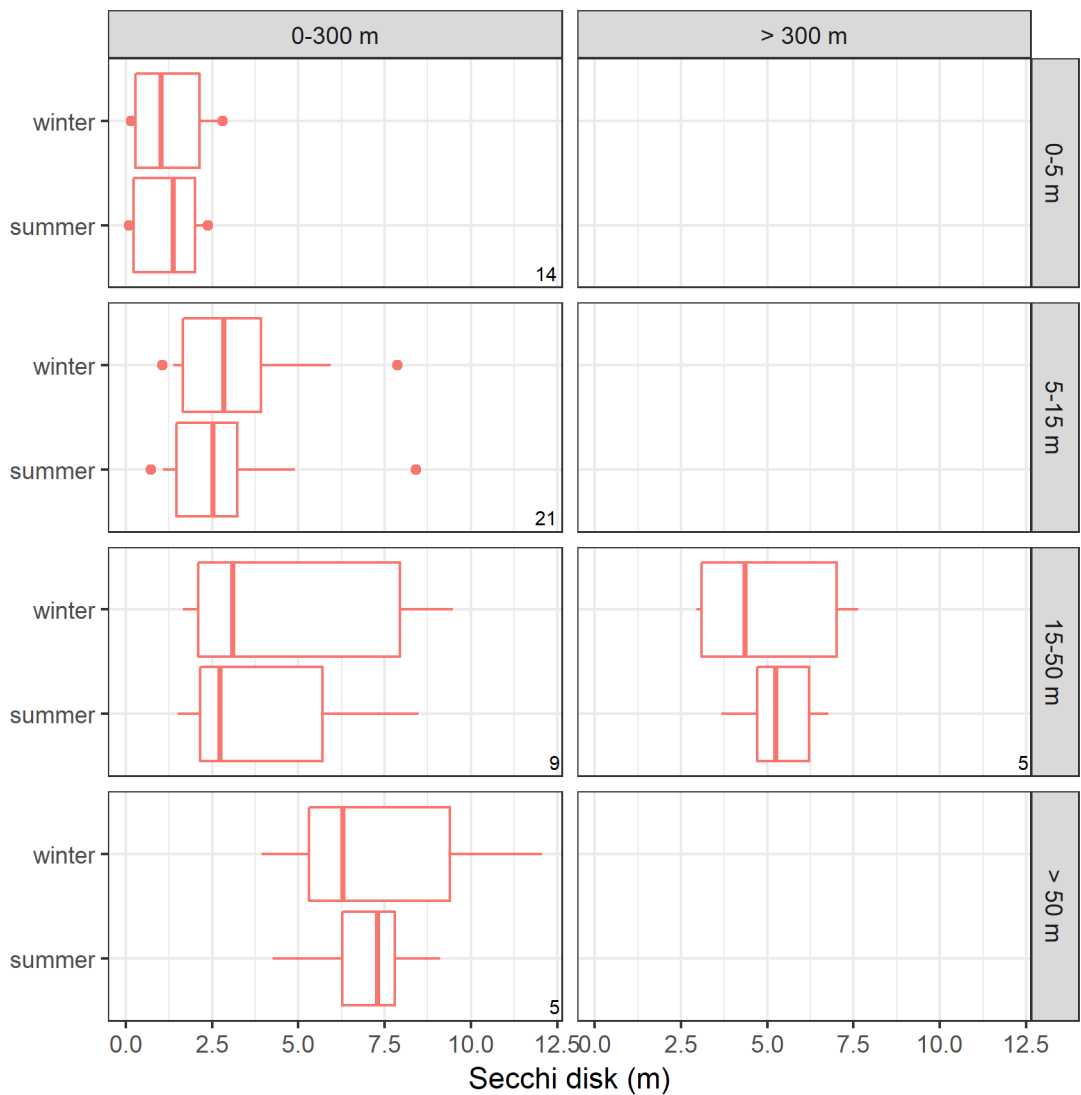


Figure 5-1: Seasonal patterns of SECCHI in lakes in different altitude and depth classes. Columns represent lakes with both summer and winter observations grouped by natural (N), exotic forest (EF), pastoral (P) and urban (U) landcover classes. The top row represents all sites irrespective of climate, while the remaining rows are sites grouped by climate classes within each landcover class. Blue boxplots indicate significant differences ($p < 0.05$) in seasonal state within a panel, while red boxplots within a panel are not significantly different. Percentiles: boxes = 25% and 75%; horizontal bars = medians; whiskers = 10% and 90%; closed circles = 5% and 95% (for classes with > 10 sites). Panel numbers indicate the number of lakes in each class, with classes with fewer than five lakes not shown.

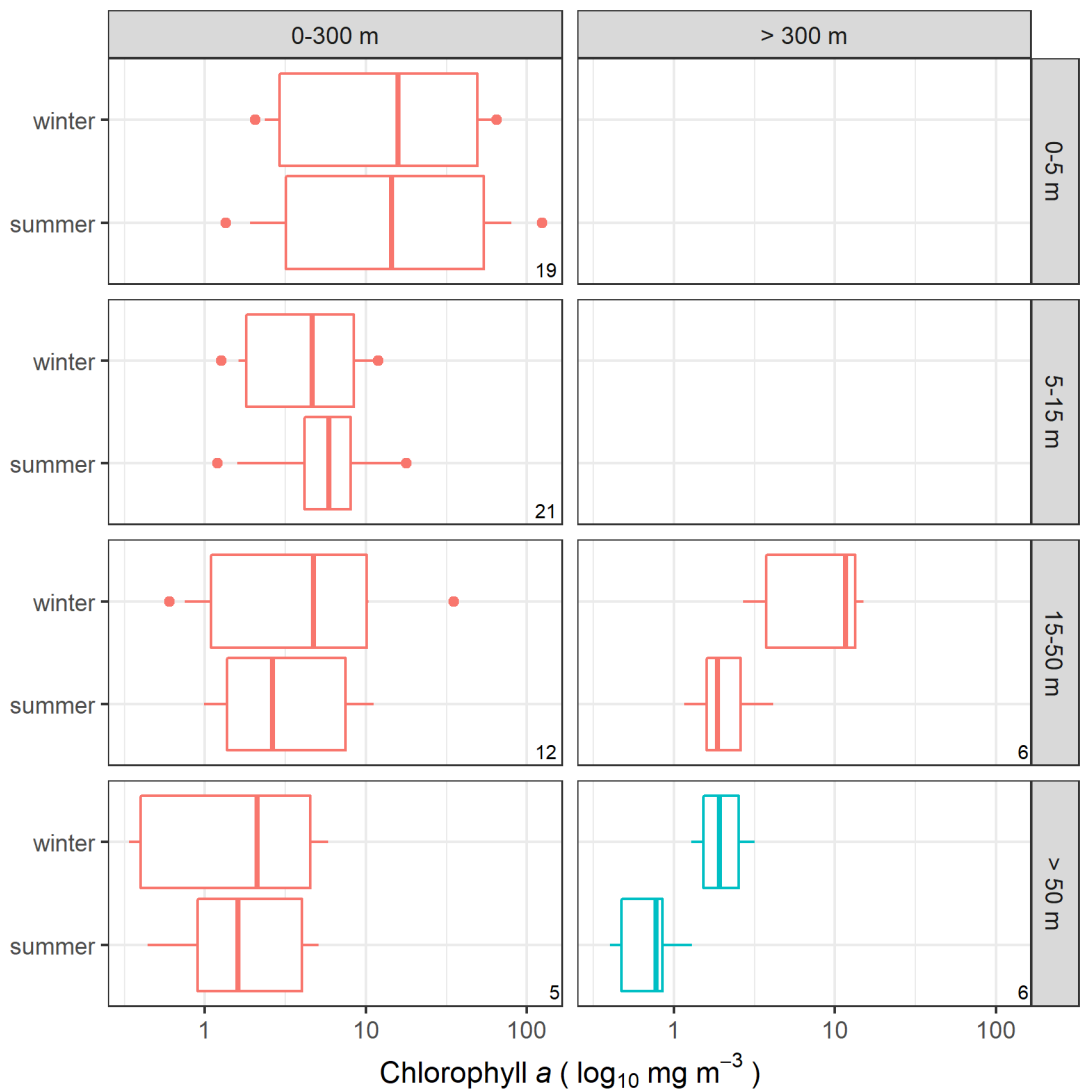


Figure 5-2: Seasonal patterns of CHLA in lakes in different altitude and depth classes. Columns and rows represent lakes with both summer and winter observations grouped by altitude and depth classes, respectively. Blue boxplots indicate significant differences ($p < 0.05$) in seasonal state within a panel, while red boxplots within a panel are not significantly different. Percentiles: boxes = 25% and 75%; horizontal bars = medians; whiskers = 10% and 90%; closed circles = 5% and 95% (for classes with > 10 sites). Panel numbers indicate the number of lakes in each class, with classes with fewer than five lakes not shown.

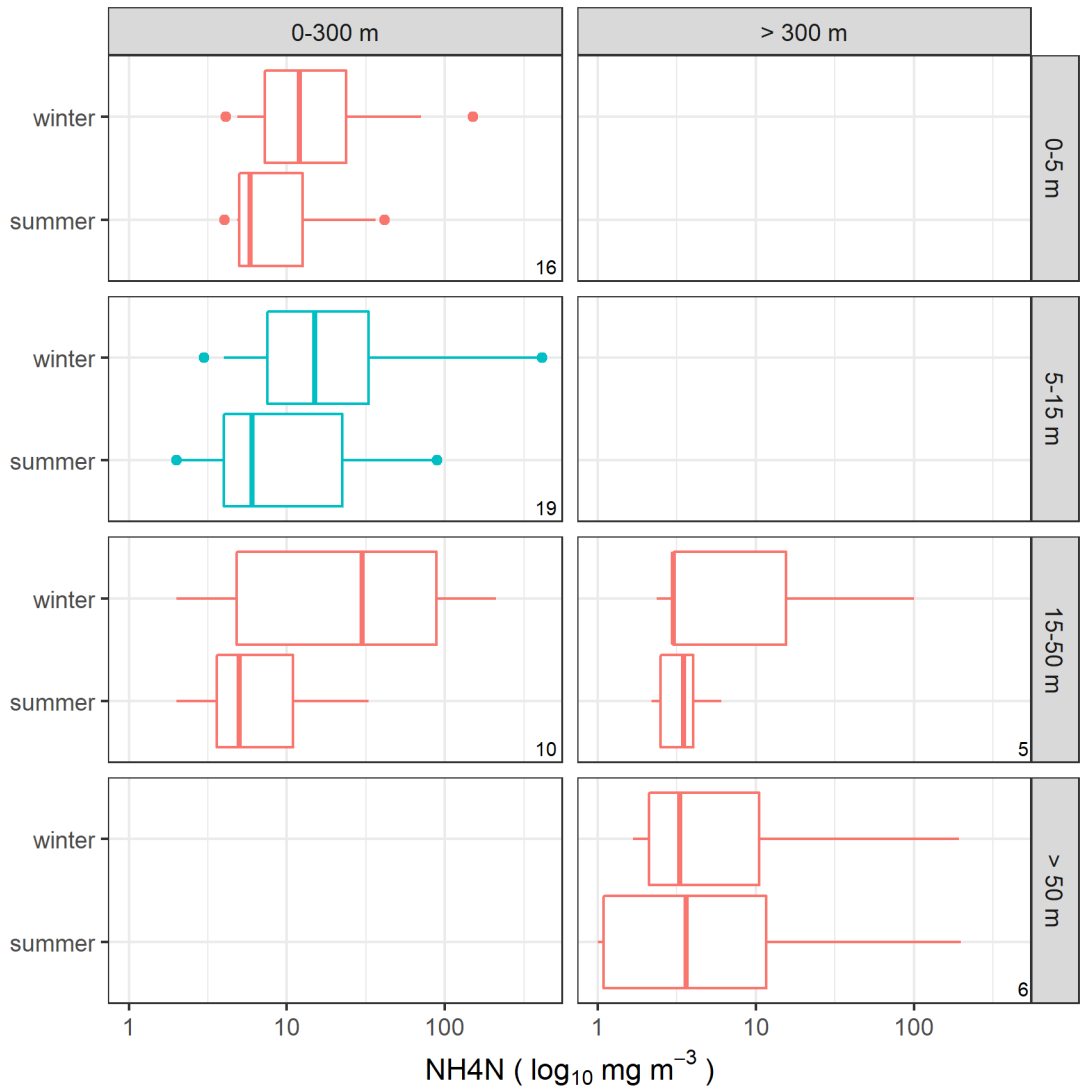


Figure 5-3: Seasonal patterns of NH₄N in lakes in different altitude and depth classes. Columns and rows represent lakes with both summer and winter observations grouped by altitude and depth classes, respectively. Blue boxplots indicate significant differences ($p < 0.05$) in seasonal state within a panel, while red boxplots within a panel are not significantly different. Percentiles: boxes = 25% and 75%; horizontal bars = medians; whiskers = 10% and 90%; closed circles = 5% and 95% (for classes with > 10 sites). Panel numbers indicate the number of lakes in each class, with classes with fewer than five lakes not shown.

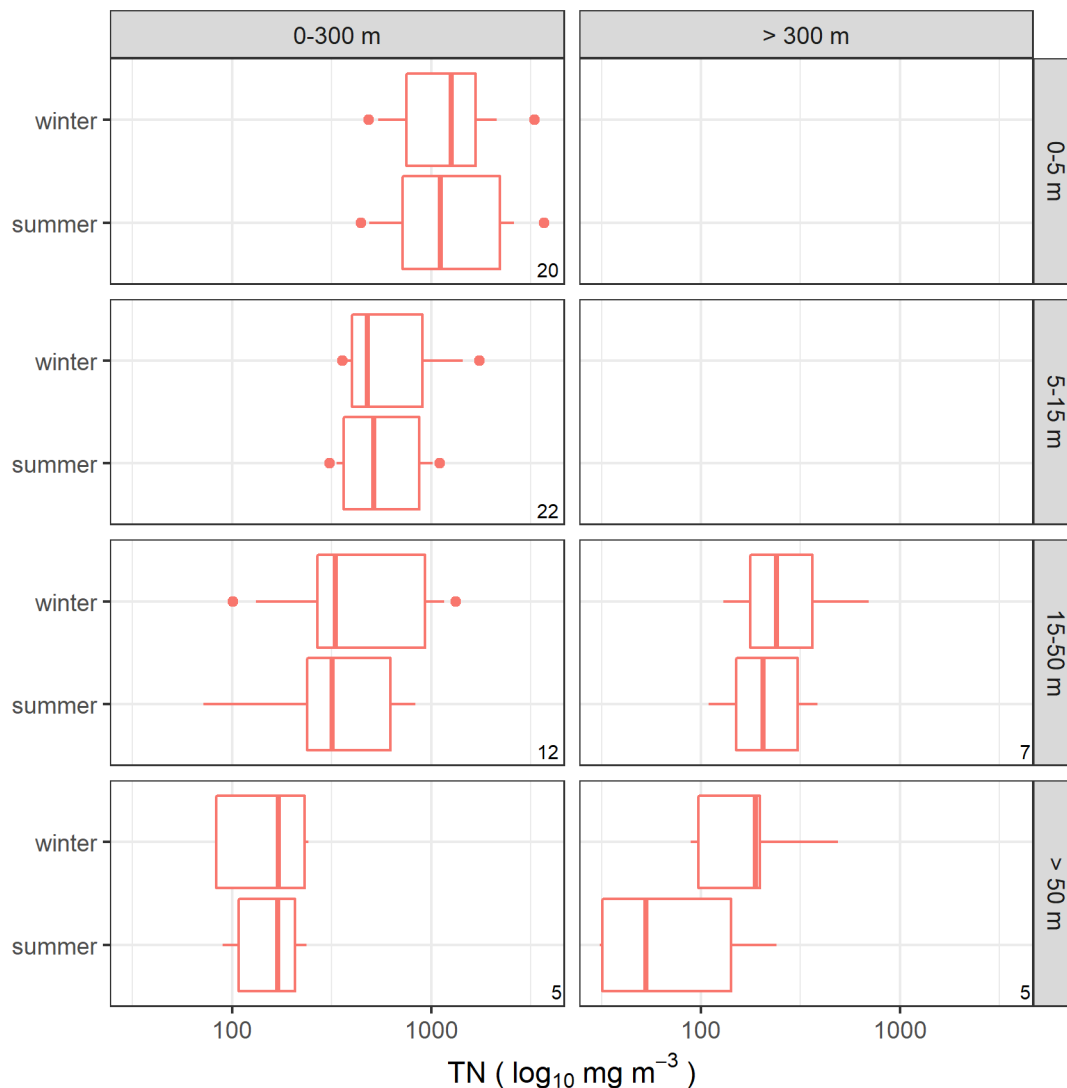


Figure 5-4: Seasonal patterns of TN in lakes in different altitude and depth classes. Columns and rows represent lakes with both summer and winter observations grouped by altitude and depth classes, respectively. Blue boxplots indicate significant differences ($p < 0.05$) in seasonal state within a panel, while red boxplots within a panel are not significantly different. Percentiles: boxes = 25% and 75%; horizontal bars = medians; whiskers = 10% and 90%; closed circles = 5% and 95% (for classes with > 10 sites). Panel numbers indicate the number of lakes in each class, with classes with fewer than five lakes not shown.

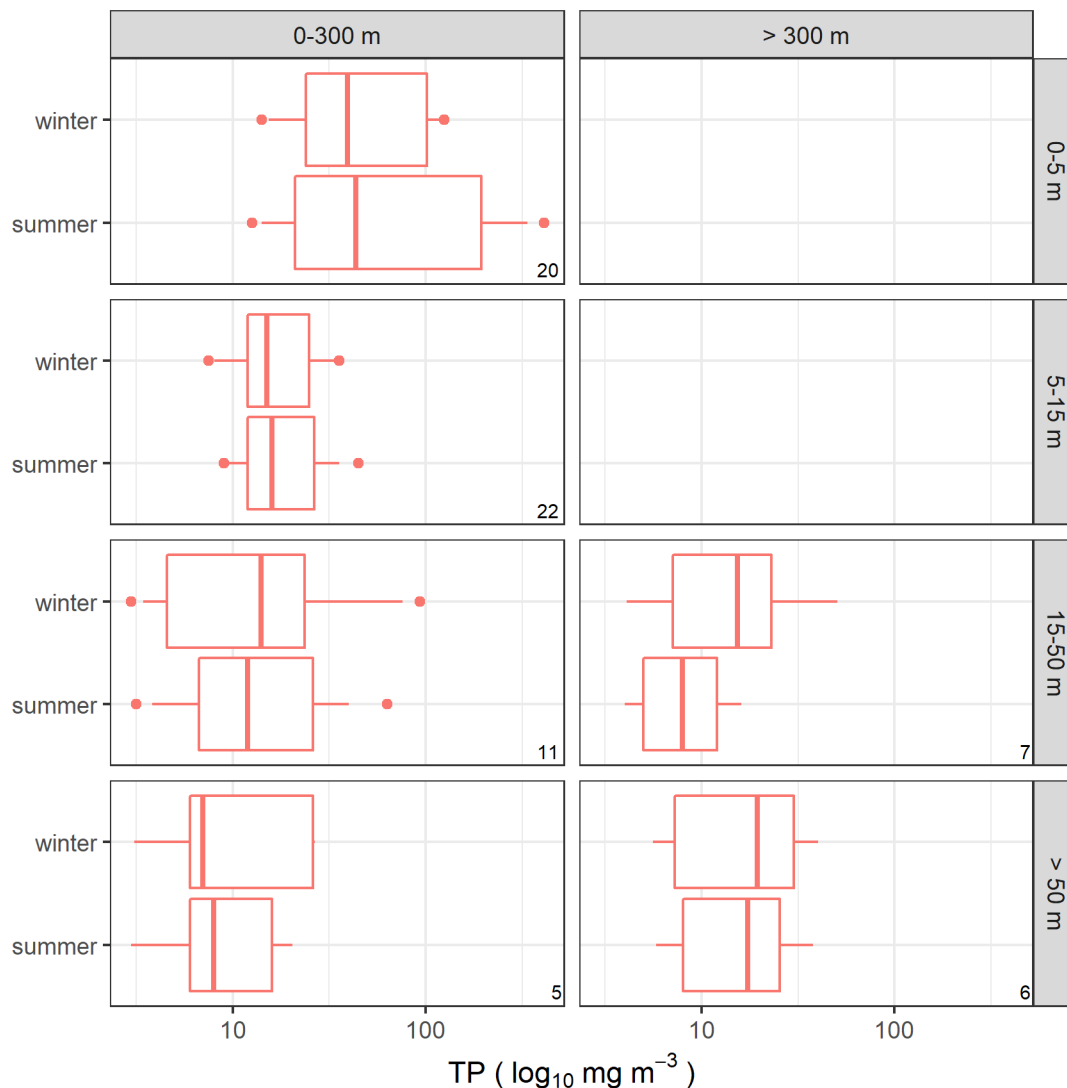


Figure 5-5: Seasonal patterns of TP in lakes in different altitude and depth classes. Columns and rows represent lakes with both summer and winter observations grouped by altitude and depth classes, respectively. Blue boxplots indicate significant differences ($p < 0.05$) in seasonal state within a panel, while red boxplots within a panel are not significantly different. Percentiles: boxes = 25% and 75%; horizontal bars = medians; whiskers = 10% and 90%; closed circles = 5% and 95% (for classes with > 10 sites). Panel numbers indicate the number of lakes in each class, with classes with fewer than lakes sites not shown.

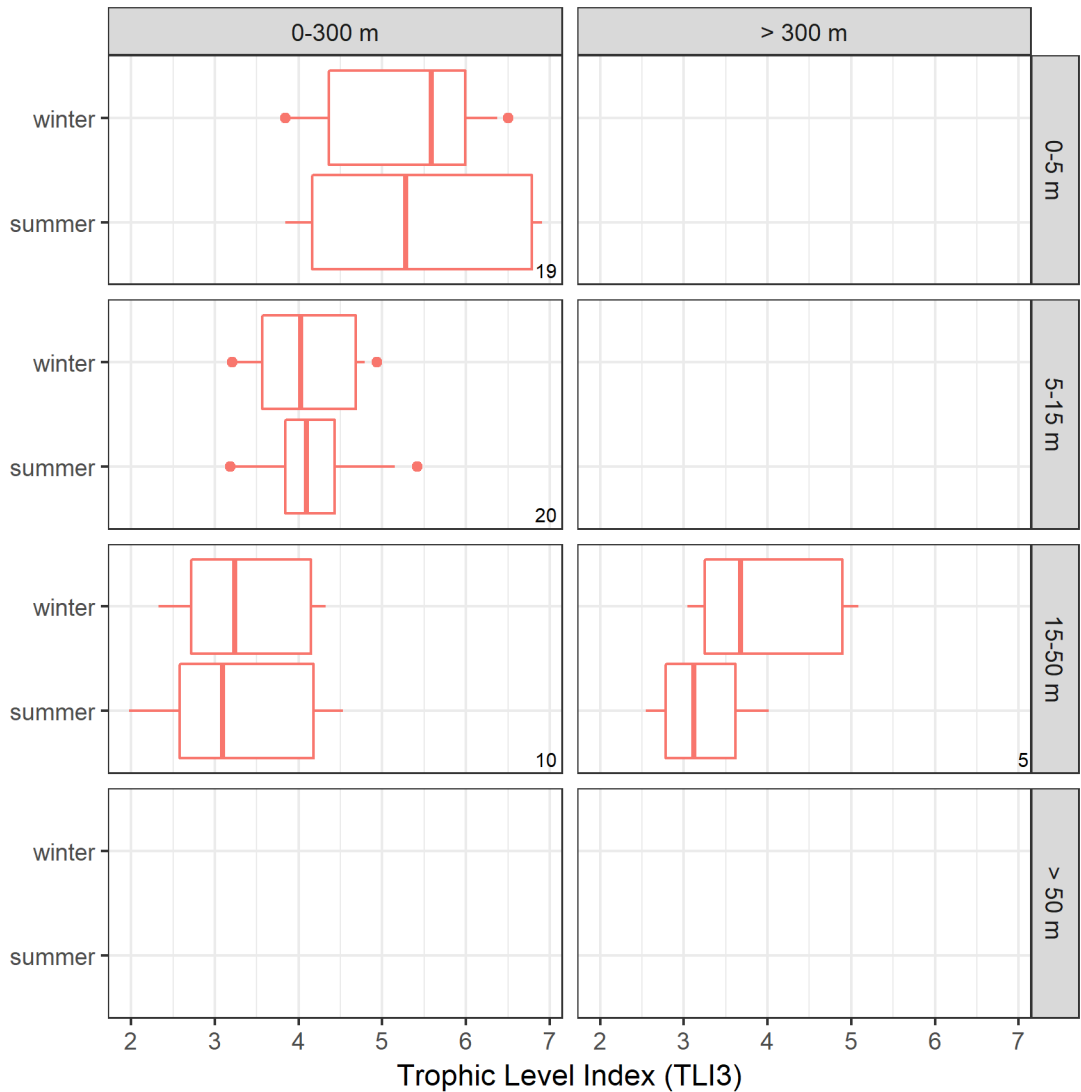


Figure 5-6: Seasonal patterns of TLI3 in lakes in different altitude and depth classes. Columns and rows represent lakes with both summer and winter observations grouped by altitude and depth classes, respectively. Blue boxplots indicate significant differences ($p < 0.05$) in seasonal state within a panel, while red boxplots within a panel are not significantly different. Percentiles: boxes = 25% and 75%; horizontal bars = medians; whiskers = 10% and 90%; closed circles = 5% and 95% (for classes with > 10 sites). Panel numbers indicate the number of lakes in each class, with classes with fewer than five lakes not shown.

5.2 Spatial models of summer and winter lake water quality state

5.2.1 Model Performance

The RF models for all water quality variables performed well, as indicated by the following statistics: $R^2 > 0.7$, $NSE > 0.7$, and $RMSD < 0.5$ for all models except NH4N (Table 5-2). Bias in the RF models was low as indicated by the close match between the line representing the regression of the observed versus predicted values (red dashed line in Figure 5-7) and the one-to-one line (blue solid line in Figure 5-7). The close match between the regression and one to one line also indicates that the models are consistent (i.e. that low or high values are not under or over-estimated). Based on NSE values, models for SECCHI, TN and TLI3 had the best overall performance, the NH4N model had the worst overall performance, and the TP and CHLA models had intermediate performance.

Table 5-2: Performance of lake water quality state random forest models. Performance was determined using independent predictions (i.e. sites that were not used in fitting the models) generated from the out-of-bag observations. Regression R^2 = coefficient of determination, NSE = Nash-Sutcliffe efficiency, RMSD = root mean square deviation). Units for RMSD and bias are the log10 transformed units of the respective water quality variables.

Water quality variable	N	Regression R^2	NSE	Bias	RMSD
SECCHI	120	0.87	0.86	-0.004	0.19
NH4N	124	0.35	0.34	0.006	0.57
TN	174	0.88	0.87	-0.002	0.16
TP	173	0.80	0.79	-0.003	0.22
CHLA	178	0.71	0.71	-0.005	0.33
TLI3	151	0.83	0.81	-0.002	0.06

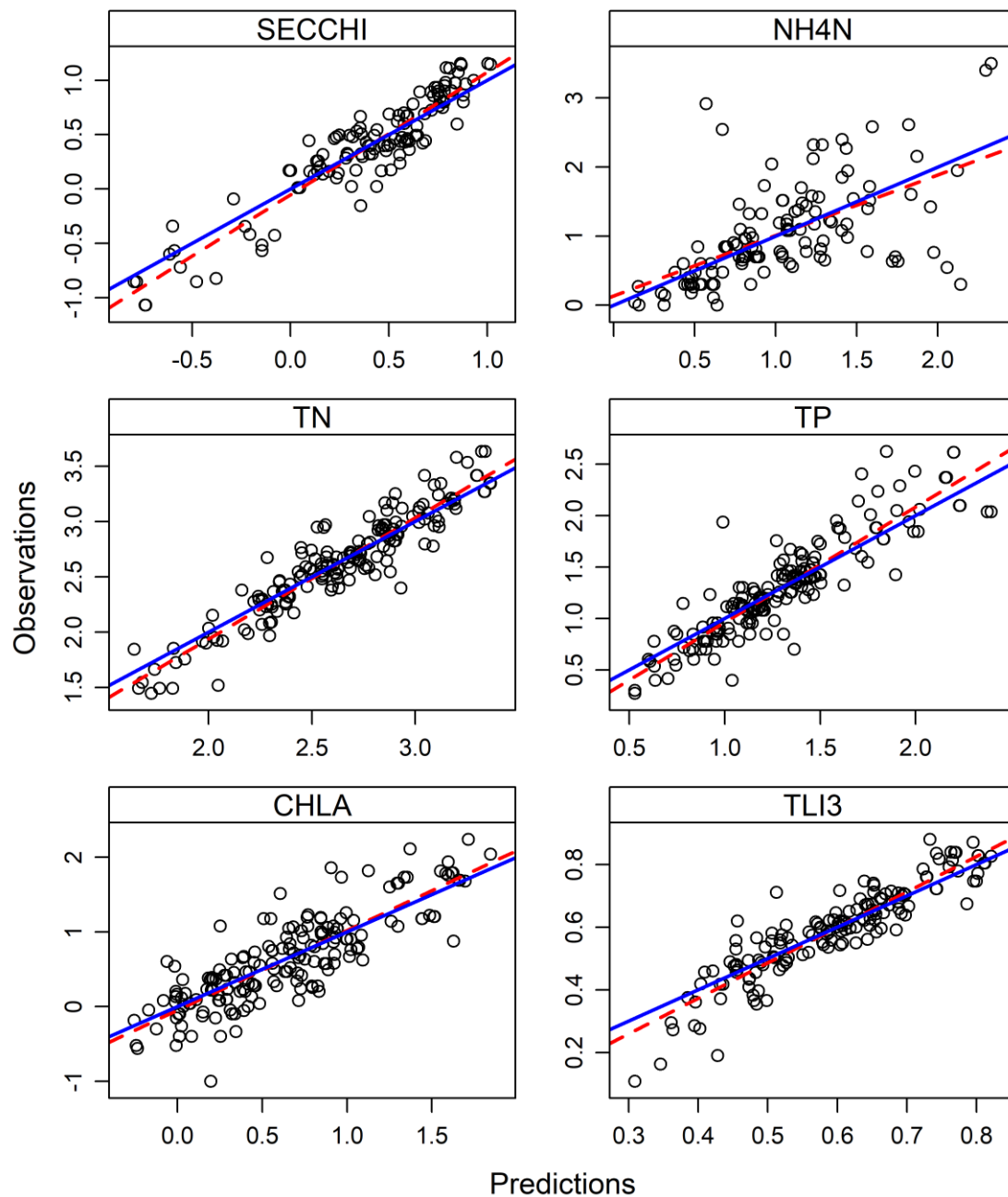


Figure 5-7: Comparison of observed lake water quality versus values predicted by the random forest models. Note that the observed values are plotted on the Y-axis and predicted values on the X-axis, following Piñeiro et al. (2008). Solid lines: best fit linear regression of the observed and predicted values for summer (red) and winter (Blue) models. Black dashed line: one-to-one line. Units are the \log_{10} transformed units of all water quality variables

5.2.2 Modelled relationships

The reduced lake RF models for all variables retained a small subset of the original set of predictors that reflected associations between water quality and lake and catchment elevation, geological and climatic factors (Table 5-3). Season was not retained in any of the lake RF models.

The lake water quality variables had logical relationships with many of the individual predictor variables included in the reduced RF models (Figure 5-8), with these patterns generally consistent with other RF modelling studies for lakes (Fraser and Snelder, 2018; Snelder et al., 2016). Nutrient concentrations and chlorophyll *a* decreased and Secchi depth increased with increasing lake and catchment elevation (lkElev, catElev) and catchment slope (catSlope). These patterns are consistent with an observed gradient in trophic conditions for lakes that is associated with altitude and climate (Sorrell et al., 2006). Predictors describing catchment landcover were not retained in any of the RF models (Figure 5-8). However, the inclusion of elevation and catchment climate is probably partly due to these predictor's correlation with catchment landcover. TLI3 and TN decreased with lake fetch (lkFetch), which may be a reflection of the generally lower trophic status of larger lakes rather the effect of wind mixing on lakes. These patterns are generally consistent with those observed in Fraser & Snelder (2018).

Table 5-3: Rank order of importance of predictor variables retained in the lake random forest models for at least one water quality variable. Blank cells indicate that the predictor was not included in the reduced model. The predictor variables in the first column are listed in descending order of the median of the rank importance over all six models.

predictor	SECCHI	NH4N	TN	TP	CHLA	TLI3
lkElev	2	1	4	3	1	1
lkArea	-	2	-	-	-	-
catSlope	-	5	-	1	2	3
lkFetch	-	4	3	-	-	2
lkSumWind	3	11	2	-	3	4
lkDistCoast	-	3	-	-	-	-
catElev	1	6	1	5	4	7
catAlluv	-	7	6	6	-	8
catCalc	-	12	8	4	-	5
lkDepth	-	10	5	-	-	-
catPsize	-	8	-	-	-	-
catWinTemp	-	15	7	-	-	9
lkDecSolRad	-	13	9	-	-	6
catFlow	-	9	-	-	-	-
catArea	-	16	-	2	-	-
catPeat	4	18	-	-	-	-
catHard	-	14	-	-	-	-
catPhos	-	17	-	-	-	-

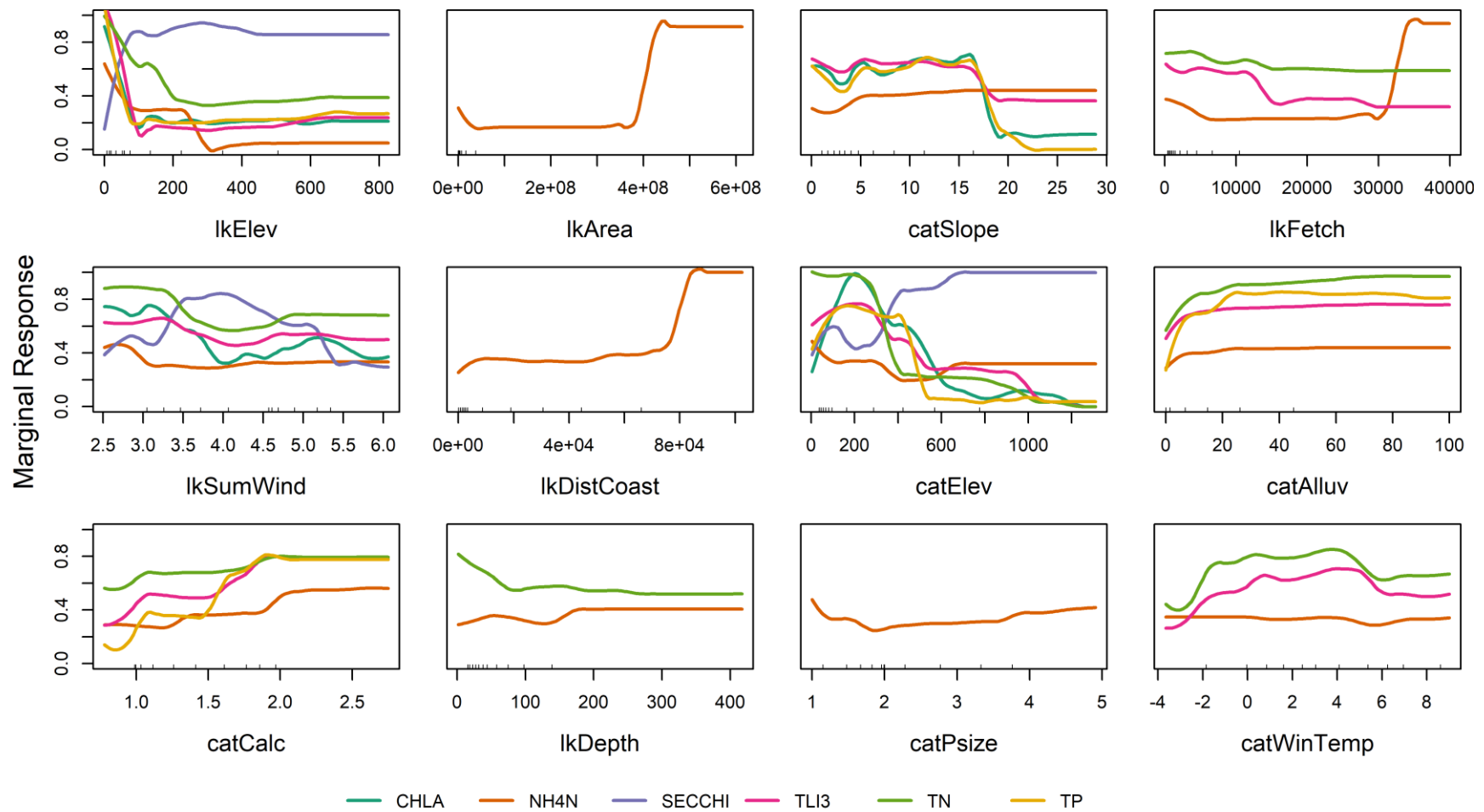


Figure 5-8: Partial plots for the 12 most important predictor variables in random forest models of lake water quality. Each panel corresponds to one predictor, with summer and winter models represented by solid and dashed lines, respectively. The Y-axis scales: standardised value of the marginal response for each of the six modelled variables. In each case, the original marginal responses over all twelve predictors were standardised to have a range between zero and one. Plot amplitude (the range of the marginal response on the Y-axis) is directly related to a predictor variable’s importance; amplitude is large for predictor variables with high importance.

5.2.3 Model predictions

The minimum values predicted by the RF models were always somewhat larger than the minimum of the observed values and the maximum predicted values were always somewhat smaller than the maximum observed values (Table 5-4). This is an expected outcome of RF models, which are based on partitioned data with predictions derived from the means of observations that are assigned to a particular partition. Therefore, the predictions for each water quality variable were always within the range of the observations.

Table 5-4: Comparisons of the minimum and maximum observed and predicted median values of seasonal lake water quality.

Variable and unit	Minimum observed value	Maximum observed value	Minimum predicted value	Maximum predicted value
SECCHI (m)	0.08	14	0.16	12
NH4N (mg m ⁻³)	1.00	3150	1.46	1320
TN (mg m ⁻³)	28.00	4300	37.06	3237
TP (mg m ⁻³)	1.88	420	2.37	230
CHLA (mg m ⁻³)	0.10	174	0.48	104
TLI3 (Unitless)	1.28	8	1.60	7

Predictions of water quality are shown in Figure 5-9 for the 3802 lakes with complete data in the FENZ dataset. These mapped predictions had similar spatial patterns, with high values of CHLA, NH4N, TN, TP and TLI3 and low values of SECCHI in low-elevation areas on the coasts of the North and South Island, apart from areas with little or no pastoral landcover (e.g., Fiordland). Values of CHLA, NH4N, TN, TP and TLI3 were also high and values of SECCHI were low further inland in areas of both islands dominated by agricultural land use such as Southland, parts of Otago, Hawkes Bay, Bay of Plenty, Waikato and Northland. Values of CHLA, TN, TP and TLI3 were generally low and SECCHI high in inland areas of the South Island. These patterns were generally consistent with the results of previous RF lake modelling studies (Fraser and Snelder, 2018; Snelder et al., 2016).

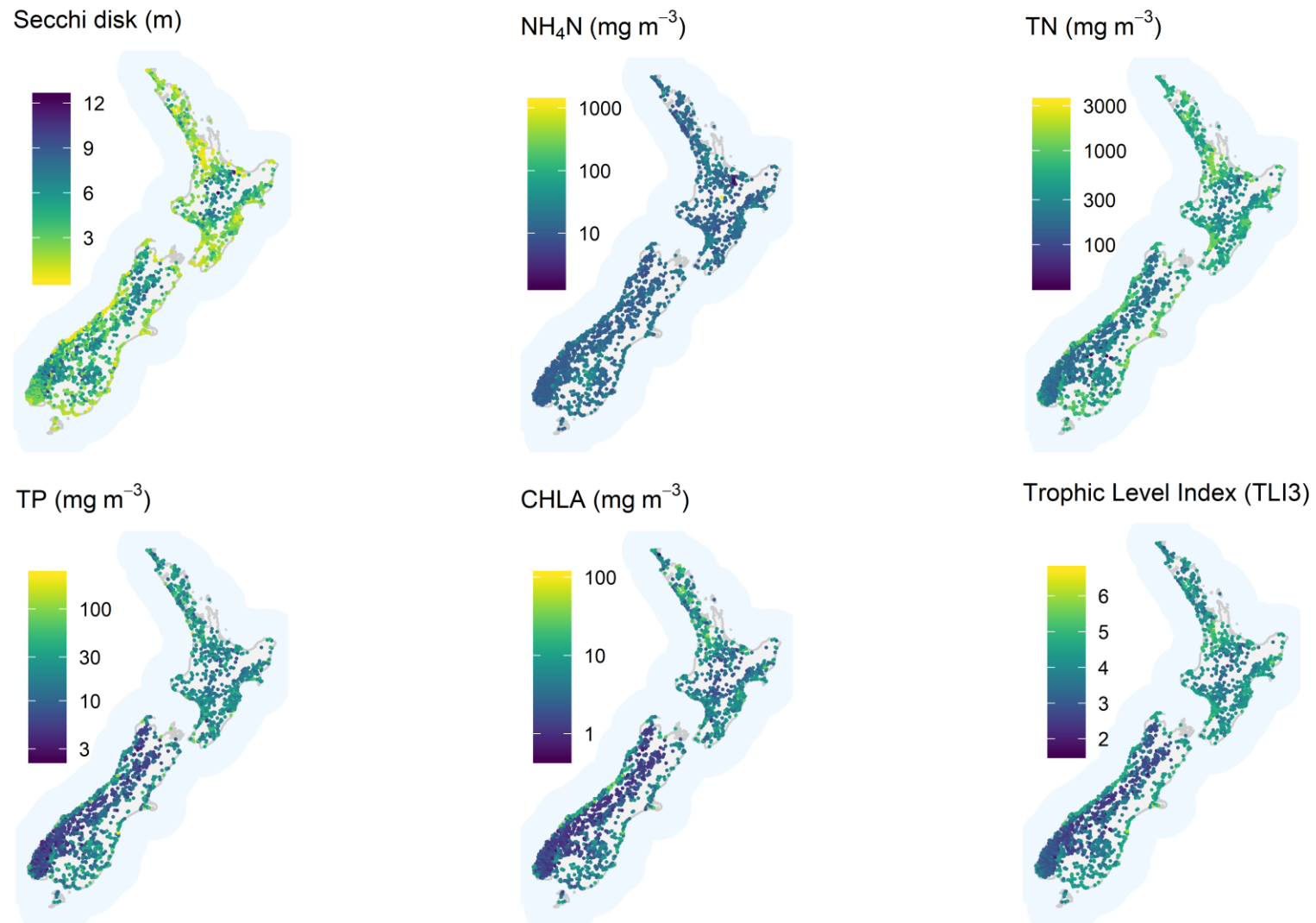


Figure 5-9: Predicted median water quality for six variables in New Zealand lakes. Predictions are based on summer and winter samples only, with season not included in the final random forest model. The lakes are indicated by points located at the lake centre.

6 Diel variation in water quality

Excessive growth of aquatic plants (blooms of algae and macrophytes) due to nutrient enrichment of freshwaters by inputs from human activities is a global problem (Chindler et al., 1997; Conley and Likens, 2009; Dodds, 2006; Dodds et al., 2009; Smith et al., 1998; Snelder et al., 2018). The nutrient enrichment response in gravel-bed rivers typically manifests as the development of abundant periphyton biomass, where other controlling factors (e.g., high light, stable flow regime, warm temperatures, low grazing pressure) are favourable. Excessive periphyton can degrade aquatic biodiversity and a wide range of freshwater ecosystem services and values and can have a marked effect on water quality on diel (i.e. 24h) time-scales. Using the Tukituki River as a case study, we show how metabolism (gross and net primary production [GPP & NPP] and ecosystem respiration [ER]) in periphyton-dominated rivers leads to variation in pH, dissolved oxygen (DO) and nitrogen concentrations between light and dark periods. We also briefly discuss the potential implications of these temporal changes, with respect to the compulsory NPS-FM values (MfE, 2017) of ecosystem and human health.



Figure 6-1: Examples of benthic periphyton blooms in the Tukituki River (Feb 2016 and Feb 2017). Left and lower right show the green filamentous *Cladophora*, and upper right image shows distinctive dark *Microcoleus* (formerly *Phormidium*).

6.1 Tukituki River case study site

The case study was carried out in the lower Tukituki River in Hawke's Bay. This section of the river is 5th and 6th order, has a median flow of 22 m³/s, and summer flows of 5-6 m³/s (Figure 6-2). The river is affected by nutrients inputs from upwelling of agriculturally N-enriched groundwaters and P-enriched secondary treated, sewage treatment plant (STP) effluent from Waipawa and Waipukurau. The Tukituki River is highly valued for trout fishing and swimming, but these uses are often adversely affected by excessive periphyton, including cyanobacterial mats, during summer. Data presented here came surveys carried out in the summers of 2016 and 2017 at sites between T7 and T12 – a distance of approximately 48 km (Figure 6-2). The median periphyton biomass (and range) for these sites during the surveys in 2016 and 2017 were 170 mg chla/m² (156-208 mg chla/m²) and 115 mg chla/m² (50-184 mg chla/m²), respectively.

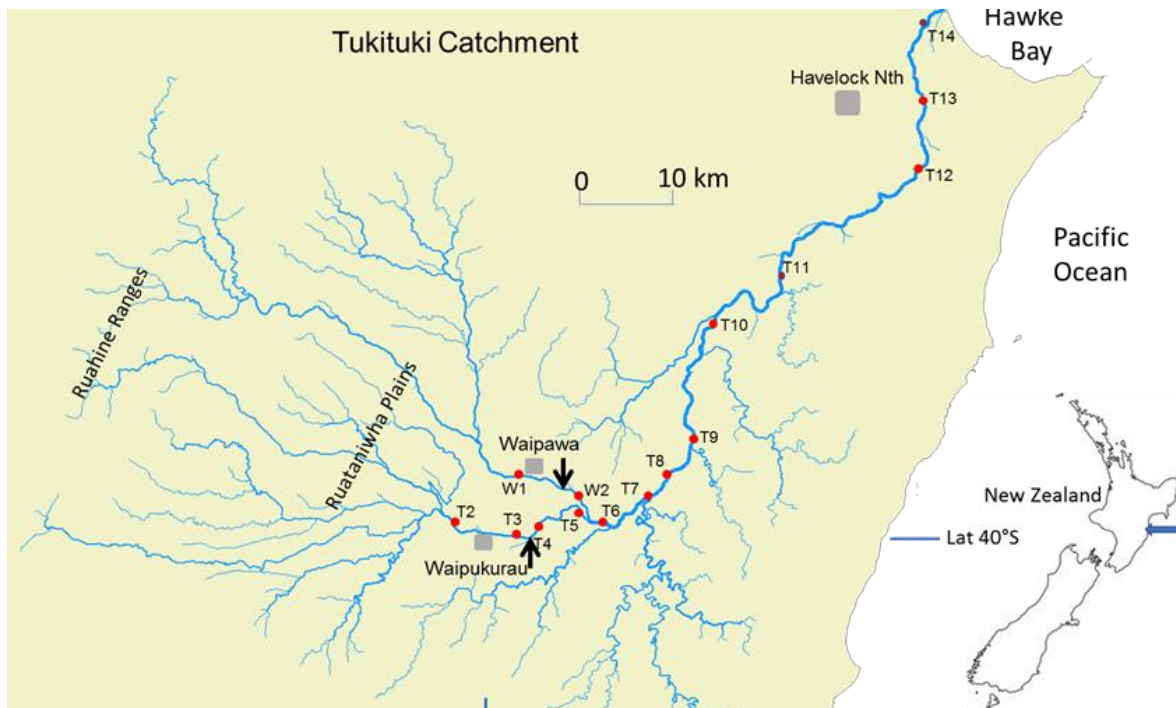


Figure 6-2: Location map of the Tukituki River showing the study sites and sewerage treatment plant discharges (black arrows).

6.2 Results

6.2.1 pH

Diel variation

The Tukituki River at T12 has high pH relative to other New Zealand rivers (Smith and Maasdam 1994). During the day, periphyton photosynthesis consumes dissolved CO_2 from the water column, decreasing hydrogen ions and increasing pH values in the river from 7.5 to 9.0-9.5 (Figure 6-3). Atmospheric CO_2 ($\text{CO}_{2(\text{atm})}$) dissolves into river water, $\text{CO}_{2(\text{diss.})}$ (Eq. 1), and then reacts relatively slowly to form carbonic acid (H_2CO_3) (Eq. 2). This acid dissociates quickly into its conjugate base (HCO_3^-) and a hydrogen ion (H^+). Photosynthesis during the day consumes the $\text{CO}_{2(\text{diss.})}$, which then pulls Eq. 2 to the left (to form more $\text{CO}_{2(\text{diss.})}$), reducing the concentration of H^+ concentration, and consequently increasing pH. The ability of river water to buffer changes in pH depends on the alkalinity – the concentration of bicarbonate and carbonate. The Tukituki River has a relatively high alkalinity compared with other NZ rivers, with a value of 65 g/m^3 (as CaCO_3), compared with median and 75th percentile values for 77 NRWQ sites of 27 and 36 g/m^3 , respectively.



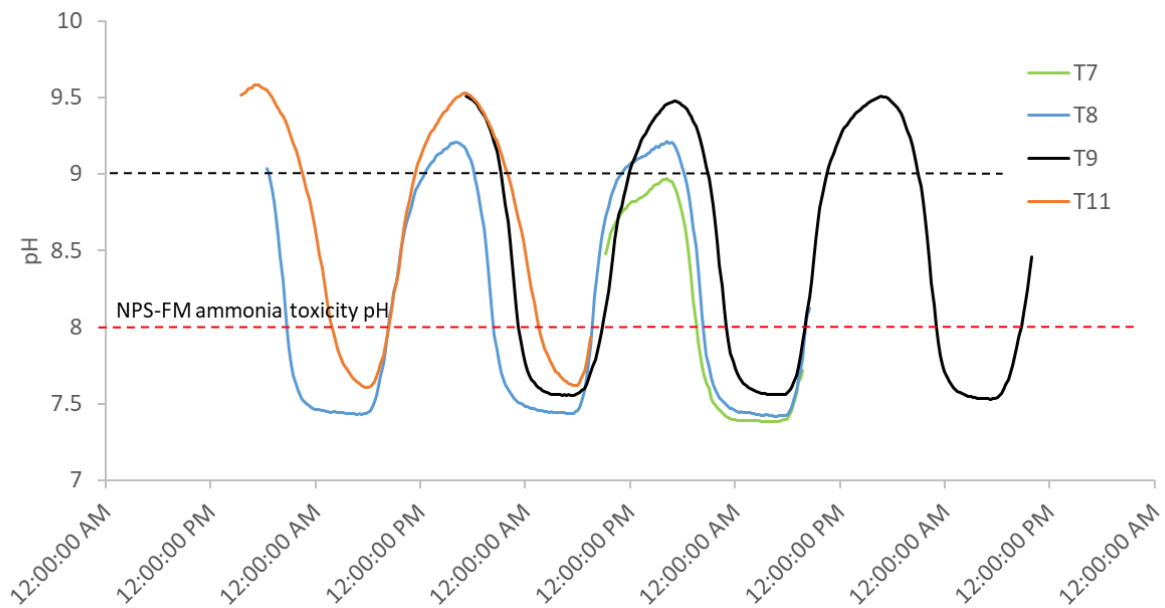


Figure 6-3: Diel pH values at Tukituki sites T7, T8, T9 and T11 (Feb 2017).

Diel pH values (over 1-4 days) are shown for sites T7, T8, T9 and T11 in Figure 6-3. At T9 and T11, the pH values increased by 2 units, from c. 7.5 to 9.5. The average length of time (h) that river water exceeded pH 9 at each site is shown in Figure 6-4. Over relatively short distances (e.g., 31 km), the number of hours where pH was ≥ 9 increased from 0 h at T7 to 11 h at T11 (refer to Figure 6-2). In Feb 2018 (data not shown), the variation in pH at the most upstream site T2 (upstream of STP discharges and near to the stabilizing influence of upwelling Ruataniwha Plains groundwater) was relatively small (<0.5 pH units), ranging between 7.5 and 7.9.

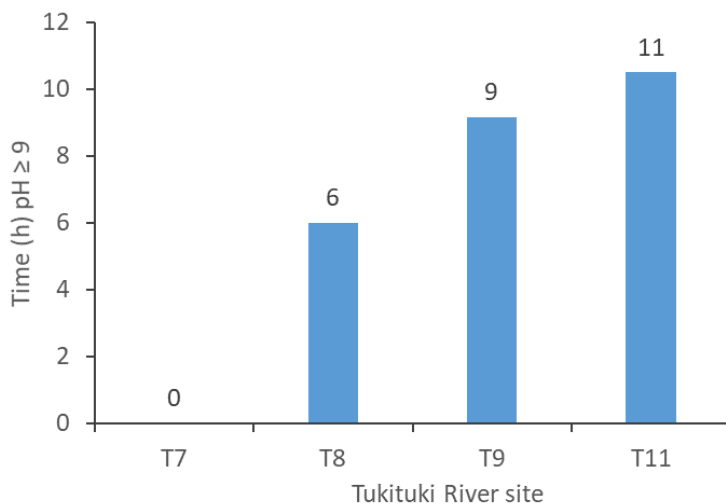


Figure 6-4: The average duration (hours) that river water pH was ≥ 9 at sites along a 31km reach of the Tukituki River (Feb 2017).

Potential implications of high diel pH values for water quality

The potential effects of large diel fluctuations in pH include toxicity (direct and via enhanced ammonia toxicity) and solubilization of particulate forms of phosphorus stored in bed sediments.

Direct toxicity

Ecosystem health effects from pH extremes tend to be associated with acidic pH ranges. For example, pH values < 5 associated with acid rain lead to increased concentrations of the free aluminium ion and have caused toxicity problems for freshwater fish (Davies-Colley et al., 2013).

West et al. (1997) investigated the response of nine New Zealand fish species to pH values in the range 3 to 11. All species exhibited pH preferences and all but inanga avoided pH values above 9.5. Given that this is close to the upper limit observed in the Tukituki River in Feb 2017 (9.5-9.6), it is probably unlikely that diel pH maxima impact on the distribution of native freshwater fish. A similar conclusion for lowland streams in New Zealand was drawn by Davies-Colley et al (2013).

Increased ammonia toxicity

Ammonia is present in two forms, ammonia (NH_3) and its conjugate acid ammonium (NH_4^+) with the former responsible for ammonia toxicity. The proportion of the toxic and non-toxic forms depends on pH (Figure 6-5). Green shading shows the diel range of pH values at the most upstream site (T2) during February 2018, which correspond to NH_3 proportions of <5%. In contrast, the high pH values of 9-9.6 associated with periphyton production at lower sites (e.g., T9 and T11) correspond to NH_3 proportions of 35-70%. NPS-FM criteria are based on a pH value of 8, corresponding to only 5% of the more toxic NH_3 form (red dashed line Figure 6-3). At the diel pH maxima (9.6), for a given ammoniacal-nitrogen concentration, the concentration of toxic NH_3 will be 14-times higher, compared to the upstream pH maximum of 8.

In 2018, diel pH maxima in the Tukituki River near STP discharges were not sufficient to cause significant pH-enhanced ammonia toxicity in the water column. However, under extreme low flow conditions (c. 2 m³/s, cf. 5-6 m³/s in 2017 and 2018), spot pH values in the afternoon were up to 9.3 at locations immediately upstream and downstream of the STP discharge. Diel pH-enhanced ammonia toxicity was an issue for the Manawatu River, with pH values > 9 upstream of the Palmerston North STP (Freeman, 1983). Fortunately, bacterial respiration associated with the discharge offset the pH increase from periphyton production, although the author indicated that future discharge changes could alter this situation (Freeman, 1983).

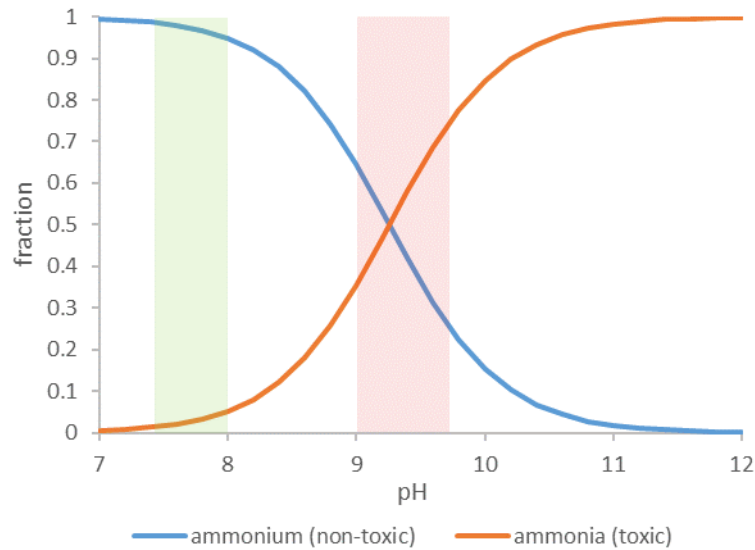


Figure 6-5: Fraction of ammonium (NH₄) and ammonia (NH₃) at different pH values. Green shading shows diel pH range at the upstream site (T2), while red shading indicates the region between 9-9.6 at which downstream sites can occur for >10h per day (refer to Figure 6-4).

Solubilisation of phosphorus in bed sediments

Control of freshwater concentrations of dissolved reactive phosphorus (DRP) is often important to preventing nuisance growths of periphyton that are aesthetically unattractive or otherwise degrade freshwater ecosystems (Biggs, 2000). Froelich (1988) observed that, in solution, DRP reacts quickly with a variety of surfaces, being taken up by, and released from particles through a complex series of 'sorption' reactions. Metal ions including iron, aluminium and calcium have the capacity to take up phosphate from river water under mildly acidic conditions. As pH increases above pH 8, hydroxyl complexes of iron, aluminium and calcium become increasingly more stable than their respective phosphates, releasing soluble phosphate into the water column (Jensen & Andersen 1992). For example, the concentration of dissolved phosphate, released by the dissolution of solid iron phosphate, increases rapidly above pH 7.5 (Figure 6-6; Golubev and Savenko, 2002).

Diel pH maxima observed in the Tukituki River are sufficiently high (e.g., >9 for several hours per day, Figure 6-4) to potentially dissolve reservoirs of inorganic phosphorus in river bed sediments. Laboratory extractions from Tukituki River sediments have shown that, on average, 3-4 times more DRP was solubilised from sediments at pH 9.5-10 versus pH 7-8 (Wilcock et al. pers. comm.).

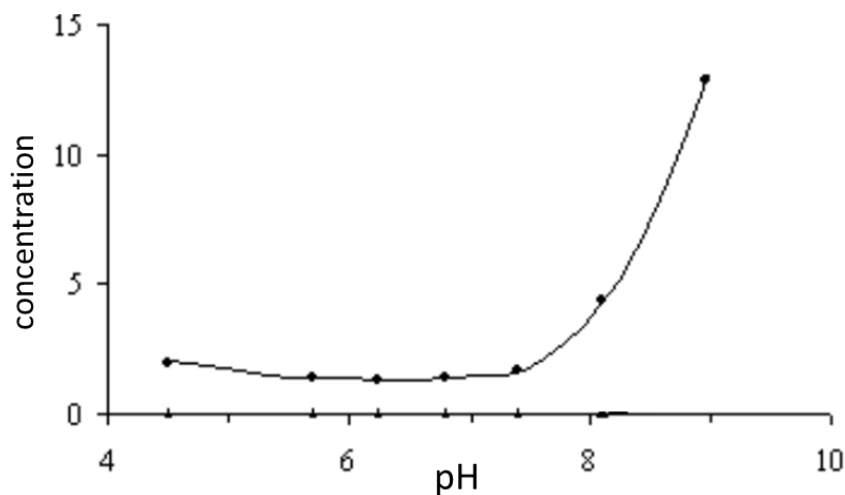


Figure 6-6: The relationship between free dissolved phosphate from the dissolution of iron(II) phosphate with increasing pH value. From Golubev and Savenko 2002.

At the upstream site (T2), nutrient N:P mass ratios of > 60 suggest that algal growth in the Tukituki River is phosphorus-limited. The removal of inorganic nitrogen at downstream sites (T11/T12) requires a large amount of phosphorus to be supplied from other sources to sustain the high N:P ratio. This was initially thought to be the STP discharges, but since late 2016, DRP from these point sources has reduced by around 95%. From simple nutrient budget calculations, we estimate that around 80% of phosphorus (under summer low flow conditions) is being provided from another source, most likely inorganic phosphorus sorped to river bed sediments. The growth of periphyton may provide a 'positive feed-back loop' for the supply of additional soluble (and bioavailable phosphorus) to the water column. That is, *increased algal growth* → *increase pH maxima* → *increased solubilisation of phosphorus to the water column* (which then fuels additional periphyton growth).

In Feb 2017, continuous monitoring of pH was accompanied by hourly automated sampling for nutrient analyses. Water column concentrations did not show the anticipated correlation between pH and DRP (data shown for T9, Figure 6-7). DRP concentrations were out-of-phase with pH, and presumably reflected phosphorus uptake by periphyton during the afternoon. We are therefore uncertain whether diel pH maxima enhanced the flux of DRP from bed sediments to the water column. Numerous studies have calculated the flux of DRP from sediments to overlying water using simple diffusion models from porewater gradient of DRP concentrations (D'Angelo and Reddy, 1994; Klump and Martens, 1981; Sundby et al., 1992). However, none of these studies observed increases in water column DRP, suggesting dynamic changes at the sediment-water interface (Reddy et al., 1999). In a review of phosphorus retention in streams and wetlands, high diel pH maxima from photosynthesis caused precipitation of water column DRP as calcium phosphate (Reddy et al., 1999).

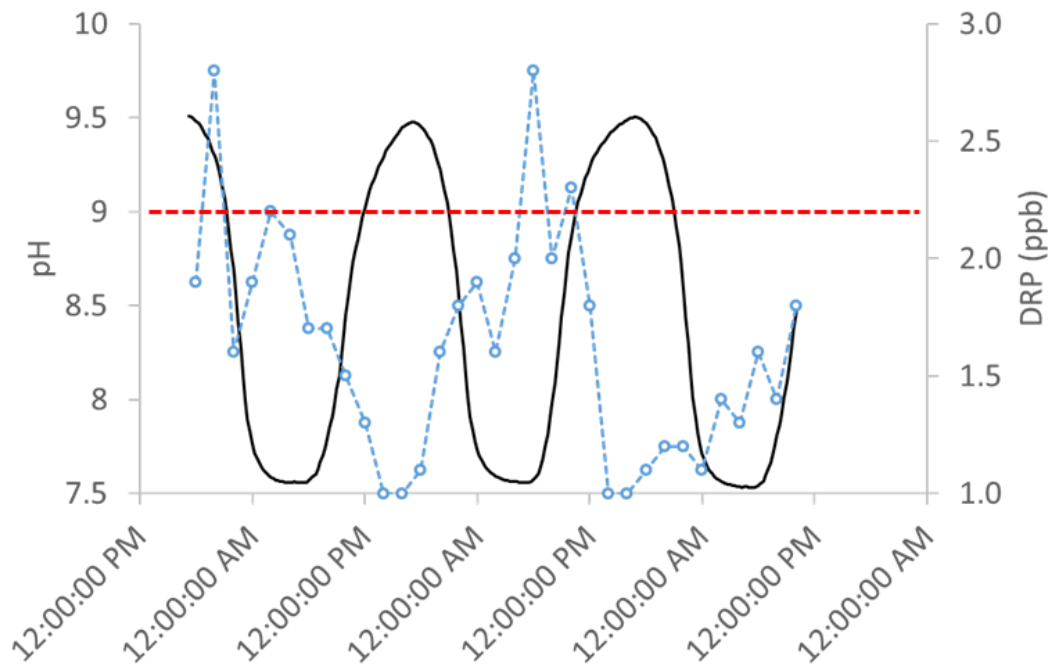


Figure 6-7: Continuous pH (black line) and two-hourly DRP concentrations (blue dashed line) for site T9, Tukituki River (Feb 2017). Red dashed line at pH 9 indicates where phosphate complexes associated with bed sediments would be expected to dissolve and release DRP to the water column.

6.2.2 Dissolved oxygen (DO)

Diel variation

Reduced dissolved oxygen (DO) concentrations (i.e., hypoxia) can impair the growth and/or reproduction of aquatic organisms and very low or zero DO concentrations (i.e. anoxia) will kill organism (Davies-Colley et al., 2013).

DO concentrations in the lower Tukituki River are strongly associated with periphyton biomass, with generally low and high biomass at site T2 and T9, respectively. Upstream (c. 7km) of the Waipukurau STP discharge (i.e., T2, c. Figure 6-2), DO concentrations in February 2018 ranged between 7.8 and 9.3 g/m³ (blue dashed curve, Figure 6-8). In contrast, at site T9 (c. 30 km downstream of T2), DO concentrations ranged between 7.8 and 15 g/m³ (black curve, Figure 6-8).

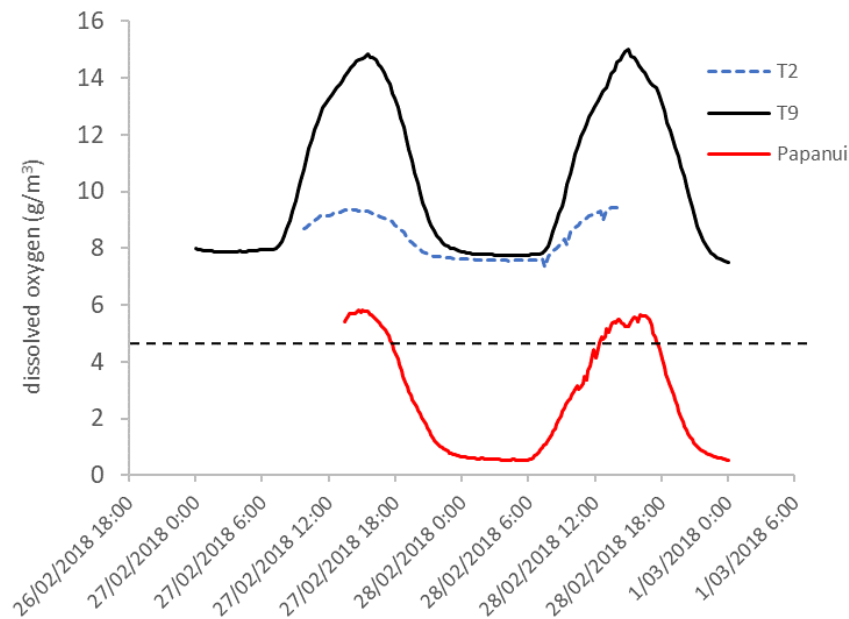


Figure 6-8: Dissolved oxygen (DO) concentrations g/m³) at two sites on the Tukituki River (T2 and T9) and one site on a tributary, Papanui Stream. The black dashed line indicates the NPS-FM bottom line value of 4.5 g/m³.

Possible implications for water quality

Ecological effects from diel variation in DO – minima and maxima

In the Tukituki River mainstem, relatively high reaeration coefficients associated with fast flowing, shallow water and high production/respiration ratios mean that summer time DO minima in the Tukituki River (even at productive sites like T9) remain well above the NPS-FM bottom line value of 4.5 g/m³ (Figure 6-8). DO maxima in the Tukituki River correspond to percent saturation levels of up to 220% (2011, data not shown). High DO saturation can result in fish gill damage, increasing the risk of secondary fungal infection and death (Machova et al., 2017). These effects have been observed at DO saturation levels between 250 to 300% (Svobodová et al., 1993). The effect of supersaturated oxygen is different to ‘gas bubble disease’, which is due to supersaturation of atmospheric gases (driven by dissolved inorganic nitrogen) (Weitkamp and Katz, 1980).

Although adverse effects of diel DO minima were not observed in the Tukituki River mainstem, tributaries like the Papanui Stream regularly have low DO concentrations during summer with DO minima close to zero (red curve, Figure 6-8). In February 2018, DO concentrations were below 1 g/m³ for approximately seven hours per day (between 10:00 pm and 7:00 am). In previous studies, common smelt (both juvenile and adult), juvenile common bullies, juvenile rainbow trout juvenile banded kokopu were reported to have 50% mortalities when exposed to a DO concentration of 1 g/m³ for 0.6, 0.6, 1 and <8h, respectively (Dean and Richardson 1999). All of these species would be expected to suffer mortality if exposed to dissolved oxygen minima in the Papanui Stream. Spot measurements taken at this site on the same day between 1200 and 1700 h would have indicated DO > 4.5 g/m³ (i.e., not ecologically threatening), demonstrating the need to at least be cognizant of diel DO variability and to select the timing of spot measurements deliberately (e.g., early morning for DO ecological suitability assessment) or to conduct 24-hour monitoring.

High diel DO: 'Gas lift effect' promotes sloughing of benthic periphyton

Under steady flows, there was five times more periphyton caught in the afternoon in drift nets at the surface than mid-water column (Paired t-test, $P < 0.05$, 2016 and 2017 data; Quinn et al., 2018), whereas surface and water column catches were similar during the morning (Figure 6-9). Surface floating periphyton was buoyed by gas bubbles indicating that photosynthesis within the periphyton mats contributed to periphyton sloughing. Our data did not differentiate *Microcoleus* and filamentous greens, but *Microcoleus* was often amongst the dominant forms of periphyton in the Tukituki River, with cover exceeding 20% at the upstream sites where DIN was $>300 \text{ mg m}^{-3}$ (Quinn et al., 2018).

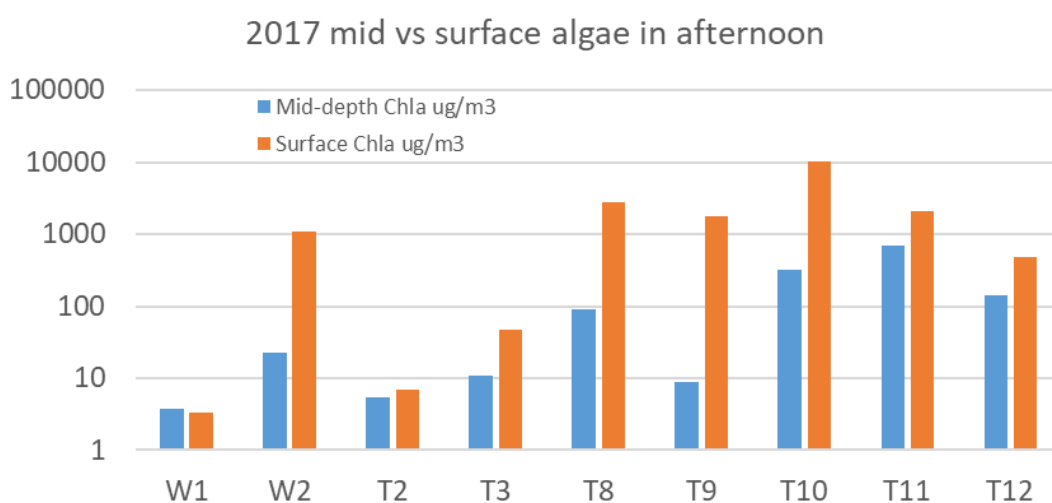


Figure 6-9: Chlorophyll-a (Chla) concentrations (a proxy measure of sloughed algal biomass) of biomass trapped in nets positioned at mid-depth and surface level. Surface net trapped benthic algae detach via gas lift which still had positive buoyancy from entrapped oxygen bubbles. Note the log-scale of y-axis.

The 'gas lift' effect corresponds to times when most contact recreation takes place in the Tukituki River (mid to late afternoon), and therefore increasing sloughing of *Microcoleus* during the afternoon increases the potential for people and pets to be exposed to algal toxins. The increased risk of exposure is associated with floating *Microcoleus* in the water column, and *Microcoleus* that accumulates on the river bank. This was consistent with advice to inform the development of a benthic cyanobacteria attribute (Wood et al., 2015), where detachment events are thought to be partly due to entrapment of oxygen within the mats caused by photosynthesis during daylight. The likelihood of contact and therefore ingestion of *Microcoleus*-dominated mats will be escalated during the photosynthesis-driven mass detachment events.

6.2.3 Nitrate-nitrogen

Diel variation – summer baseflow

Uptake of nitrate-N from the water column by periphyton results in marked diel changes in nitrate-N concentrations (Figure 6-10). Nitrate-N concentrations are 'out of phase' with DO concentrations. In contrast to DO, which has an external source (atmospheric reaeration), nitrate-N is progressively

removed as the water flows downstream. Maxima and minima were 500 and 340 mg/m³ at T8, 450 and 230 mg/m³ at T9, and 120 and 20 mg/m³ at T11 (Figure 6-10).

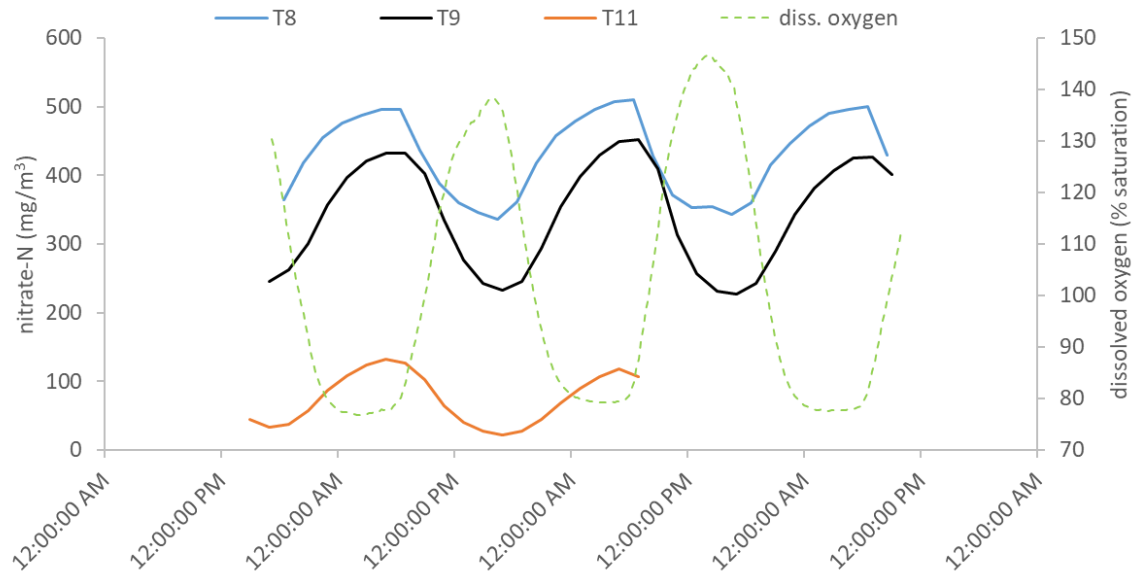


Figure 6-10: Diel variations in nitrate-N concentrations at Tukituki sites T8, T9 and T11 (Feb 2017). The dissolved oxygen curve (green dashed) is a proxy for photosynthetic activity by benthic periphyton, which is driving the diel variation in nitrate-N concentrations. The distance between T8 and T9 and T8 and T11 is 5 and 27 km, respectively.

Possible implications for water quality

State of the environment monitoring involves generally monthly ‘grab’ samples, which are usually collected at the same time on each sampling date. The marked decrease in nitrate-N between 0700 and 1700 in the Tukituki River highlights the potential for monitoring records to be influenced by diel variations caused by benthic periphyton photosynthesis, particularly in summer months when periphyton biomass is high. Nutrient uptake by periphyton may have spatial and/or temporal implications for water quality that need to be considered, as mentioned by Smith and Maasdam (1994).

Temporal considerations

Diel fluctuations in nitrate-N concentrations during summer low flows can cause additional variability that is not apparent in data from grab samples. For example, at T9 in the Tukituki River, the nitrate-N concentration between 0900 and 1500 h decreased by 180 mg/m³ (from 410 to 230 mg/m³). At site T11, the nitrate-N concentration at 0900 and 1500 h was 102 and 27 mg/m³, respectively. As such, the timing of water sampling at this site can result in greater than three-fold variation in nitrate-N concentration.

Spatial considerations

Based on nitrate-N maxima (at night in the absence of uptake) in the 27 km between T8 and T11, nitrate-N concentrations decreased almost 300 mg/m³, from 510 to 120 mg/m³. This instream attenuation is important when determining nutrient concentrations/loads delivered to potentially sensitive downstream receiving environments (e.g., lakes and estuaries), particularly in summer with high biomass and low flows. Amendments to the NPS-FM periphyton attribute made in August 2017 require regional councils to set instream nutrient criteria to meet periphyton objectives in their freshwater management units. In addition, these criteria must also consider the trophic-state objectives of potentially sensitive downstream receiving environments. In the case of the Tukituki River, if T8 was the monitoring site used to estimate summer nutrient concentrations (or loads) discharged to the estuary, this may result in an overestimate of actual nutrient loads, and hence the risk to meeting trophic state objectives. This is not the case for the Tukituki River as there is a state of the environment monitoring site at T12 (17 km downstream of T11, refer to Figure 6-2).

Temporal and spatial considerations

To determine nutrient attenuation, the net reduction in nutrient concentration between an upstream and downstream site are compared. Here we use nutrient attenuation between site T8 and T9 as an example. These sites are approximately 5 km apart, with a travel time of around 2 hours. In the absence of marked diel changes in nitrate-N concentrations, the uptake occurring between site T8 and T9 would involve collecting a sample of the same water mass – that is, sampling T9 approximately 2 hours after sampling T8. However, diel variation observed at each site is greater than the uptake between the sites (i.e., intra-site variation > inter-site uptake). Assuming a travel time of 2.5 hours, subtracting T9 nitrate-N concentrations from T8, yields uptake concentrations of between 60 and 120 mg/m³ of nitrate-N (Figure 6-11). The influence of intra-site diel concentrations is apparent, with the lower (50-60 mg/m³) and upper (100-120 mg/m³) range of nitrate-N uptake corresponding to travel times during dark (black dots) and daylight hours (orange dots, Figure 6-11).

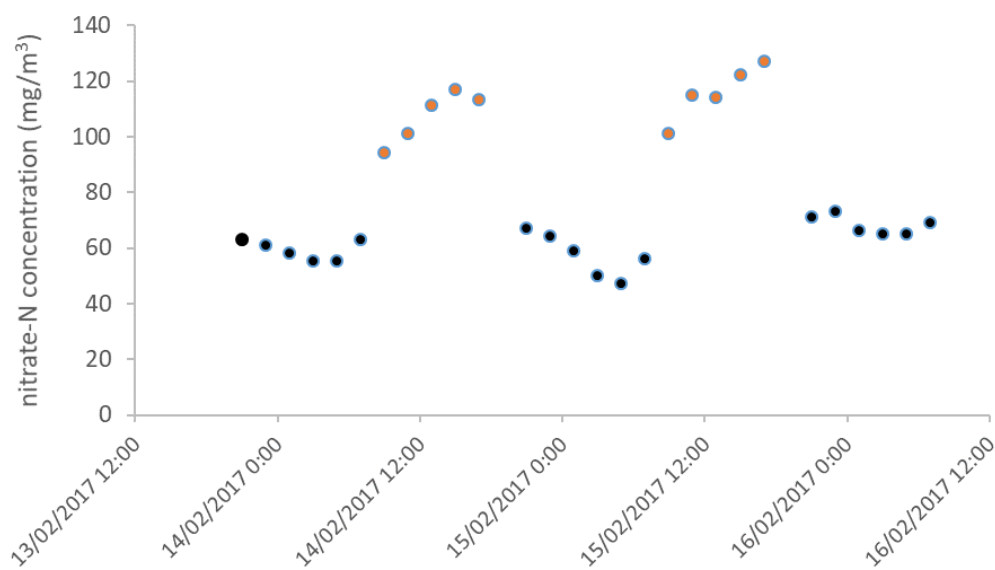


Figure 6-11: Concentration of nitrate-N attenuated between sites T8 and T9 (3 km distance) on the Tukituki River. Black and orange circles indicate nitrate-N uptake occurring under dark and light conditions, respectively.

The data show that nitrate-N attenuation was occurring in the light and dark, with higher attenuation in the light (Figure 6-11). Nitrate-N uptake in nitrogen-sufficient cells takes place much more rapidly in the light than in the dark (Syrett, 1981). However, nitrogen-starved cells with high carbon reserves show rapid dark uptake (Grant and Turner, 1969; Syrett, 1981; Thacker and Syrett, 1972). Quinn et al. (2018) have shown that periphyton in the lower reaches of the Tukituki River become progressively depleted in nitrogen (evident from increasing trend in periphyton C:N ratios).

Stormflow events— effects on summer periphyton biomass and nutrient transported to downstream receiving environments

Short-term increases in river flow (termed variously as spates, freshets, floods) can cause marked changes in periphyton biomass (Biggs et al., 1999; Biggs and Close, 1989; Peterson, 1996; UEHLINGER et al., 1996) and nutrient concentrations (especially particulate nutrients in sloughed periphyton).

Relatively large stormflow events that scour the attached periphyton transport substantial quantities of particulate periphyton nitrogen and phosphorus downstream but also “reset” the system to a low periphyton condition with less marked diel variations. Figure 6-12 shows changes in diel patterns of nitrate at sites T9 and T11 following an 85 m³/s spate on 20 Feb 2017 that reduced CHLA at T9 from 135 mg/m² on 15 Feb 2017 to 2 mg/m² on 1 Mar 2017. After the spate, nitrate concentrations increased at both sites and diel variations were lower, likely reflecting less uptake by the lower periphyton biomass present.

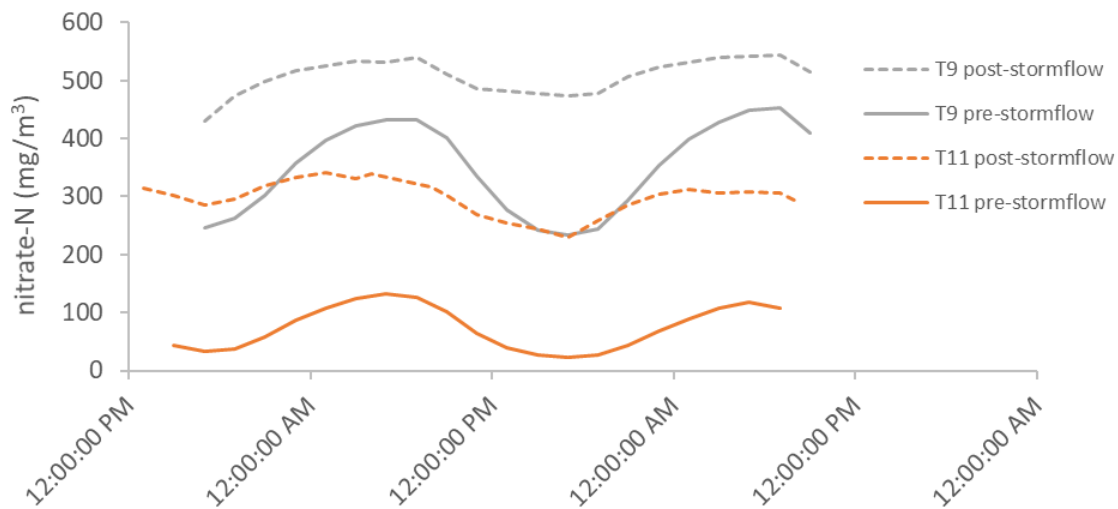


Figure 6-12: Diel concentrations of nitrate-N at sites T9 and T11 (22 km apart) on the Tukituki River before (solid line) and one week after (dashed line) a 85 m³/s stormflow event on 20 Feb 2017. The baseflow rate prior to the storm event was c. 5 m³/s.

The effect of the 85 m³/s stormflow event on 20 Feb 2017 on downstream particulate nutrient transport was calculated using the average periphyton nitrogen and phosphorus densities for all surveys of 1.6 g/m² and 0.1 g/m², respectively; and a mean river width of 41 m and depth of 0.5 m over the 80 km study reach. We estimate that >5000 kg nitrogen and >300 kg phosphorus was stored in periphyton within the reach under normal summer steady flow conditions. If this periphyton was scoured and exported to the coast over a day (as is plausible), the nitrogen and phosphorus loads would be 20- and 28-times higher than the daily average TN and TP loads under our survey conditions at baseflow. This indicates that a scouring flow event in a river with abundant periphyton, such as the Tukituki, can deliver a substantial pulse of particulate organic nitrogen and phosphorus to downstream lakes, estuaries and coastal receiving environments. Such transport of organic nitrogen is likely to have implications for downstream receiving environments, particularly if they have long residence times (e.g., lakes, estuaries).

7 Discussion and conclusions

7.1 Patterns of seasonal water quality

Season was an important predictor in all river water quality models (Table 4-1, Table 4-3). Winter months were associated with lower CLAR and higher TURB and nutrient concentrations than during summer (Figure 4-11). In contrast, ECOLI concentrations were higher in summer than in winter (Figure 4-8, Figure 4-11). These patterns were typically strongest in areas dominated by high-intensity agriculture, although similar relationships were also noted in natural and urban areas for some variables (Table 4-1, Table 4-3). Higher NO₃N during the winter months is a common and expected result in New Zealand, likely driven by high winter runoff, higher nitrogen uptake by algae in summer and seasonal differences in land management (Howard-Williams et al., 1982; Quinn and Stroud, 2002; Wilcock et al., 1999). Our study supports previous research showing higher ECOLI concentrations and greater exceedances during the summer months in rivers (Muirhead and Meenken, 2018; Snelder et al., 2016). Regional councils are required to monitor ECOLI year-round to assess water quality with respect to human health for recreation. There has been some suggestion that ECOLI monitoring is only necessary during the summer when contact recreation (i.e., swimming) primarily occurs. Our study indicates that summer grades are most likely to be poorer than grades derived from annual data at sites with catchments dominated by agricultural and urban land use.

In contrast, season was not an important predictor of lake water quality for most variables, although CHLA and NH₄N had significantly higher winter concentrations in some lakes (Table 5-1). However, season was not included in the lake spatial models for any water quality variable (Table 5-3, **Error! Reference source not found.**). Higher winter CHLA may be driven by increased nutrient levels in winter due to the breakdown of the thermocline in stratified lakes. In contrast, the higher winter concentrations of NH₄N in deep oligotrophic lakes may be due to reduced rates of nutrient uptake and denitrification in the winter. However, our results suggest that most lake water quality variables are not strongly affected by seasonal variation. This result may be due to low stratification of many lakes or lag effects that reduce the impacts of the seasonal patterns observed in rivers.

The distribution of monitoring sites in both geographic and environment space determines the ability of a RF model to produce realistic spatial predictions. The river monitoring sites were well-distributed geographically (Figure 2-1, Larned et al., 2018b), with most regions of the country well represented. However, monitoring sites were over-represented in low elevation, low slope catchments of and under-represented in catchments dominated by native forest landcover and minimal intensive agricultural landcover. In contrast, the lake dataset had a more restricted geographic coverage (Figure 2-2; Fraser and Snelder, 2018). In particular, there was no or very limited data available for the Hawkes Bay, Taranaki and Gisborne regions in the North Island, the top and west coast of the South Island. Monitored lakes were slightly over-representative of low elevations and lakes in regions with warmer climates and were under-representative of lakes in regions with colder climates (Fraser and Snelder, 2018).

The correlative rather than causative nature of the relationships between these predictors and nutrient loads to rivers and lakes is not relevant when considering the statistical measures of predictive performance of the models. However, it does mean that the lake model predictions may be unrealistic in situations where the relationship between catElev, lkElev and catWinTemp and the actual causative variables (catchment nutrient loads) is significantly different to the fitting dataset. The most obvious situations where this is likely are lakes at low-elevations whose catchments are

largely unmodified, and lakes with cold climates but low-elevation. The model predictions are therefore likely to be less reliable in geographic regions that have low-elevation lakes and lake catchments with relatively unmodified catchment landcover such as the West Coast of the South Island, Fiordland and Stewart Island.

7.2 Comparison with previous studies

7.2.1 Rivers

The seasonal river water quality models presented in this study build on previous modelling work carried out by Unwin et al. (2010), Larned et al. (2016a) and Whitehead (2018). The models in Unwin et al. (2010) and Larned et al. (2016a) were based on data from 1996-2007 and 2009-2013, respectively, while Whitehead (2018) and the current models are based on data from 2013-2017. The current report assessed the influence of seasonal patterns on water quality, a predictor not included in the previous reports. However, the results and model performance of the current study were generally consistent with these previous studies.

Improvements in the modelling methodology and predictor variables between the 2010 and 2016 studies (see Larned et al., 2016a) increased the performance of the RF models. In the current study, we used the same modelling procedures and predictor variables as Whitehead (2018), including the use of the most current landcover data available at a national scale (LCDB4).

7.2.2 Lakes

The spatial lake water quality models represented in this study build on previous modelling work carried out by Snelder et al. (2016) and Fraser and Snelder (2018). These studies used the same methodologies but varied in time period (2009-2013, Snelder et al. 2016b; 2013-2017, Fraser and Snelder 2018, current study). The differences between studies led to differences in the number of lakes used and small differences in model performance. This study is the first national-scale report to include season as a predictor variable for lake water quality. However, our results suggest that lake water quality does not vary significantly by season for most variables, meaning that the broad-scale conclusions are the same for all three studies.

8 Acknowledgments

We thank Dan Elder, Annabelle Ellis and Sheree De Malmanche (Ministry for the Environment) for support of this project and for feedback, enthusiasm, and patience. We thank Abi Loughnan and the LAWA team for data updates. And we thank the many regional council staff who provided additional data and information about monitoring programmes. Thanks also to Ton Snelder and Caroline Fraser for provision of analysis code and statistical advice. We thank Rachel Wright, Ton Snelder and Scott Larned for formatting and reviewing the report.

9 References

- Alexander, R.B., Elliott, A.H., Shankar, U., McBride, G.B. (2002) Estimating the sources and transport of nutrients in the Waikato River Basin, New Zealand. *Water Resources Research* 38: 4-1-4-23.
- Biggs, B.J.F. (2000) New Zealand periphyton guideline: detecting, monitoring and managing enrichment of streams. NIWA Christchurch.
- Biggs, B.J.F., Close, M.E. (1989) Periphyton biomass dynamics in gravel bed rivers: the relative effects of flows and nutrients. *Freshwater Biology* 22: 209-231.
- Biggs, B.J.F., Tuchman, N.C., Lowe, R.L., Stevenson, R.J. (1999) Resource stress alters hydrological disturbance effects in a stream periphyton community. *Oikos* 85: 95-108.
- Booker, D.J., Snelder, T.H. (2012) Comparing methods for estimating flow duration curves at ungauged sites. *Journal of Hydrology* 434: 78–94.
- Breiman, L. (2001) Random Forests. *Machine Learning* 45: 5–32.
- Breiman, L. (1984) *Classification and regression trees*. Wadsworth International Group, Belmont, California.
- Burns, N., Rutherford, J., Clayton, J. (1999) A monitoring and classification system for New Zealand lakes and reservoirs. *Lake and Reservoir Management* 15: 255–271.
- Chindler, D.A.W.S., Chlesinger, W.I.H.S., Iلمان, D.A.G.T., Vitousek, P.M., Aber, J.D., Howarth, R.W., Likens, G.E., Matson, P.A., Schindler, D.W., Schlesinger, W.H., Tilman, D.G. (1997) Human alteration of the global nitrogen cycle: sources and consequences. *Ecological Applications* 7: 737–750.
- Clapcott, J.E., Goodwin, E., Snelder, T.H. (2013) Predictive models of benthic macroinvertebrate metrics, Cawthron Institute Report 2301. Cawthron Institute, Nelson.
- Close, M.E., Davies-Colley, R.J. (1990) Baseflow water chemistry in New Zealand rivers 2: influence of environmental factors. *New Zealand Journal of Marine and Freshwater Research* 24: 343–356.
- Conley, D., Likens, G. (2009) Controlling eutrophication: nitrogen and phosphorus. *Science* 323: 1014–1015.
- Cutler, D.R., Edwards, T.C., Beard, K.H., Cutler, A., Hess, K.T., Gibson, J., Lawler, J.J. (2007) Random forests for classification in ecology. *Ecology* 88: 2783–2792.
- D’Angelo, E.M., Reddy, K.R. (1994) Diagenesis of organic matter in a wetland receiving hypereutrophic lake water: I. Distribution of dissolved nutrients in the soil and water column. *Journal of Environment Quality* 23: 928–936.
- Davies-Colley, R.J., Franklin, P., Wilcock, R.J., Clearwater, S., Hickey, C. (2013) National Objectives Framework – temperature , dissolved oxygen & pH. Proposed thresholds for discussion. NIWA Client Report HAM2013–056 prepared for the Ministry for the Environment.

- Dodds, W.K. (2006) Eutrophication and trophic state in rivers and streams. *Limnology and Oceanography* 51: 671–680.
- Dodds, W.K., Bouska, W.W., Eitzmann, J.L., Pilger, T.J., Pitts, K.L., Riley, A.J., Schloesser, J.T., Thornbrugh, D.J. (2009) Eutrophication of U.S. freshwaters: Analysis of potential economic damages. *Environmental Science and Technology* 43: 12–19.
- Duan, N. (1983) Smearing estimate: a nonparametric retransformation method. *Journal of the American Statistical Association* 78: 605–610.
- Eden, D., Parfitt, R. (1992) Amounts and sources of phosphate in hill country rocks, south-eastern North Island, New Zealand. *Soil Research* 30: 357–370.
- Elith, R.J., Leathwick, J.R. (2012) Boosted regression trees for ecological modeling. 1–22.
- Fraser, C., Snelder, T.H. (2018) Spatial modelling of lake water quality state: incorporating monitoring data for the period 2013 to 2017. LWP Client Report 2018–16. Land Water People, Christchurch.
- Freeman, M. (1983) Periphyton and water quality in the Manawatu River, New Zealand. PhD thesis, Massey University.
- Froelich, P.N. (1988) Kinetic control of dissolved phosphate in natural rivers and estuaries: A primer on the phosphate buffer mechanism. *Limnology and Oceanography* 33: 649–668.
- Golubev, S., Savenko, A. (2002) Solubility of iron(III) and aluminum phosphates in aqueous solutions. Goldschmidt Conference Abstracts 2002: A285.
- Grant, B.R., Turner, I.M. (1969) Light-stimulated nitrate and nitrite assimilation in several species of algae. *Comparative Biochemistry and Physiology* 29: 995–1004.
- Hastie, T.J., Tibshirani, R., Friedman, J.H. (2001) The elements of statistical learning, data mining, inference and prediction (2nd edition). Springer Series in Statistics. Springer-Verlag, New York.
- Howard-Williams, C., Davies, J., Pickmere, S. (1982) The dynamics of growth, the effects of changing area and nitrate uptake by watercress *Nasturtium officinale* R. Br. in a New Zealand Stream. *Journal of Applied Ecology* 19: 589–601
- Joy, M.K., Death, R.G. (2001) Control of freshwater fish and crayfish community structure in Taranaki, New Zealand: dams, diadromy or habitat structure? *Freshwater Biology* 46: 417–429.
- Klump, J.V., Martens, C.S. (1981) Biogeochemical cycling in an organic rich coastal marine basin—II. Nutrient sediment-water exchange processes. *Geochimica et Cosmochimica Acta* 45: 101–121.
- Larned, S.T., Unwin, M.J. (2012) Representativeness and statistical power of the New Zealand river monitoring network. National Environmental Monitoring and Reporting: Network Design, Step 2. NIWA Client Report CHC2012–079 prepared for Ministry for the Environment. NIWA, Christchurch.

- Larned, S.T., Snelder, T.H., Unwin, M.J. (2016a) Water quality in New Zealand rivers: modelled water quality state. NIWA Client Report CHC2016–070 prepared for the Ministry for the Environment. NIWA, Christchurch.
- Larned, S.T., Snelder, T.H., Unwin, M.J., McBride, G., (2016b) Water quality in New Zealand rivers: current state and trends. *New Zealand Journal of Marine and Freshwater Research* 50, 389–417.
- Larned, S.T., Snelder, T.H., Whitehead, A.L., Fraser, C. (2018a) Water quality state and trends in New Zealand lakes: analyses of national data ending in 2017. NIWA Client Report 2018359CH prepared for the Ministry for the Environment. NIWA, Christchurch.
- Larned, S.T., Whitehead, A.L., Snelder, T.H., Fraser, C., Yang, J. (2018b) Water quality state and trends in New Zealand rivers: analyses of national data ending in 2017. NIWA Client Report 2018347CH prepared for the Ministry for the Environment. NIWA, Christchurch.
- Leathwick, J.R., Overton, J.M., McLEOD, M. (2003) An environmental domain classification of New Zealand and its use as a tool for biodiversity management. *Conservation Biology* 17: 1612–1623.
- Leathwick, J.R., Snelder, T.H., Chadderton, W.L., Elith, R.J., Julian, K., Ferrier, S. (2011) Use of generalised dissimilarity modelling to improve the biological discrimination of river and stream classifications. *Freshwater Biology* 56: 21–38.
- Machova, J., Faina, R., Randak, T., Valentova, O., Steibach, C., Kocour Kroupova, H., Svobodová, Z. (2017) Fish death caused by gas bubble disease: a case report. *Veterinární Medicína* 62: 231–237.
- McDowell, R.W., Snelder, T.H., Cox, N., Booker, D.J., Wilcock, R.J. (2013) Establishment of reference or baseline conditions of chemical indicators in New Zealand streams and rivers relative to present conditions. *Marine and Freshwater Research* 64: 387–400.
- MfE (2017) Clean Water. Ministry for the Environment, Publication number: ME 1293. Ministry for the Environment, Wellington.
- Moriasi, D.N., Arnold, J.G., Van Liew, M.W., Bingner, R.L., Harmel, R.D., Veith, T.L. (2007) Model evaluation guidelines for systematic quantification of accuracy in watershed simulations. *Transactions of the ASABE* 50: 885–900.
- Muirhead, R.W., Meenken, E.D. (2018) Variability of *Escherichia coli* concentrations in rivers during base-flow conditions in New Zealand. *Journal of Environment Quality* 47: 967.
- Nash, J.E., Sutcliffe, J.V. (1970) River flow forecasting through conceptual models part I — a discussion of principles. *Journal of Hydrology* 10: 282–290.
- Peterson, C.G. (1996) Mechanisms of lotic microalgal colonization following space-clearing disturbances acting at different spatial scales. *Oikos* 77: 417
- Piñeiro, G., Perelman, S., Guerschman, J.P., Paruelo, J.M. (2008) How to evaluate models: Observed vs. predicted or predicted vs. observed? *Ecological Modelling* 216: 316–322.

- Quinn, J., Rutherford, K., Wilcock, R.J., Depree, C., Young, R., Schiff, S. (2018) Nutrient-periphyton interactions along a temperate river and response to phosphorus input reduction. Proceedings of the 4th International Conference on Water Resources and Wetlands. Tulcea, Romania.
- Quinn, J.M., Stroud, M.J. (2002) Water quality and sediment and nutrient export from New Zealand hill-land catchments of contrasting land use. *New Zealand Journal of Marine and Freshwater Research* 36: 409–429.
- R Core Team (2017) R: A language and environment for statistical computing. R Foundation for Statistical Computing, Vienna, Austria. <https://www.R-project.org/>.
- Reddy, K.R., Kadlec, R.H., Flaig, E., Gale, P.M. (1999) Phosphorus retention in streams and wetlands: a review. *Critical Reviews in Environmental Science and Technology* 29: 83–146.
- Smith, D.G., Maasdam, R. (1994) New Zealand's national river water quality network 1. design and physico-chemical characterisation. *New Zealand Journal of Marine and Freshwater Research* 28: 19–35.
- Smith, V.H., Tilman, G.D., Nekola, J.C. (1998) Eutrophication: Impacts of excess nutrient inputs on freshwater, marine, and terrestrial ecosystems. *Environmental Pollution* 100: 179–196.
- Snelder, T.H., Biggs, B.J.F. (2002) Multiscale river environment classification for water resources management. *Journal of the American Water Resources Association* 38: 1225–1239.
- Snelder, T.H., Leathwick, J.R., Kelly, D. (2006) Definition of a multivariate classification of New Zealand lakes. NIWA, Christchurch.
- Snelder, T.H., Wood, S., Atalah, J. (2016) Strategic assessment of New Zealand's freshwaters for recreational use: a human health perspective Escherichia coli in rivers and planktonic cyanobacteria in lakes LWP Client Report 2016–011. Land Water People, Christchurch.
- Snelder, T.H., Larned, S.T., McDowell, R.W. (2018) Anthropogenic increases of catchment nitrogen and phosphorus loads in New Zealand. *New Zealand Journal of Marine and Freshwater Research* 52: 336–361.
- Sorrell, B., Unwin, M.J., Dey, K., Hurren, H. (2006) A snapshot of lake water quality. NIWA, Christchurch.
- Sundby, B., Gobeil, C., Silverberg, N., Alfonso, M. (1992) The phosphorus cycle in coastal marine sediments. *Limnology and Oceanography* 37: 1129–1145.
- Svetnik, V., Liaw, A., Tong, C., Wang, T. (2004) Application of Breiman's random forest to modeling structure-activity relationships of pharmaceutical molecules, in: Roli, F., Kittler, J., Windeatt, T. (Eds.), *Multiple Classifier Systems*. Springer Berlin Heidelberg, Berlin, Heidelberg, pp. 334–343.
- Svobodová, Z. (1993) Water quality and fish health. Food and Agriculture Organization of the United Nations.

- Syrett, P.J. (1981) Nitrogen metabolism of microalgae, in: Platt, T. (Ed.), *Physiological bases of phytoplankton ecology*. Canadian Bulletin of Fisheries and Aquatic Science, Vol. 210. Canadian Government Publishing Centre, Ottawa, pp. 182–210.
- Thacker, A., Syrett, P.J. (1972) Disappearance of nitrate reductase activity from *Chlamydomonas reinhardi*. *The New Phytologist* 71: 435–441.
- Timperley, M.H. (1983) Phosphorus in spring waters of the Taupo Volcanic Zone, North Island, New Zealand. *Chemical Geology* 38: 287–306.
- Uehlinger, U., Bühner, H., Reichert, P. (1996) Periphyton dynamics in a floodprone pre-alpine river: evaluation of significant processes by modelling. *Freshwater Biology* 36: 249–263.
- Unwin, M.J., Snelder, T.H., Booker, D., Ballantine, D., Lessard, J. (2010) Predicting water quality in New Zealand rivers from catchment-scale physical, hydrological and land cover descriptors using Random Forest models. NIWA Client Report CHC2010–037. NIWA, Christchurch.
- Weitkamp, D.E., Katz, M. (1980) A review of dissolved gas supersaturation literature. *Transactions of the American Fisheries Society* 109: 659–702.
- West, D.W., Boubée, J.A.T., Barrier, R.F.G. (1997) Responses to pH of nine fishes and one shrimp native to New Zealand freshwaters. *New Zealand Journal of Marine and Freshwater Research* 31: 461–468.
- Whitehead, A.L. (2018) Spatial modelling of river water-quality state: incorporating monitoring data from 2013 to 2017. NIWA Client Report 2018360CH prepared for the Ministry for the Environment. NIWA, Christchurch.
- Wilcock, R.J., Nagels, J.W., Rodda, H.J.E., O'Connor, M.B., Thorrold, B.S., Barnett, J.W. (1999) Water quality of a lowland stream in a New Zealand dairy farming catchment. *New Zealand Journal of Marine and Freshwater Research* 33: 683–696.
- Wood, S., Hawes, I., McBride, G.B., Truman, P., Dietrich, D. (2015) Advice to inform the development of a benthic cyanobacteria attribute. Cawthron Report No. 2752 prepared for Ministry for the Environment. Cawthron Institute, Nelson.